# BIOCONVERSION OF XYLAN INTO FUNCTIONAL XYLOOLIGOSACCHARIDES (XOS) BY RECOMBINANT ENDO-β-1,4-XYLANASE

NGUYEN CAO CUONG



A Thesis Submitted in Partial Fulfillment of the Requirements for the
Degree of Doctor of Philosophy in Biotechnology
Suranaree University of Technology
Academic year 2024

# การเปลี่ยนไซแลนให้เป็นไซโลโอลิโกแซ็กคาไรด์เชิงหน้าที่ (ซอซ) โดยใช้เอนไซม์ปรับแต่งพันธุกรรมเอนโด-เบต้า-1,4-ไซแลเนส

เหงียน เคา เคิ่ง



วิทยานิพนธ์นี้เป็นส่วนหนึ่งของการศึกษาตามหลักสูตรปริญญาปรัชญาดุษฎีบัณฑิต
สาขาวิชาเทคโนโลยีชีวภาพ
มหาวิทยาลัยเทคโนโลยีสุรนารี
ปีการศึกษา 2567

BIOCONVERSION OF XYLAN INTO FUNCTIONAL XYLOOLIGOSACCHARIDES (XOS) BY RECOMBINANT ENDO-β-1,4-XYLANASE

Suranaree University of Technology has approved this thesis submitted in partial fulfillment of the requirements for the Degree of Doctor of Philosophy.

Thesis Examining Committee

.....
(Prof. Dr. Dietmar Haltrich)
Chairperson

.....
(Assoc. Prof. Dr. Apichat Boontawan)
Member (Thesis Advisor)

.....
(Prof. Dr. Montarop Yamabhai)
Member (Thesis co-advisor)

.....
(Assoc. Prof. Dr. Nguyen Hoang Anh)
Member

.....
(Assoc. Prof. Dr. Prakit Sukyai)
Member

.....
(Assoc. Prof. Dr. Phimchanok Jaturapiree)
Member

.....
(Assoc. Prof. Dr. Yupaporn Ruksakulpiwat)
Vice Rector for Academic
Affairs and Quality Assurance

.....
(Prof. Dr. Neung Teaumroong)
Dean of Institute of Agricultural
Technology

เหงียน เคา เคิ่ง : การเปลี่ยนไซแลนให้เป็นไซโลโอลิโกแซ็กคาไรด์เชิงหน้าที่ (ซอซ) โดยใช้เอนไซม์ปรับแต่งพันธุกรรมเอนโด-เบต้า-1,4-ไซแลเนส (BIOCONVERSION OF XYLAN INTO FUNCTIONAL XYLOOLIGOSACCHARIDES (XOS) BY RECOMBINANT ENDO-β-1,4-XYLANASE) อาจารย์ที่ปรึกษา : รองศาสตราจารย์ ดร.อภิชาติ บุญทาวัน, 106 หน้า

คำสำคัญ: บาซิลัส สับซิลิส/ ไซแลเนส/โปรตีนจับมัลโตส/ฮิสติดีน/ติดป้าย/ไซแลน/ไซโลโอลิโกแซ็กคาไรด์/ซอซ/พรีไบโอติก/ต้านการอักเสบ

ไซแลนเป็นทรัพยากรประเภทคาร์โบไฮเดรต ที่สามารถหมุนเวียนมาใช้ใหม่ ซึ่งมีปริมาณมากเป็นอันดับสองของโลก ไซแลนเป็นสารโพลีแซ็กคาไรด์ที่มีโครงสร้างหลากหลาย และมีศักยภาพในการนำไปใช้งานได้หลากหลายรูปแบบ ในงานวิจัยเพื่อเป็นส่วนหนึ่งของวิทยานิพนธ์นี้ ได้ทำการโคลนยีน BsXynA11 จากเชื้อ บาซิลัส สัปซิลิส เข้าในพลาสมิส pMAL-p5x และ pMY202 เพื่อผลิตเอนไซม์ปรับแต่งพันธุกรรมไซแลเนส ๒ ชนิด คือ MBP-*Bs*XynA11 และ *Bs*XynA11-His จากนั้นได้ทำการประเมินความสามารถของเอนไซม์ทั้งสองในการเปลี่ยนไซแลนจากไม้บีช (Beechwood; BW) และชานอ้อย (Sugarcane Bagasse; BG) ให้เป็นไซโลโอลิโกแซ็กคาไรด์ (ซอซ) เชิงหน้าที่

ผลการศึกษาพบว่าสภาวะที่เหมาะสมในการผลิต MBP-BsXynA11 ในเชื้อแบคทีเรียเอสเชอริเชีย โคไล คือการใช้สาร IPTG ที่ความเข้มข้น ๐.๒ มิลิโมลาร์ เป็นเวลา ๒๐ ชั่วโมง ที่อุณหภูมิ ๓๒ องศาเซลเซียสในขณะที่ BsXynA11-His นั้นจะให้ผลการผลิตที่ดีที่สุดเมื่อใช้ IPTG ที่ความเข้มข้น ๐.๑ มิลิโมลาร์ ที่อุณหภูมิ ๒๗ องศาเซลเซียส เป็นเวลา ๒๐ ชั่วโมง ภายใต้สภาวะดังกล่าว MBP-BsXynA11 มีผลผลิตสูงกว่า โดยอยู่ที่ ๔๔.๖ มิลิกรัมต่อลิตร เมื่อเทียบกับ BsXynA11-His ซึ่งมีผลผลิตที่ ๔๔.๖ มิลิกรัมต่อลิตร ผลการวิเคราะห์ด้วย SDS-PAGE พบว่า MBP-BsXynA11 มีน้ำหนักโมเลกุล ๖๖ กิโลดาลตัน ในขณะที่ BsXynA11-His มีน้ำหนักโมเลกุล ๒๓ กิโลดาลตัน ทั้งสองเอนไซม์แสดงประสิทธิภาพสูงสุดที่อุณหภูมิ ๖๐ องศาเซลเซียสและ ค่าความเป็นกรด-ด่าง ที่ ๖.๕ แต่ MBP-BsXynA11 มีค่ากิจกรรมจำเพาะ (specific activity) สูงกว่า โดยอยู่ที่ ๗,๙๐๐ ยูนิตต่อนาโนโมล ในขณะที่ BsXynA11-His มีค่า ๔,๘๐๐ ยูนิตต่อนาโนโมล

MBP-BsXynA11 ยังมีความคงทนต่อความร้อนได้ดีกว่า โดยหลังการบ่มที่ ๔๐ องศาเซลเซียส เป็นเวลา ๗๒ ชั่วโมง ค่ากิจกรรมของ MBP-BsXynA11 คงเหลืออยู่ที่ร้อยละ ๗๖.๕ และ ๘๑ ในสภาวะที่มีและไม่มีไซแลนจากไม้บีชตามลำดับ ในขณะที่ BsXynA11-His มีค่าคงเหลือเพียง ร้อยละ ๖๕.๕ และ ๒.๓ สำหรับอุณหภูมิ ๕๐ องศาเซลเซียส กิจกรรมที่คงเหลือของ MBP-BsXynA11 อยู่ที่ร้อยละ ๕๘.๕ และ ๒๒.๕ ในสภาวะที่มีและไม่มีไซแลนจากไม้บีชตามลำดับ ส่วน BsXynA11-His มีค่าคงเหลือเพียง ร้อยละ ๑๐.๗ และ ๑.๖

การวิเคราะห์จลนพลศาสตร์พบว่า MBP-BsXynA11 มีค่า Vmax และ kcat สูงกว่าที่ ๔,๕๓๐ ไมโครโมล ต่อนาทีต่อนาโนโมล และ ๕,๙๗๖ ต่อวินาทีตามลำดับ ในขณะที่ BsXynA11-His มีค่า ๓,๔๗๐ ไมโครโมล ต่อนาทีต่อนาโนโมล และ ๔,๗๘๘ ต่อวินาทีตามลำดับ อย่างไรก็ตาม BsXynA11-His มีความสามารถในการจับกับสารตั้งต้นคือไซแลนจากไม้บีชได้ดีกว่า โดยมีค่า Km ที่ ๑๒.๙ มิลิกรัมต่อมิลิลิตร เมื่อเทียบกับ MBP-BsXynA11 ซึ่งมีค่า Km ที่ ๑๙.๓ มิลิกรัมต่อมิลิลิตร

ในกระบวนการเปลี่ยนไซแลนให้เป็น ซอซ ที่ความเข้มข้น 2% (w/v) ที่ ค่า pH 6.5 และอุณหภูมิ ๕๐ องศาเซลเซียสเป็นเวลา ๔๘ ชั่วโมง ซอซ ถูกผลิตได้ร้อยละ ๕๒ และ ๕๐ เมื่อใช้เอนไซม์ MBP-BsXynA11 และ BsXynA11-His ตามลำดับ และผลิตภัณฑ์ ซอซ มากกว่าร้อยละ ๙๐ ประกอบด้วยไซโลไบโอส ไซโลไตรโอส และไซโลเตตราโอส ซึ่งเป็นองค์ประกอบที่มีฤทธิ์ทางชีวภาพสูง

จากนั้นได้ทำการศึกษากิจกรรมทางชีวภาพของ **MBPBW-XOS** (ซอซ ที่ได้จากไซแลนจากไม้บีชโดยใช้เอนไซม์ MBP-BsXynA11) ผลการศึกษาแสดงให้เห็นถึงคุณสมบัติพรีไบโอติกที่เด่นชัดในอาหารสังเคราะห์ต่อเชื้อโปรไบโอติก ๗ สายพันธุ์ ได้แก่ *Bifidobacterium longum* (Omniflora, Austria), *Lactobacillus acidophilus* DSM20079 (DSMZ), *L. amylovorus* DSM20552 (DSMZ), *L. delbrueckii subsp. bulgaricus* DSM20081 (DSMZ), *L. gasseri* (Omniflora, Austria), *Streptococcus salivarius* DSM2059 (DSMZ), *S. thermophilus* APC151 นอกจากนี้ ยังพบว่า **MBPBW-XOS** สามารถสนับสนุนการเจริญเติบโตของโปรไบโอติกสองสายพันธุ์ (*L. delbrueckii subsp. bulgaricus* และ *S. thermophilus*) ในโยเกิร์ตหลังจากการเก็บรักษาเป็นเวลา ๓ สัปดาห์ที่อุณหภูมิ ๔ องศาเซลเซียส

ที่สำคัญที่สุด การศึกษานี้พบว่า **MBPBW-XOS** และ **MBPBG-XOS** (ซอซ ที่ได้จากไซแลนจากชานอ้อยโดย MBP-BsXynA11) และ **XOSBW-HIS** (ซอซ ที่ได้จากไซแลนจากไม้บีชโดย BsXynA11-His) รวมทั้ง **XOSBG-HIS** (ซอซ ที่ได้จากไซแลนจากชานอ้อยโดย BsXynA11-His) มีฤทธิ์ต้านการอักเสบในเซลล์โมโนไซต์ของมนุษย์ที่ถูกกระตุ้นด้วย LPS โดยมีฤทธิ์ในลักษณะที่ขึ้นกับปริมาณที่ใช้ โดยความเข้มข้นที่เหมาะสมที่สุดคือ ๕๐ ไมโครกรัมต่อมิลิลิตร 50 μg/mL แม้ว่าจะยังจำเป็นต้องมีการศึกษาต่อเนื่องเพื่อประเมินความเป็นพิษของ ซอซในปริมาณที่สูง แต่อย่างไรก็ตามผลการวิจัยนี้ได้เน้นย้ำถึงศักยภาพของ ซอซ ที่ผลิตด้วยเอนไซม์ในการเป็นส่วนผสมในอาหารเชิงหน้าที่ ที่ช่วยส่งเสริมสุขภาพ ทั้งมนุษย์และสัตว์



สาขาวิชาเทคโนโลยีชีวภาพ
ปีการศึกษา 2567

ลายมือชื่อนักศึกษา.....
ลายมือชื่ออาจารย์ที่ปรึกษา.....
ลายมือชื่ออาจารย์ที่ปรึกษาร่วม.....
ลายมือชื่ออาจารย์ที่ปรึกษาร่วม.....

NGUYEN CAO CUONG : BIOCONVERSION OF XYLAN INTO FUNCTIONAL XYLOOLIGOSACCHARIDES (XOS) BY RECOMBINANT ENDO-β-1,4-XYLANASE. THESIS ADVISOR : ASSOC. PROF. APICHAT BOONTAWAN, Ph.D. 106 PP.

Keywords: *Bacillus subtilis*/xylanase/Maltose-binding protein/Histidine/Tag/ Xylan/Xylooligosaccharides/Prebiotic/Anti-inflammatory

Xylan, the second most abundant renewable carbohydrate resource globally, is a heterogeneous polysaccharide with diverse potential applications. In this study, the BsXynA11 gene from *Bacillus subtilis* was cloned into pMAL-p5x and pMY202 vectors to express two recombinant xylanases, namely MBP-*Bs*XynA11 and *Bs*XynA11-His. These recombinant xylanases were evaluated for their ability to convert xylan from beechwood (BW) and sugarcane bagasse (BG) xylan into functional xylooligosaccharides (XOS). The optimal conditions for the MBP-*Bs*XynA11 expression in *Escherichia coli* were 0.2 mM IPTG for 20 h, at 32 °C, while *Bs*XynA11-His expression was optimal using 0.1 mM IPTG at 27 °C for 20 h. Under these conditions, MBP-*Bs*XynA11 exhibited a higher expression yield of 44.6 mg/L compared to 5.5 mg/L for *Bs*XynA11-His. SDS-PAGE analysis showed molecular weights of 66 kDa for MBP-*Bs*XynA11 and 23 kDa for *Bs*XynA11-His. Both enzymes demonstrated optimal activity at 60 °C and pH 6.5; however, MBP-*Bs*XynA11 displayed a higher specific activity of 7,900 U/nmol, compared to 4,800 U/nmol for *Bs*XynA11-His. In comparison with *Bs*XynA11-His, the thermostability of MBP-*Bs*XynA11 was superior. In the presence and absence of the BW-xylan, the remaining activity of MBP-*Bs*XynA11 after 72 h of incubation at 40 °C was 76.5% and 81%, and at 50 °C, 58.5% and 22.5%, respectively. For *Bs*XynA11-His, 65.5% and 2.3% of the activity were retained at 40 °C, and 10.7% and 1.6% were retained at 50 °C, in the presence and absence of BW substrate, respectively. Kinetic analysis revealed that MBP-*Bs*XynA11 also exhibited a higher *Vmax* of 4,530 μmol·min$^{-1}$·nmol$^{-1}$ and *kcat* of 5,976 s$^{-1}$, compared to 3,470 μmol·min$^{-1}$·nmol$^{-1}$ and 4,788 s$^{-1}$ for *Bs*XynA11-His, respectively. However, *Bs*XynA11-His showed better substrate affinity for BW-xylan, i.e., at *Km* of 12.9 mg·mL$^{-1}$, compared to 19.3 mg·mL$^{-1}$ for MBP-*Bs*XynA11. At the optimal bioconversion reaction of 2% (w/v) WB xylan, pH 6.5 at 40 °C for 48 h, 52% and 50% of XOS could be generated from BW-xylan using 500 U/mL MBP-*Bs*XynA11 and *Bs*XynA11-His, respectively. Remarkably, over 90% of the XOS products comprised xylobiose, xylotriose, and xylotetraose, which are highly bioactive components.

Next, the biological activities of MBPBW-XOS (XOS derived from beechwood xylan by MBP-*Bs*XynA11) was investigated. The results showed a notable prebiotic effect in synthetic media on seven probiotic strains, i.e., *Bifidobacterium longum* (Omniflora, Austria), *Lactobacillus acidophilus* DSM20079 (DSMZ), *L. amylovorus* DSM20552 (DSMZ), *L. delbrueckii* sub. *bulgaricus* DSM20081 (DSMZ), *L. gasseri* (Omniflora, Austria), *Streptococcus salivarius* DSM2059 (DSMZ), and *S. thermophilus* APC151. Moreover, MBPBW-XOS's ability to support the growth of two probiotic strains (*L. delbrueckii* subsp. *bulgaricus* and *S. thermophilus*) in yogurt after three weeks of storage at 4 °C was also revealed. Most importantly, the anti-inflammatory activity of MBPBW-XOS, MBPBG-XOS (XOS from sugarcane bagasse xylan by MBP-*Bs*XynA11), XOSBW-HIS (XOS from beechwood xylan by *Bs*XynA11-His), and XOSBG-HIS (XOS from sugarcane bagasse xylan by *Bs*XynA11-His) were also demonstrated on LPS-induced human mature monocytes, in a dose-dependent manner, with the optimal concentration at 50 μg/mL. While further studies are needed to assess XOS toxicity at high doses, these findings underscore the potential of enzymatically produced XOS as functional food ingredients with health-promoting effects for humans and animals.



School of Biotechnology
Academic Year 2024

Student's Signature: .....
Advisor's Signature: .....
Co-Advisor's Signature: .....
Co-Advisor's Signature: .....

# ACKNOWLEDGEMENT

I am truly grateful for your reading of my thesis. You know, 40 years ago, I was a boy born in a poor rural area in Central Vietnam. My parents were workers in a local tea processing factory. They worked year-round without daring to get sick so that they could take care of my brother and me. Growing up, I understood the hardships my parents went through, and in that circumstance, I couldn't even imagine what my future would be like. However, somehow, our family overcame all difficulties. Both my brother and I graduated from university and gradually grew up. Two years ago, my father had a stroke and is now paralyzed on one side. My mother is the caregiver for my father so that my brother and I can focus on our studies and work. I want to express my deepest gratitude to my family, parents, brother and sister, and nieces-who have always been by my side, encouraging and supporting me so that I could complete this PhD program. I dedicate this work to my family.

In Vietnam, we have a saying: *"Without teachers, you cannot achieve anything."* I could not have become a lecturer or completed my master's and PhD programs without my esteemed teachers' guidance, instruction, and devoted help. In this thesis, I would like to express my heartfelt thanks to **Dr. Le Thanh Long** (HUAF, Vietnam) and **Prof. Dr. Do Thi Bich Thuy** (HUAF and DTU, Vietnam), laid the first bricks on my scientific research path. I also sincerely thank my advisor, **Assoc. Prof. Dr. Apichat Boontawan** (SUT, Thailand), for his kindness, selflessness, and the invaluable knowledge he has imparted.

I would like to thank all the professors at the School of Biotechnology, SUT, who have imparted valuable knowledge to me throughout my studies.

I sincerely thank the members of the thesis committee:
Prof. Dr. Dietmar Haltrich (BOKU-Austria, Chairperson)
Assoc. Prof. Dr. Apichat Boontawan (SUT-Thailand, Thesis Advisor)
Prof. Dr. Montarop Yamabhai (SUT-Thailand, Thesis Co-Advisor)
Assoc. Prof. Dr. Nguyen Hoang Anh (VNUA-Vietnam, Member)
Assoc. Prof. Dr. Prakit Sukyai (KU-Thailand, Member)
Assoc. Prof. Dr. Phimchanok Jaturapiree (SU-Thailand, Member)

The esteemed teachers have enthusiastically participated and provided valuable feedback, helping me learn and further refine my thesis.

I would like to thank my dear friends at MY LAB, AB LAB, SUT Tennis Club, and HUAF for always being reliable, helping, and sharing with me during my journey at SUT.

Thank you, Anna, my girlfriend; life as a Ph.D. student is beautiful and meaningful with you by my side.

This is an important milestone, a beautiful period in my life that I will always remember.

Thank you very much! I love you all!

NGUYEN CAO CUONG

# CONTENTS

Page

# CONTENTS (Continued)

Page

# LIST OF TABLES

**Table** **Page**

# LIST OF FIGURES

**Figure** **Page**

# LIST OF FIGURES (Continued)

**Figure** **Page**

# LIST OF ABBREVIATIONS

| | | |
|---|---|---|
| XOS | = | Xylooligosaccharides |
| LCB | = | Lignocellulose |
| BW | = | Beechwood |
| SCB | = | Sugarcane bagasse |
| DNS | = | 3,5-dinitrosalicylic acid |
| HPLC | = | High-performance liquid chromatography |
| SCFA | = | Short-chain fatty acids |
| DP | = | Degree of polymerization |
| TLC | = | Thin layer chromatography |
| BSA | = | Bovine Serum Albumin |
| SDS-PAGE | = | Gel electrophoresis |
| CFU | = | Colony-forming unit |
| MBPBW-XOS | = | XOS delivery from beechwood xylan by MBP-*Bs*XynA11 |
| HISBW-XOS | = | XOS delivery from beechwood xylan by *Bs*XynA11-His |
| MBPBG-XOS | = | XOS delivery from sugarcane bagasse xylan by MBP-*Bs*XynA11 |
| HISBG-XOS | = | XOS delivery from sugarcane bagasse xylan by *Bs*XynA11-HIS |

# CHAPTER 1
# INTRODUCTION

Climate change poses a significant challenge to humanity, with agricultural production being one of the primary contributors. A substantial portion of agricultural by-products, such as rice straw, wheat straw, rice husk, corn stover, and sugarcane bagasse, are typically left in fields after harvesting and are often burned to prepare for the next planting season. This practice not only contributes to air pollution but also results in the wastage of renewable resources. The rapid growth of the global population and increasing energy demands have spurred research efforts aimed at developing new energy sources and utilizing agricultural by-products to produce high-value products. However, challenges remain, particularly regarding the sustainable utilization of biomass and the difficulties associated with scaling up these processes to an industrial level.

Lignocellulose (LCB) is the most crucial component in agricultural biomass with significant potential for bioconversion. It consists of cellulose, hemicellulose, and lignin, providing an abundant and cost-effective raw material for conversion into value-added products such as biofuels, organic acids, oligosaccharides, and other chemicals (Kumar et al., 2021). Among these, the production of oligosaccharides from lignocellulose materials has gained considerable attention from researchers.

Xylo-oligosaccharides (XOS) are prebiotic compounds widely utilized in food and pharmaceutical industries. With the high demand for XOS, significant research efforts are being directed towards developing sustainable and environmentally friendly technologies and bioprocesses for their production. XOS can be produced from lignocellulose waste using various methods, including auto-hydrolysis and chemical hydrolysis; however, these methods are less sustainable and environmentally detrimental. Furthermore, they often result in products of low quality and purity, limiting their applicability in food products. The bioconversion of XOS from lignocellulose biomass through enzymatic hydrolysis presents an effective solution to these challenges, offering a cleaner and more sustainable approach.

Xylanase is a group of hydrolytic enzymes crucial for xylose and xylo-oligosaccharides (XOS) production. Endo-β-1,4-xylanase (EC 3.2.1.8) is an enzyme that specifically cleaves β-1,4 glycosidic bonds within xylan, producing xylobiose and xylo-oligomers. This enzyme is found in various microorganisms, including fungi (e.g., *Aspergillus*, *Trichoderma*, *Thermomyces*, *Fusarium*) and bacteria (e.g., *Lactobacillus*, *Streptomyces*, *Bifidobacteria*) (Bhardwaj et al., 2019b). However, species of *Bacillus* have been identified as particularly promising sources of xylanases due to their tolerance to high temperatures and broad pH ranges. Among these, *Bacillus subtilis* is recognized as a significant industrial microorganism with high potential for XOS production (Rashid & Sohail, 2021).

The enzymatic method for XOS production offers several advantages, including high yields and product purity due to the specificity of enzymatic reactions, mild operational conditions, minimal equipment corrosion, and reduced pollutant residue. Despite these benefits, the enzymatic production of XOS remains an expensive and complex process, even with high market value and demand. The high cost of enzymes and the complexities involved in biomass pretreatment present significant barriers to the industrial-scale production of XOS. In this study, pure xylanase from *Bacillus subtilis* was produced using various purification approaches. Then, a xylanase with superior characteristics was used to hydrolyze xylan into XOS. In the next step, the functional properties of XOS, such as prebiotic and anti-inflammatory activities, were explored.

*The objective of the research:* To produce the functional xylooligosaccharide from xylan using recombinant xylanase from *Bacillus subtilis.*

The sub-objectives:

- Cloning, expression, purification, and characterization of two xylanase from *B. subtilis.*
- Optimize condition to convert xylan into functional xylooligosaccharide using recombinant xylanase.
- Investigate the biological activity of XOS.

# CHAPTER 2
# LITERATURE REVIEWS

## 2.1 Xylan

Xylan is the main component of hemicellulose, there are L-arabino-(4-O-methyl-D-glucurono)-D-xylan (Sun et al., 2004), composed of 43-93% xylose units. Hemicellulose shows branch groups of acetyl, arabinose, and uronic acid groups with a high amount of arabinose (Figure 1). Xylose units are linked by β-1,4 linkages with branch groups at C-2 and C-3. Arabinose is linked to the xylan chain by α-1,2 or α-1,3 linked, galactose is linked by β-1,5 linked to the xylan backbone. Glucuronic acid can be linked to xylan at O-5, and ferulic acid can be attached to arabinose residues at O-5.

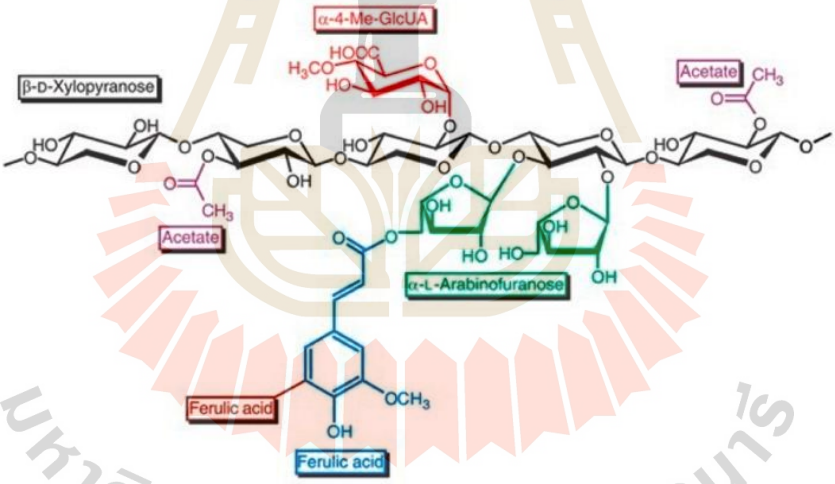


**Figure 1.** Structure of xylan showing different intermolecular bonds and substitutions (Palaniappan et al., 2021)

Xylans are classified into different subclasses depending on their degree of substitution (DS) and the types of branch groups in their structure (de Freitas et al., 2019):

a) Homoxylans: a single polysaccharide made by D-xylopyranosyl (Xylp) groups linked by β-(1,3)-linkages (X3), β-(1,4)-linkages (X4), and a mixed β-(1,3, 1,4)-linkages (Xm).

b) Glucuronoxylans: polysaccharides composed of a single side chain of α-D-glucuronic acid (GA) and its 4-O-methyl derivative (MeGA) linked to Xylp at C-2.

c) Arabino glucuronoxylans (AGX): polysaccharides have α-L-arabinofuranosyl (α-Araf) residue attached to Xylp at C-3.

d) Arabinoxylans (AX): these polysaccharides have α-Araf residues attached to Xylp at C-2 and C-3. Phenolic acids (ferulic acid and p-coumaric acid) can be attached to O-5.

e) Glucurono arabinoxylans (GAX): polysaccharides similar to AGX disubstituted by Araf residues.

To produce the added value products from lignocellulosic biomass (LCB), it has to be extracted by pre-treatment as a substrate for the next processes. Pretreatment is necessary in order to remove lignin in LCB and to obtain sugars from cellulose or hemicellulose. Hemicellulose xylan is heterogeneous and durable it requires complex processing for its extraction (Chaudhary et al., 2021). Xylan has a more branched chain leading to easier solubility in solvents. Water and dilute alkaline can remove acetyl content from xylan and also breaks alpha-ether linkages of lignin to release hemicellulose chain.

The selection of LCB hemicellulose extraction method depends on the target, application and cost. There are several methods for LCB pretreatment such as autohydrolysis, liquid hot water extraction, steam explosion, and acid or alkaline. Among them, acid and alkaline pretreatments were more applied. The different methods lead to different degrees of polymerization, degree of branching/substitution, residual lignin content, solubility, and reactivity of hydrolysate. For recovering polysaccharides or monosaccharides, the alkaline or acid pretreatment was considered. Acid pretreatment and processes after that lead to a final product based on monosaccharides and oligosaccharides. For XOS production, acid pretreatment results in high xylose and low XOS yield with unwanted compounds of chemical inhibitors (organic acids, 5-hydroxymethylfurfural (HMF), and furfural). On the other hand, alkaline pretreatment breaks down the cell wall, disrupting the macromolecule components and making xylan and lignin solubilized. The hydrolysis process produces a final product based on polysaccharides with a high degree of polymerization. The effect of alkaline is saponification of the ester bond, separating hemicellulose from

lignin, and releasing acid acetic. Alkaline also causes swelling cellulose structure, and absorption of water leads to disrupting the interaction between lignin and carbohydrates. Alkaline pretreatment is more advantageous with a high yield of XOS, but it needs a second step to produce XOS, such as acid or enzymatic hydrolysis, to break the polysaccharides and consequently release oligomers.

## 2.2 Sugarcane bagasse

Sugarcane (*Saccharum officinarum*) bagasse (SCB) is a biomass of agricultural residue from sugarcane processing. The overview of the general compositions of sugarcane is shown in Figure 2.

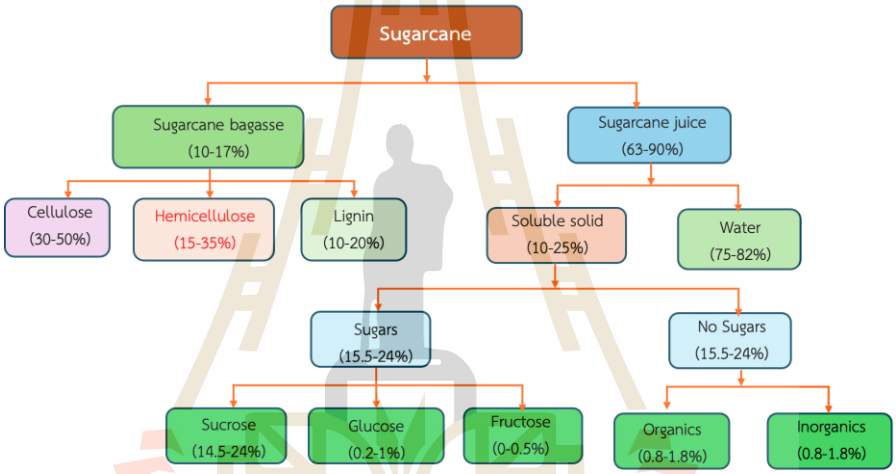


**Figure 2**. The general compositions of sugarcane (Canilha et al., 2012; Mai-Moulin et al., 2019)

The SCB has two kinds of fiber (microfibril): the cellulose fiber in the rind and fiber in the pith. The fibers in the pith are mainly of parenchyma cells and in the rinds of sclerenchyma cells. Smaller than cellulose fibers are cellulose microfibrils, which bind to hemicellulose to form a network structure, surrounded by lignin (Figure 3). The main component of lignocellulose is hemicellulose polysaccharides. Furthermore, the major component of hemicellulose is xylan, constituted of xylose unit.

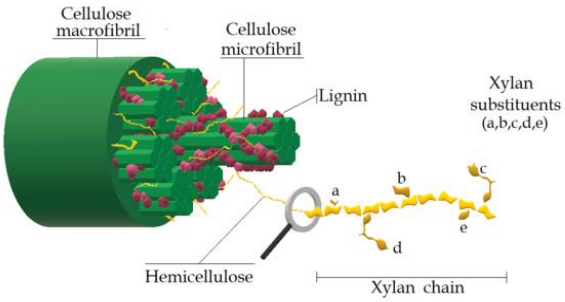


**Figure 3.** Structure of lignocellulose biomass with xylan and its main substituents. a) acetyl; b) 4-O-methyl-α–Dglucuronopyranosyl; c) α-L-arabinoferuloyl; d) α-L-arabinocoumaroyl; e) α-L-arabinose (Santibanez et al., 2021)

SCB includes 30-50% cellulose, 10-20% lignin, 15-35% hemicelluloses, xylan ~21%. Lignocellulose biomass is generated in sugar factories (18-28% of sugarcane) and is considered an important source of renewable material, available in large quantities at low cost. Cellulose can be used to produce solvents, biofuels, and other cellulose products such as carboxymethyl cellulose, and cellulose nitrate. Hemicellulose can be used in fermentation to solvents and biofuels, biofilms, and xylooligosaccharides. Lignin can be used to produce phenols, activated carbon, and carbon fiber (Brienzo, 2016). A comparison of SCB components with other agricultural residues shows in Table 1.

SCB has great potential in bioconversion to form value-added products. However, its complex and heterogeneous structure presents a significant challenge for technological processes. Cellulose is the largest component, consisting of β-D-anhydroglucopyranose units linked by β-(1,4)-glycosidic linkages to make a linear homopolysaccharide. Cellulose chains are linked by hydrogen bonds, forming macro and microfibrils. Cellulose is a part of the plant cell wall, so it was difficult to separate it from hemicellulose and lignin. Hemicelluloses are the second most abundant in SCB dry biomass.

**Table 1**. The comparison of SCB components with other agricultural wastes

| Agricultural source | Cellulose (% w/w) | Hemicellulose (% w/w) | Lignin (% w/w) | Xylan (% w/w) | References |
|---|---|---|---|---|---|
| Sugarcane bagasse | 40–43 | 25–28 | 23–28 | 21.1 | (Poletto et al., 2020) |
| Wheat straw | 38–41 | 22–28 | 20–22 | 21.2 | (Poletto et al., 2020) |
| Corncob | 30–42 | 31–38 | 18–22 | 34.8 | (Yang et al., 2015) |
| Rice straw | 35 | 25 | 12 | 24.5 | (Otieno & Ahring, 2012a) |
| Birch wood | 40 | 24 | 24 | ND | (Huang et al., 2017) |
| Beech wood | 42.5 | 34.3 | 22.2 | 20.8 | (Demirbaş, 2006) |

* ND No data found

## 2.3 Endo-1,4-β-xylanases

Xylanase is the group of enzymes that degrade xylan into simple monosaccharides and xylooligosaccharides by catalyzing the hydrolysis of glycosidic linkage (β-1,4). Xylanase is a group of hydrolase enzymes, including endo β-1,4-xylanases (EC 3.2.1.8), β-d-xylosidases (E.C.3.2.1.37), α-glucuronidase (EC 3.2.1.139) acetylxylan esterase (EC 3.1.1.72), α-l-arabinofuranosidases (E.C.3.2.1.55), p-coumaric esterases (3.1.1.B10) and ferulic acid esterase (EC 3.1.1.73). Xylanase is classified into three types based on (1) molecular weight and pI, (2) based on the crystal structure, and (3) based on enzyme kinetics and substrate specificity. Based on the classification of families, xylanase is separated into family 10 (GH10) and family 11 (GH11). GH10 enzymes consist of enzymes that have a high molecular weight (high molecular weight with low isoelectric point-HMWLI) while GH11 enzymes consist of enzymes that have low molecular weight (low molecular weight with high isoelectric point-LMWHI) (Bhardwaj et al., 2019b).

Endo β-1,4-xylanases (EC 3.2.1.8) belong to Glycoside hydrolase Family 11 (LMWHI, <30 kDa), it is called “real xylanase”. This enzyme randomly cleaves the xylan chain by catalyzing the removal of xylose monomers from the xylooligosaccharides chain and nonreducing xylobiose terminal, while several other enzymes such as α-D-glucuronidase, α-L-arabinofuranosidase, and acetyl xylanesterase catalyze the removal of the side chain groups, Figure 4 (Chaudhary et al., 2021).

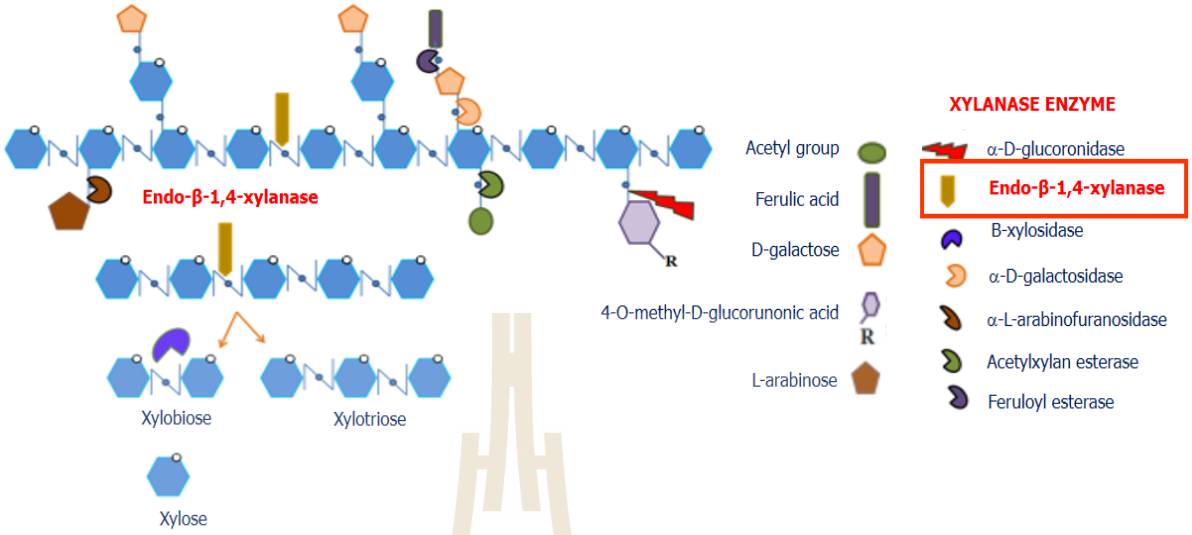


**Figure 4.** Structure of xylan showing bonds that are attacked by a specific xylanolytic enzyme for complete hydrolysis of xylan to its constituents (Bhardwaj et al., 2019b)

Endo β-1,4-xylanase can be produced by some bacteria and fungi such as *Bacillus* sp., *Clostridium* sp., *Streptomyces* sp., *Flavobacterium* sp., *Lactobacillus* sp., etc. (Table 2). Microorganisms have rapid growth, mild culture, and high xylanolytic secretion. Furthermore, xylanase from microorganisms has high specificity with the substrate, mild reaction conditions, and low by-products. Therefore, microbial xylanases have many potential for industrial application.

Xylanase from fungi has a high activity, however, their optimal pH is in the acidic range. Furthermore, the fungi culture process requires a low pH, and a long generation time, and is more complicated in subsequent downstream processing. Bacteria has a short generation time, and their xylanase is more advantageous than fungi xylanase. They require the neutral or alkaline pH range. Notably, *Bacillus* has emerged as a significant source of xylanases due to its tolerance to high temperatures and broad pH range (Bhardwaj et al., 2019b). Among *Bacillus* species, *Bacillus subtilis* is recognized as a major industrial microorganism with substantial potential for XOS production (Rashid & Sohail, 2021). Table 3 shows various xylanase purification strategies have been employed, including ammonium sulfate precipitation followed by dialysis, gel permeation chromatography, and ion exchange chromatography. While these methods may meet enzyme purification requirements, their major disadvantages include being time-consuming, costly, and challenging to scale up. Therefore,

simplifying the enzyme purification process for industrial applications is essential. Utilizing a fusion tag with affinity chromatography presents an effective approach for large-scale enzyme purification, saving time and reducing costs. Using fusion tags for protein production in *E. coli* has been widely implemented (Costa et al., 2014), with Hig-tag and MBP-tag demonstrating efficacy in protein purification (Mahmoudi Gomari et al., 2020). However, no current studies have compared the effectiveness of His-tag and MBP-tag in the production and purification of xylanase from *B. subtilis* expressed from an *E. coli* expression system

Xylanase has many applications in the industry. For example, in paper and pulp industries for pre-bleaching purposes (Sharma & Sharma, 2017; Walia et al., 2017). In food and drink industry: to increase juice yield obtained from vegetables and fruits, improve the quality of bread, or produce functional food (Butt et al., 2008; Chaudhary et al., 2021). In animal feeds: improving the animal's digestive (Bedford, 2018). However, the most prominent application of xylanase is the bioconversion of xylan from agricultural by-products to XOS. Bioconversion of XOS production by xylanase has several advantages, such as no or low production of undesirable by-products, easy to XOS downstream processing, and environment protection. XOS products from enzymatic hydrolysis methods are important strategy for the development of new functional foods due to their prebiotic effects (Ávila et al., 2020).

**Table 2** The recombinant source of xylanase, its expression system, and application

| Source of xylanase gene | Expression System | Applications | Reference |
|---|---|---|---|
| Bacillus subtilis Lucky9 | E. coli BL21 | XOS production | (Chang et al., 2017b) |
| Myceliophthora thermophila ATCC 42464 | P. pastoris | Biofuel | (Basit et al., 2018) |
| Trichoderma reesei | B. subtilis 3610 | XOS production | (Amorim et al., 2019a) |
| Trichoderma reesei | B. subtilis 3610 | XOS production | (Amorim et al., 2019b) |
| B. amyloliquefaciens | Pichia pastoris | XOS production | (Liu et al., 2017) |
| *A. fumigatus* | E. coli BL21 | XOS production | (Hu et al., 2019) |
| B. subtilis RTS | E. coli BL21 | Biofuel | (Saleem *et al.*, 2021) |

**Table 3.** Different xylanase purification methods from several microorganisms

| Source organism | Methods | Specific activity (IU/mg) | Fold purification | Recovery (%) | Application of purified enzyme | References |
|---|---|---|---|---|---|---|
| Thermotoga thermarum | Ni-affinity chromatography | 192 | 6.9 | 82.3 | XOS production | (Shi et al., 2014) |
| Trichoderma inhamatum | Ion exchange chromatography (DEAE Sephadex A-50 column), dialysis | 1257.7 | 1.9 | 62.7 | XOS production | (Silva et al., 2015) |
| Penicillium chrysogenum | Ion exchange chromatography (CM Sephadex C-50 column) | 438.3 | 9.8 | 49.3 | XOS and ethanol production | (Terrone et al., 2018) |
| Aspergillus tamarii Kita | Carboxymethyl-cellulose (CM-cellulose) chromatography | 1215.89 | 7.43 | 36.72 | XOS production | (Heinen et al., 2018) |
| Aspergillus oryzae LC1 | Ammonium sulfate, dialysis | 631 | 4.1 | 21 | XOS production | (Bhardwaj et al., 2019a) |
| | Anion exchange Chromatography (DEAE-Sephadex A-50) | 469 | 3 | 31.9 | | |
| | Gel Filtration Chromatography (Sepharose G-100) | 101.5 | 6.6 | 78.7 | | |
| | ATPS with Triton X-114 | 508.9 | 3.3 | 69.4 | | |
| | ATPS with PEG | 2004.3 | 13 | 86.8 | | |

For enzyme assay, both qualitative and quantitative analyses were used. These assays differ not only in assay conditions (temperature, pH, buffer, incubation time, substrate, etc) but also in their principles. Detection of reducing sugars from the substrate is used for quantitative enzyme activity (DNS, Nelson-Somogyi), Remazol Brilliant Blue. Detection of dye released from covalently dyed xylan, measurement of viscosity, or monitoring the turbidity are used for qualitative (SDS-PAGE (coomassie blue), Zymogram (Congo Red).

For qualitative, SDS-PAGE assay provides information about protein molecular weight. Congo red assay (Zymogram) is the most common method to confirm xylanase activity based on the diffusion principle. After electrophorese xylanase on polyacrylamide gel containing xylan, the gel is soaked in Congo red solution. Congo red strongly binds to xylan containing β-1,4-glycosidic linkages. The advantage of this method is based on the high specificity of xylanase with xylan helping to its qualitative test. However, the cons of this method are cumbersome and time-consuming. On the other hand, it uses large amounts of chemicals (Congo red for staining and sodium chloride for de-staining).

For quantitative enzyme activity, reducing sugars liberated from xylan is measured through DNS (3,5-dinitrosalicylic acid) or Nelson-Somogyi (copper and arsenomolybdate) are the most popular methods. Other methods, such as using 4-O-methylglucuronoxylan covalently dyed with Remazol Brilliant Blue (RBB xylan) as substrate, or sodium 2,2'-bicinchoninate, p-hydroxybenzoic acid hydrazide, or potassium ferricyanide were less used (Gusakov et al., 2011). There are also some commercial methods for xylanase activity assays, such as the fluorescence-based method EnzChek® Ultra Xylanase Assay Kit (Invitrogen, Carlsbad, CA), Xylazyme tablet (Megazyme, Bray, Ireland), which employs azurine-crosslinked arabinoxylan (AZCLArabinoxylan) as substrate and its hydrolysis by xylanase produces water soluble dyed fragments (L et al., 2013).

Because xylose is the monomer of xylan, to determine enzyme activity, xylose is usually used as the standard for calculation. However, the product of endo-1,4-β-d-xylanase hydrolysis from xylan is XOS, which has a higher color response with DNS than xylose. Therefore, the DNS method gives much higher enzyme activity values than the Nelson-Somogyi (NS) reducing sugar method.

To compare DNS and NS methods in xylanase activity assay, McCleary et al., (2015) used different substrates (glucuronoxylan from birchwood, glucuronoxylan from beechwood, and arabinoxylan from wheat) to determine endo-xylanase activity from *Aspergillus niger*. The results of different enzyme activity are shown in Table 4.

The results showed that endo-xylanase activities from NS assay were much lower than those obtained with the DNS assay. DNS assay led to different activity with different substrates (Wheat arabinoxylan is the highest enzyme activity) and xylose standard is highest among xylose, with the same substrate, using xylose, xylobiose, xylotriose or xylotetraose. These are the cons of DNS assay.

**Table 4.** A comparison of polysaccharide substrates and reducing sugar methods for the measurement of endo-1,4-β-xylanase (McCleary & McGeough, 2015)

| Substrate | Xylose | | Xylobiose | | Xylotriose | | Xylotetraose | |
|---|---|---|---|---|---|---|---|---|
| | U/mL | % | U/mL | % | U/mL | % | U/mL | % |
| DNS assay | | | | | | | | |
| Wheat arabinoxylan | 26,760 | 100 | 19,020 | 71 | 9950 | 37 | 8405 | 31 |
| Birchwood 4-O-methyl glucuronoxylan | 11,350 | 100 | 6595 | 58 | 4056 | 38 | 3400 | 29 |
| Beechwood 4-O-methyl glucuronoxylan | 13,680 | 100 | 7750 | 57 | 5170 | 38 | 4160 | 30 |
| NS assay | | | | | | | | |
| Wheat arabinoxylan | 1470 | 100 | 1420 | 97 | 1519 | 103 | 1516 | 103 |
| Birchwood 4-O-methyl glucuronoxylan | 1913 | 100 | 1928 | 101 | 2029 | 106 | 1904 | 100 |
| Beechwood 4-O-methyl glucuronoxylan | 1831 | 100 | 1751 | 96 | 1857 | 101 | 1976 | 108 |

The pros of NS assay: it is not affected by whether xylose, xylobiose, xylotriose, or xylotetraose (XOS with DP 2-4) are used as standards with beechwood and birchwood glucuronoxylans. NS method is as simple to use as DNS method. However, the cons of NS are poisonous chemicals are employed.

Despite its disadvantages, DNS is still the most commonly used method for the determination of xylanase activity (Table 5)

**Table 5.** Characterize xylanase and its activity assay from different microbial sources

| Source of xylanase | Strain type | Analysis method | Optimal pH, Temp. | Enzyme activity | Km (mg/mL) | Vmax | References |
|---|---|---|---|---|---|---|---|
| Bacillus amyloliquifaciens NRRL B-14393 | Wild | Colorimetric, Nelson Somogyi | 6.0, 35 °C | 99.7 U/g | - | - | (Rashad et al., 2015) |
| Bacillus subtilis | Recombinant (E. coli) | Colorimetric, DNS | 6.5, 60 °C | 436.5 (U/mL) | 3.1 | 318.9 (μmol/mg) | (Chang et al., 2017b) |
| Myceliophthora thermophila | Recombinant (Pichia pastoris) | Colorimetric, Remazol Brilliant Blue-xylan | 6.0, 60 °C | 1,533.7 (U/g) | 8.80 | 2,380 (U/mg) | (Basit et al., 2018) |
| B. amyloliquefaciens | Recombinant Pichia pastoris | Colorimetric, DNS | 5.0, 50 °C | 128.75 (U/mg) | 5.41 | 22.42 (μmol/mL) | (Liu et al., 2017) |
| Trichoderma reesei | Recombinant (Pichia pastoris) | Colorimetric, DNS | 5.0, 50 °C | 1299 (U/mL) | - | - | (Hu et al., 2019) |
| B. pumilus B20 | Wild | Colorimetric, DNS | 6.5, 60 °C | 755.81 (U/mg) | 2.3 | 50 (μmol/mL) | (Geetha & Gunasekaran, 2017a) |
| Anoxybacillus kamchatkensis NASTPD13 | Wild | Colorimetric, DNS | 9.0, 65°C | 33 (U/mg) | 0.7 | 66.64 (μmol/mg) | (Yadav et al., 2018) |
| Pediococcus acidilactici GC25 | Wild | Colorimetric, DNS | 7.0, 40 °C | 318.45 (U/mg) | 3.10 | 4.66 (U/mg) | (Adiguzel et al., 2019) |
| Pediococcus pentosaceus | Recombinant (Lactococcus lactis) | Colorimetric, Nelson Somogyi | 7.2, 37 °C | 49.70 (U/mL) | - | - | (Roslan et al., 2020) |

## 2.4 Xylo-oligosaccharide

Oligosaccharides are known as a variety of carbohydrates that involve 2–10 monosaccharide units, linear or branched, connected by **α**- and/or **β**-glycosidic linkages. These molecules can be formed from different monosaccharides. The main chain of oligosaccharides is composed the units of fructose (fructooligosaccharides, FOS), galactose (galactooligosaccharides, GOS), D-glucose (cellooligosaccharides, COS), arabinose (arabinooligosaccharides, AOS), mannose (mannooligosaccharides, MOS), D-glucosamine or N-acetyl-d-glucosamine (chitooligosaccharides, CHOS) and xylose (xylooligosaccharides, XOS). Oligosaccharides can be used as a substrate in many bioconversions, but they are also well-known for their prebiotic activity in promoting the growth of beneficial bacteria. These properties can be applied to many products to improve human health (de Freitas et al., 2019).

Among oligosaccharides, XOS have great potential to be applied in functional foods based on its physicochemical properties such as low viscosity, high water solubility, tolerance to high temperature, acidic pH, and undigested by the gastrointestinal system. XOS consist of xylose units linked through **β**-1,4 glycosidic bonds. XOS from xylobiose (X2), xylotriose (X3), xylotetrose (X4), xylopentose (X5), and xylohexose (X6) show high biological activity. In nature, XOS present in fruits, vegetables, milk, and honey. However, the commercial XOS is produced from xylan (lignocellulosic material from agricultural residues), which contains 25–35% in dry biomass.

With wide applicability, XOS market is increasing and predicts reach to $135.7 million by 2029 from $119.26 by 2022, with a compound annual growth rate of approximately 6%. Nowadays, the Asiatic's XOS market is the most extensive, with Japan being the biggest country of XOS production and consumption (Santibanez et al., 2021). Thailand is a tropical country with developmental agriculture, the biomass from those can be an abundant source for XOS production. In the sugar industry alone, the annual production of sugarcane is estimated at 74.9 million tons, which generated approximately 21 million tons of bagasse.

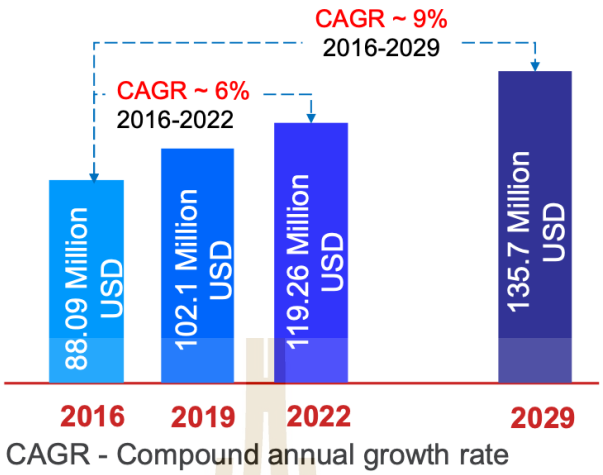


**Figure 5.** Global xylooligosaccharides market 2016-2029

The strategy of XOS production from agricultural residues

XOS production from agricultural residue has been conducted through two main strategies (Figure 6). One-step process or Two-step processes.

For one-step process, is known as autohydrolysis, which includes thermal treatment with the steam of liquid water at high temperatures or pressures. During the autohydrolysis treatment, hydronium ions were formed to make the acid condition. Hemicellulose was depolymerized to XOS under that condition. The main pros of the autohydrolysis method are low or noncorrosive chemical requests, and being labeled as an environmentally friendly process (Otieno & Ahring, 2012b). However, autohydrolysis and direct chemical methods present high energetic requirements, low XOS yield, and high production of unwanted by-products such as other oligomers, monosaccharides, acetic acid, furfural, hydroxymethylfurfural (HMF), formic acids, levulinic acid, phenolic compounds, and others (Chen et al., 2014). The unwanted compound in XOS mixtures leads to difficulty in XOS recovery, increasing production costs.

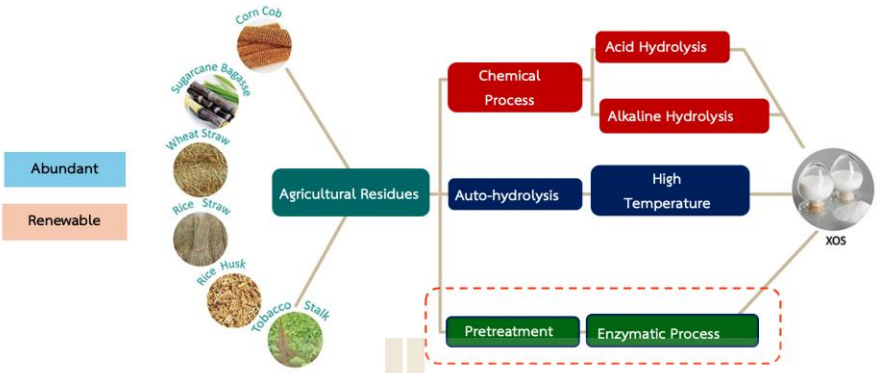


**Figure 6**. XOS production from agricultural residues (Chen et al., 2021a)

To resolve those problems, another strategy is two-step process combining pretreatment with enzymatic methods. First is pre-treatment to obtain xylan with a wide range of DP. The pretreatment is usually carried out by thermal, acid, or alkaline treatment, where hemicellulose is released from the LCB. Then, xylan is recovered from dissolved hemicellulose. The second step is hydrolysis, where xylan depolymerizes by xylanase into XOS (Carrillo et al., 2018; Poletto et al., 2020).

Currently, this two-stage approach is the most employed strategy for XOS production. Figure 7 describes more details of XOS production from LCB with or without the pretreatment step, enzyme hydrolysis, and XOS purification.

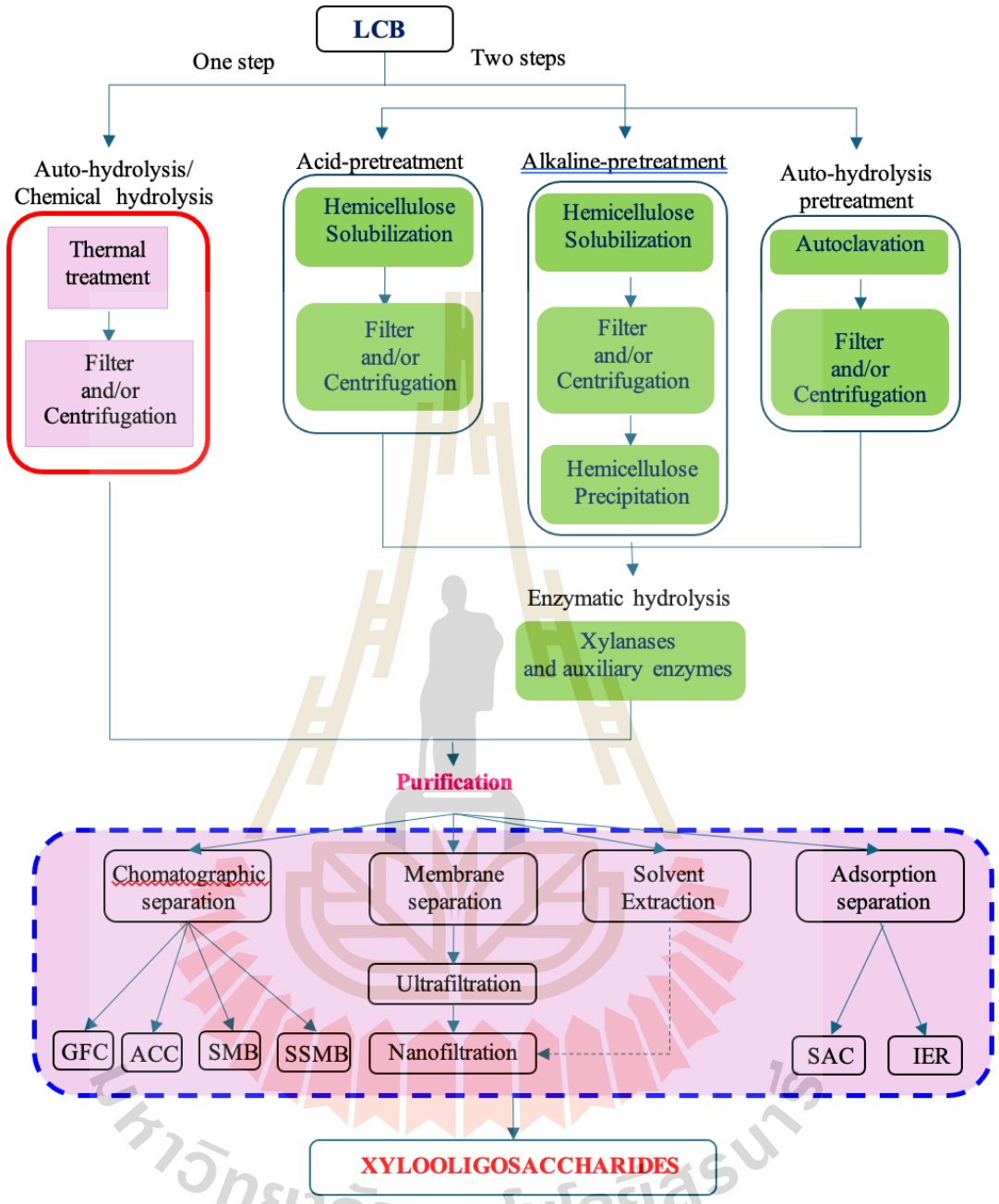


**Figure 7.** Diagram of the most common strategies for XOS production. LCB-lignocellulose biomass, GFC-Gel filtration chromatography, ACC-Activated charcoal column chromatography, SMB-Simulated moving bed, SSMB-Sequential SMB, SAC-Soluble activated charcoal, IER-Ion-exchange resins

Table 6 lists the XOS production from SCB with the two-step strategies. The different pretreatment methods and sources of xylanase were reported with XOS ranges from X2-X6. Alkaline pretreatment is commonly used for bagasse pretreatment (NaOH, KOH). Alkaline can be used alone or in combination with other alkalis or acids under normal conditions or at high temperatures and pressures. The xylan content obtained from SCB after pretreatment ranged from 6-28% of dry biomass. Pretreatment is an important first step to effectively use SCB as biomass for subsequent conversion processes.

To obtain xylan from SCB to produce XOS, Khaleghipour et al. (2021) have optimized pretreatment by 0.5M NaOH followed by autoclave (thermochemical pretreatment with alkali combined with autoclaving) at 121 °C, 60min. To recover xylan, the liquid part was collected and adjusted pH to 5.0 by acetic acid (99% v/v). Then, ethanol (99%, v/v) was used to precipitate xylan at 4 °C overnight. The solid xylan was separated by centrifugation and washed 3 times with ethanol (50% v/v). After that, xylan was dialyzed in 3 times of DI water using 10 kDa of cut-off membrane for 8 h. The xylan yield is 85.6% from initial xylan in SCB and the XOS yield is 42.3% from xylan (Khaleghipour et al., 2021). In another study, xylan from SCB was pretreated with 4% NaOH (solid-liquid ratio of 1:15 w/v) at a lower temperature (30 °C) for 24 h. The liquid was then separated by centrifugation and neutralized by hydrochloric acid to pH 7.0. After incubation overnight with 1:2 v/v 96% ethanol, precipitated xylan was collected and used for XOX hydrolysis. The xylan yield from this process was 13.8% initial xylan in SCB (Tseng et al., 2022). Mahak Gupta *et al.* (2022) provided another strategy for SCB xylan extraction. NaClO was used for delignification, and then NaOH was used to extract xylan from delignified SCB. For the delignification step, the optimal conditions were: 51.86 °C, solid-liquid 12.91% w/v, 75.12 min. For xylan extraction step, the best conditions were: 89.03°C, solid-liquid 11.80% w/v, and time 20.14 h. The xylan yield was obtained at 96.11% from SCB after 1$^{st}$ step (Gupta et al., 2022). This report is similar to (Hesam et al., 2020) when using $H_2O_2$ 5.63%, NaOH 12.91%, 17.51 h as the best condition for xylan extraction from SCB with the xylan yield 95.84%.

The overview shows that alkaline pretreatment is the most used method for xylan extraction from SCB. Alkaline can cleave the linkage between cellulose and hemicellulose, dissolve lignin, and avoid hydrolysis to sugar monomers. However, using alkaline in SCB pretreatments can generate harmful by-products for the environment

(Valladares-Diestra et al., 2022). In addition, after alkaline pretreatment, its have to follow other steps such as neutralization, and xylan precipitation by ethanol, increasing the total cost. That is a barrier to scaling up XOS products in the industry.

To resolve that problem, imidazole was recently employed in the pretreatment of LCB. Based on high basicity, safety, and low cost, it is a replacement catalyst for alkaline pretreatment (Valladares-Diestra et al., 2021b). Valladares *et al*., (2022) treated SCB with imidazole (solid-liquid 1:9) at 160 °C for 1 h. After separation by vacuum filtration, the cellulose-rich solid part was obtained. The liquid part contains a hemicellulose-rich fraction that was evaporated and then mixed with 96% ethanol to precipitate xylan. Xylan was recovered by centrifugation, washed, and lyophilized for enzymatic XOS production. The results showed that 28.9% xylan and 55.7 g of XOS per 1 kg of SCB were obtained (Valladares-Diestra et al., 2022).

**Table 6.** XOS production through enzymatic hydrolysis of the pretreated lignocellulosic biomass from SCB.

| Pretreatment | Enzymatic hydrolysis | Xylan/Biomass (XB,%), Xylan yield (%, XY) | XOS/ Biomass (XB, %), XOS/Xylan (XX,%) | XOS composition | References |
|---|---|---|---|---|---|
| KOH 1.9%, 50 min, 120 °C followed by $H_3PO_4$ 3.9%, for 44 min at 54 °C | Hlxyn11A xylanase from *Pichia pastoris*, 822 U/g, 48h | 12.17, XB<br>64.18, XY | 7.15, XB,<br>58.7, XX | X2-X4 | (Zhao et al., 2021) |
| NaOH 40%, 2 h, 60 °C | Xylanase from *Aspergillus niger*, 16% xylan, 5 U.m/L, 50 °C, 1 h | - | 19.3, XY | X2-X4 | (Valladares-Diestra et al., 2021a) |
| NaClO 0.53%, 89.03 °C, 20.14 min and NaOH 14.19% | *A. flavus* MG-7 xylanase, 120 IU | 96.11, XY | 91.12, XX | X2-X4 | (Gupta et al., 2022) |
| NaOH 15%, 20 min at 121 °C | Xyn11A xylanase *from Bacillus firmus* K-1 and CbXyn10C xylanase from *Caldicellulosiruptor bescii,* 300U/ml, 50 °C, 72h | - | 11.0, XY<br>11,2, XY | X2-X5 | (Gufe et al., 2022) |
| NaOH 4% at 30 °C for 24 h | Endoxylanase from *Bacillus Halodurans*, 0.225 U/mL, 60 °C | 13.8, XB | 44.91, XY | X2-X3 | (Tseng et al., 2022) |
| $C_3H_4N_2$ (imidazole),160 °C, 1h | Xylanases from *A. niger*, 250 U/g, 1h | 6.29, XB | 88.5, XY | X2-X6 | (Valladares-Diestra et al., 2022) |

The creation of target desired XOS is very necessary to the pharmaceutical and food industries because not all XOS have potential in health. The yield and composition of xylan hydrolysates are influenced by the xylan source (Gufe et al., 2022). Almost all reports demonstrated that XOS X2-X6 have health benefits. Controlling the hydrolysis parameters can generate the desired XOS during enzymatic hydrolysis. The parameters of hydrolysis include pH, temperature, substrate concentration, enzyme dosage, and reaction time.

Diaz et al., (2022) used the response surface methodology (RSM) technique aimed to optimize the key condition in the enzymatic hydrolysis influencing XOS yield and composition. The parameters conditions are: 1) pH of the reaction medium (4.0, 5.5. 7.0), 2) incubation temperature (25, 37.5, 50 oC), 3) substrate concentration (1, 2, 3% w/v), 4) enzyme dosage (50, 62.5, 75 U/mL) and 5) reaction time (30, 60, 90 min). The results showed that maximum X1 yield at pH 7.0, temperature 50 oC, reaction time 90 min, enzyme dose 75 U/mL, and xylan concentration 3% w/v. Maximum X2 was obtained at the same pH, enzyme dose, and xylan concentration but at different temperatures and reaction time (25 oC, 30 min). The highest yield for X2-X6 were 314.2, 76.6, 38.4, 17.8, and 5.3 mg/g xylan (Diaz-Arenas et al., 2022).

The yield and composition of XOS are also influenced by the xylan source and need to optimize separately XOS composition for each substrate (Gufe et al., 2022).

XOS purification

To be able to apply in food or pharmaceutical, XOS with a high degree of purity is required (75%-95%) (Santibanez et al., 2021). XOS purification is an important step to recover XOS in the hydrolysis media containing many compounds. XOS purification can be single or combine various techniques to remove unwanted compounds, named downstream processing. Finally, XOS can form a liquid or solid with high purity. The cost and the yield are important parameters to evaluate the effectiveness of XOS recovery.

**Table 7.** XOS purification approach

| Main product | Purification techniques | Substrate | Recovery % | Reference |
|---|---|---|---|---|
| XOS (X2-X3) | Activated charcoal (10%) chromatography | Corncob xylan | 80 | (Chapla et al., 2012) |
| XOS (X2-X6) | Ion exchange resin | Miscanthus | 89.1 | (Chen et al., 2016) |
| XOS (X5-X29) | Nanofiltration membrane and anion exchange resin | Corn stover | 89.0 | (Buruiana et al., 2017) |
| XOs | Ultrafiltration and nanofiltration | - | 57.0 | (Singh et al., 2019) |
| Xylobiose | Nanofiltration | Empty fruit bunch | 90.1 | (Wijaya et al., 2020) |
| XOS (X2-X5) | Ultrafiltration | Wheat bran | 44.4 | (Geetha & Gunasekaran, 2017b) |
| XOS | Anion-exchange resin and Cation exchange resin | Wheat bran | 96.5 | (Wang et al., 2022) |

Some processes have been discovered (Table 7) to purify XOS in raw media including membrane separation, chromatographic techniques, adsorption, and solvent extraction.

Membrane separation technology is currently considered the most promising technique to purify XOS in industrial due to its low cost, and easy to scale-up. Ultrafiltration (UF) and Nanofiltration (NF) can be used separately or combined. UF can separate oligosaccharides from high molecular weight, while NF can concentrate and remove low molecular weight compounds. In membrane technique, the membrane material, pore size of the membrane, the operational conditions, temperature, and pressure flow decide for efficient of filtration.

Kumar et al. (2015) used two UF (10 kDa and 1 kDa MWCO) to purify XOS produced by enzymatic hydrolysis with 78% purity of XOS (X2-X5) (Kumar & Satyanarayana, 2015b). Singh et al. (2012) purified XOS by using a combination of membranes (UF, 10 kDa and NF, 150 Da) followed by anion exchange resin (Diaion WA-30) to purify XOS produced by autohydrolysis. The DP2-3 were obtained with 72.2% of XOS purity (Singh et al., 2021). To remove the color compound and ions, chromatographic techniques (gel filtration chromatography (GFC), high-performance

liquid chromatography (HPLC), and activated carbon column chromatography), have been used (Santibanez et al., 2021). The adsorption technique with activated carbon is the most popular adsorbent used for removing unwanted compounds from XOS, special color compounds, and residual lignin from pretreatment step. Chen et al. (2014) used 10% activated carbon and then eluted by ethanol elution (5%) to purify XOS, the DP range is 1-9 with 47.9% purity. Another method, ion exchange resin is a suitable choice to remove the salts contained in XOS solution (Chen et al., 2014). Jiang et al. (2021) combined a variety of methods (activated carbon, UF membrane (10 kDa), cation exchange resin, and NF membrane (100-300 Da) to increase the XOS purification and reach 92.3% (Jiang et al., 2021).

XOS application

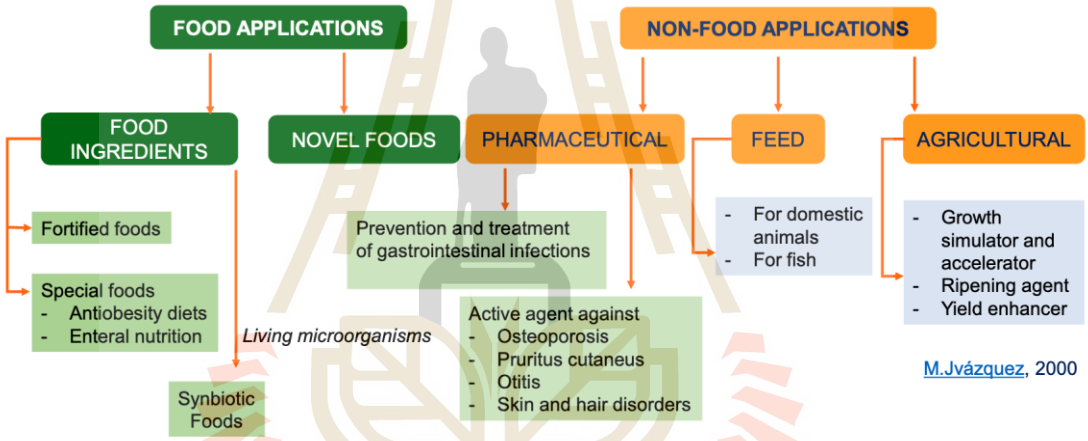


**Figure 8.** Application of xylooligosaccharides (M.J. Va´zquez, 2000)

Based on the physicochemical properties of XOS are special: water-soluble, low-calorie, less sweet (less than sucrose 50%), hydration, stable in acidic media, and non-digestible oligosaccharides (NDO), XOS can be widely applied in the agricultural, pharmaceutical, food, and cosmetic industries.

XOS is an important prebiotic, although the mechanism of XOS is not fully studied, the general mechanism of prebiotics to health benefits can be explained:

a) Prebiotics reduce adiposity by reducing the expression of G-protein, leading to lipolysis. Prebiotics also decrease the size of adipocytes as the large-sized adipocytes have increased levels of fatty acids, insulin resistance, and tumor necrosis factor-alpha (TNF-$\alpha$), IL-1$\beta$, and IL-6 (Chen et al., 2021a; Dewulf et al., 2011).

b) Prebiotics promote the growth and activity of gut-beneficial bacteria, which metabolize prebiotics to short-chain fatty acids (SCFA) (Figure 9). SCFA, including acetate, propionate, butyrate, and other compounds such as lactate, are known as metabolites for intestinal health. SCFA influences the cell integrity of the gastrointestinal tract (GI) tract, controls glucose homeostasis, modulation of immune function, and reduces the luminal pH to inhibit pathogenic bacteria (Chen et al., 2021a; Koh, 2016).

c) Prebiotics' role in reducing energy intake by altering satiety hormones like ghrelin, peptide YY (PYY), and Glucagon-like peptide (GLP-1), thereby resulting in decreasing weight (A. Parnell & A. Reimer, 2012).

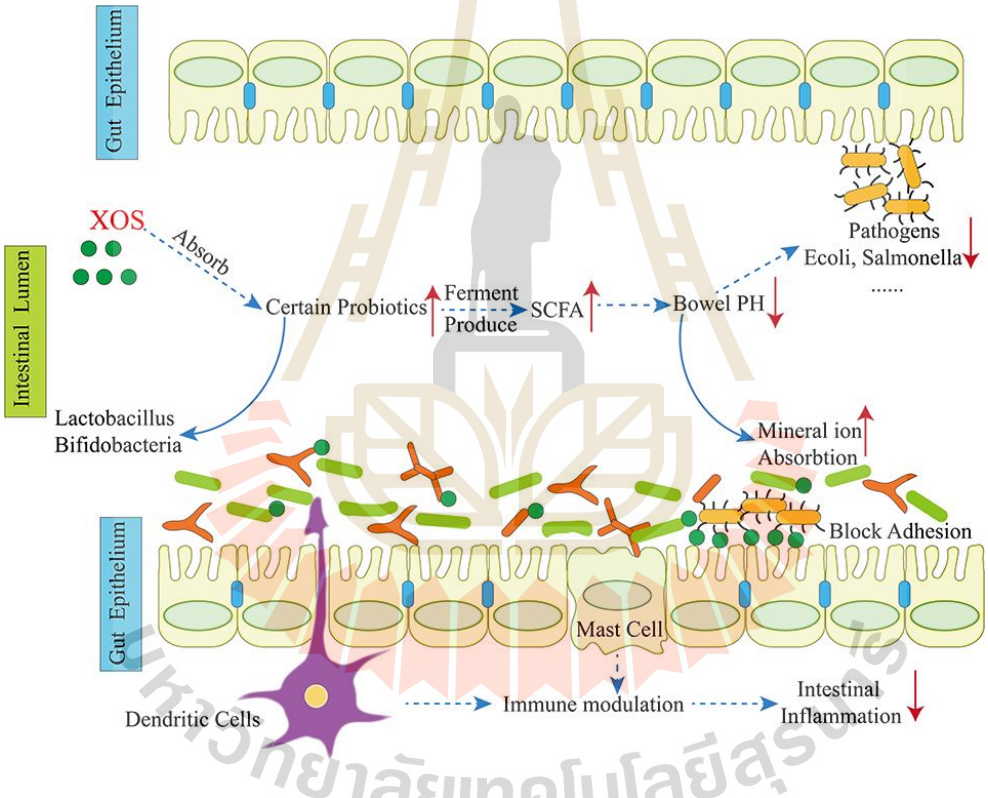


**Figure 9** Mechanism of health benefits of prebiotics (Chen et al., 2021a)

Besides the prebiotic potential, XOS demonstrate various activities in human health: immune modulation, anti-tumor, antioxidant, and anti-microbial effects. XOS can inhibit the growth of pathogenic bacteria (*Clostridium perfringens, E. coli*, and *Staphylococcus aureus* (de Freitas et al., 2019). XOS can release inflammatory mediators, and XOS is thus suggested to be an immunomodulator to prevent adverse immune-related conditions (Chen et al., 2021a; Hansen et al., 2013; hen, 2012; Lecerf et al., 2012; Nabarlatz et al., 2007). On the other hand, XOS can control the level of

cholesterol, anti-hyperlipidemic activity (L et al., 2013; Li et al., 2010); anti-allergy, anti-inflammatory (Aachary et al., 2015); anticancer (Aachary et al., 2015; Ando et al., 2004; Gupta et al., 2018; Maeda et al., 2012); anti-microbial (Hsu et al., 2004); inhibit pathogen adhesion (Ebersbach et al., 2012); antioxidant (Bouiche et al., 2020; Mohanta et al., 2022; Rashad et al., 2016; Valls et al., 2018; Yu et al., 2015); or used as a primary compound of drug for Alzheimer treatment (Maccioni et al., 2022).

The properties of XOS depend on the structure and their degree of polymerization (DP) (Brienzo, 2016). Most reports indicate that only XOS DP from X2-X6 has health benefits. In there, X2 and X3 cannot be hydrolyzed by saliva, pancreatin, gastric juice, or intestinal mucosa homogenate so that intestinal bacteria can use them (M.J. Va´zquez, 2000).

Although many reports refer to other health effects of XOS, it is nevertheless possible that the source of the substrate for XOS production determines the other functions of XOS (the composition of biomass). The prebiotic and anti-inflammatory activity of XOS will be studied in this study.

XOS characterization and quantification

*Qualitative analysis of XOS:* qualitative analyses involve the structure, molecular mass, DP, and branch chains present in XOS mixtures. The structural analysis provides information on the sequence and glycosyl linkage composition.

Nuclear Magnetic Resonance Spectroscopy (NMR) analysis determines the substituents on xylan chains such as methyl glucuronic acids (MeGlcA) (Martínez et al., 2015). It helps to understand the composition of LCB for using a suitable pretreatment method but it is hard to operate and expensive. Mass Spectroscopy (MS) analysis is used to determine the molecular mass of XOS. Fourier Transform Infrared Spectroscopy (FTIR) is a technique used to obtain information on conjugation between function groups in the XOS chain (-OH, C-O, C=O and C=C, C-O-H or C-O-C) (Jagtap et al., 2017; Khangwal & Shukla, 2022). Thin layer chromatography (TLC) determines the XOS composition (DP) and its distribution (Kumar & Satyanarayana, 2015a). TLC is a simple technique, cost-effective, and easy to operate. Ion chromatography (IC) and Size exclusion chromatography (SEC) has been used to analyze XOS's DP. Nevertheless, the disadvantage of IC is a high concentration of mobile phase (NaOH) can degrade

oligosaccharides (ZHANG et al., 2007). SEC has cons is hard to separate basic oligomers (Pu et al., 2016).

Among qualitative analysis techniques, TLC is the most frequently applied to show the elements of XOS during hydrolysis. To know the amount of each oligosaccharide, DP, and molecular weight, quantitative techniques can provide more details.

*Quantitative analysis of XOS:* the purpose of quantitative analysis is to determine the amount of different compounds in XOS, thereby, can also calculate the DP of XOS. Determination of the total amount of XOS can be done by DNS (dinitrosalicylic acid) and NS (Nelson-Somogyi) assay. Nevertheless, DNS reflects the different color responses with the different DP of XOS (DNS reagent gives a stronger color response with high DP), resulting in higher total XOS than actual. Nowadays, many modern techniques can accurately detect the amount of XOS.

The most popular technique is High-Performance Liquid Chromatography (HPLC). HPLC consists of cation-exchange columns coupled with an RI detector used for quantitative oligosaccharides (Palaniappan et al., 2021). Other monosaccharides can use Bio-Rad Aminex HPX-87H and HPX-42A HPLC columns. For determining total XOS by HPLC with Aminex HPX-87H columns, XOS must be hydrolyzed to monomers to detect and calculate based on equivalent monomers (Singh et al., 2019). HPLC with Aminex HPX-42A column is suitable to be used for oligosaccharides detection with DP lower than 6 (Akpinar et al., 2009). In our study, HPLC with Aminex HPX-42A column will be used for XOS quantitative.

The second most common technique for XOS quantification is High-Performance Anion-Exchange Chromatography with Pulsed Amperometric Detection (HPAEC-PAD). HPAEC-PAD is more selective and sensitive than HPLC, which can detect XOS with a wide DP range. Dionex columns Carbopac PA1, PA100, and PA200 in HPAEC have been used for XOS and other oligosaccharides (Palaniappan et al., 2021)

Gas chromatography (GC) also can be used for XOS quantification. However, carbohydrates have high polarity and low volatility, so XOS must be converted to volatile compounds before injecting into GC. So, this technique is not commonly used for XOS quantification.

# CHAPTER 3
# RESEARCH METHODOLOGY

## 3.1 Materials and bacteria strains

*Bacillus subtilis* strain 168 (ATCC 23857), which was used as the source of the xylanase gene (*Bs*XynA11), was purchased from the American Type Culture Collection. The bacteria were grown on Luria–Bertani (LB) agar media at 37 °C. *E. coli* DH5α (Life Technologies Co., OR, USA) and *E. coli* TOP10 (Invitrogen, Eragny, France) were used for enzyme cloning and expression, respectively. Plasmid pMAL-p5x (NEB, Ipswich, England, #N8109S) and pMY202 (Yamabhai et al., 2011) were used for the cloning and expression of MBP-*Bs*XynA11 and *Bs*XynA11-His, respectively. Xylan practical grade (CAS #9014-63-5) from Beechwood with purity >95% contains 86% xylose was purchased from Megazyme (Wicklow, Ireland). Xylooligosaccharides standard composes of xylose (X1), purchased from Sigmar-Aldrich (Darmstadt, Germany), and xylooligosaccharides (xylobiose, xylotriose, xylotetraose, xylopentaose, xylohexaose; X2–X6) from Megazyme. Seven strains of probiotics, including *Bifidobacterium longum* (Omniflora, Austria), *Lactobacillus acidophilus* DSM20079 (DSMZ), *L. amylovorus* DSM20552 (DSMZ), *L. delbrueckii* sub. *bulgaricus* DSM20081 (DSMZ), *L. gasseri* (Omniflora, Austria), *Streptococcus salivarius* DSM2059 (DSMZ), and *S. thermophilus* APC151 (isolated from yogurt), were used for prebiotic activity assay as previously described (Cuong et al., 2024). The human monocyte cell line THP-1 (Catalog #300356) was purchased from DSMZ Cell Line Services (Germany).

## 3.2 Cloning of xylanase gene from *B. sutilis* 168 into *E. coli*

To produce the recombinant xylanase from *B. subtilis* 168, the gene *Bs*xynA11 of the mature endo-1,4-β-xylanase was amplified by a PCR-based method. The primers were designed to amplify *Bs*XynA11 without the native signal peptide using the published sequence from the genomic database of *B. subtilis* 168 (NCBI accession number NC_000964.3, *XynA* regions: 2054194-2054835). For MBP-*Bs*XynA11, primers FWpMAL: 5’-GCT AGC ACA GAC TAC TGG C-3’ and RVpMAL: 5’-GCA CAG AAG CTT TTA CCA CAC TGT TAC GTT AGA AC-3’, compatible with the *XmnI* and *HindIII* (underline) cloning sites of the pMAL-p5x vector were used. For *Bs*XynA11-His, primers FWpMY: 5'-

CTG TGC AAG CTT CGG CTA GCA CAG ACT AC TGG CAA AAT TG-3' and RVpMY: 5'-GCA CAG GTC GAC CCA CAC TGT TAC GTT AGA ACT TCC AC-3' (Macrogen, Korea), compatible with the *HindIII* and *SalI* (underline) cloning sites of pMY202, were used. Templates were prepared by boiling a single colony of *B. subtilis* 168 in 100 μL of ultra-pure water for 5 min, and 20 μL was used as the template for the PCR reaction. The PCR reaction (total volume of 50 μL ) consisted of 0.3 μM of primers, 0.2 mM dNTPs, 0.02 U/μL of KOD Hot Start DNA polymerase (Sigma-Aldrich), and 10X reaction buffer. The PCR cycling conditions: initial denaturation at 95 °C for 2 min; 35 cycles of denaturation at 95 °C for 20 sec, annealing at 58 °C or 59 °C (for MBP-*Bs*XynA11 or *Bs*XynA11-His, respectively) for 10 sec, extension at 70 °C for 10 sec (Songsiriritthigul et al., 2010). The genes were then cloned into the *XmnI* and *HindIII* sites of the pMAL-p5x vector, or the *HindIII* and *SalI* sites of the pMY202 vector, such that the native signal peptide of *Bs*XynA11 was replaced by the *malE* or *OmpA* signal peptides to facilitate the secretion of the recombinant MBP-*Bs*XynA11 and *Bs*XynA11-His. The clones were screened for positive recombinants by restriction fragment analysis technique and confirmed by the Sanger DNA sequencing method (Macrogen, Korea). The xylanase 3D structure was analyzed using AlphaFold3 (AF3) model (Abramson et al., 2024).

### 3.3 Xylanase expression and purification

Terrific Broth (TB) media containing 100 μg/mL ampicillin (TB-Amp) were used to express both extracellular recombinant xylanases according to a previously published protocol with some modifications (Pechsrichuang et al., 2013). Two to five colonies of the freshly transformed *E. coli* TOP10 on LB-Amp agar with corresponding constructs were picked and grown in 2 mL TB-Amp media at 37 °C, 250 rpm overnight. The overnight cultures were pooled together, mixed well, and 1–2% (v/v) of the overnight culture were seeded into 200–400 mL of TB-Amp media. The cultures were incubated under the same conditions until the $OD_{600}$ reached 0.5–0.7 (MBP-*Bs*XynA11) or 0.8–1.0 (*Bs*XynA11-His). Subsequently, 1M isopropyl-β-D-thiogalactopyranoside (IPTG) was added to the culture broth to a final concentration of 0.2 (MBP-*Bs*XynA11) or 0.1 mM (*Bs*XynA11-His), and continued incubation for 20 h at 250 rpm at the optimal expression temperatures of 32°C for MBP-*Bs*XynA11 or 27 °C for *Bs*XynA11-His. The culture supernatants were then harvested by centrifugation at 4 °C, 4000 × g for 30 min, and kept on ice before purification.

The MBP-*Bs*XynA11 was purified according to the instruction manual of the pMAL protein fusion and purification system (NEB #E8200). The crude fusion enzyme from the supernatant was bound to amylose on the affinity resin by rotating incubation at 4 °C for 1 h. Subsequently, the amylose beads were loaded into the affinity chromatography column and washed 3 times with column buffer (20 mM Tris-HCl, 200 mM NaCl, 1 mM EDTA). The pure MBP-*Bs*XynA11 was collected by eluting with the elution buffer (column buffer containing 20 mM maltose). *Bs*XynA11-His was purified by immobilized metal affinity chromatography (IMAC) using Ni-NTA agarose (Qiagen) (Pechsrichuang et al., 2013). After incubating the crude enzyme with Ni-NTA at 4 °C for 1 h, the beads were transferred to the column and washed 3 times with wash buffer (30 mM Tris-HCl, 300 mM NaCl, 20 mM imidazole). The pure *Bs*XynA11-His was obtained by eluting with elution buffer (30 mM Tris-HCl, 300 mM NaCl, 250 mM imidazole). Both enzymes were stored at 4 °C for further analysis.

### 3.4 Enzyme activity and protein concentration assay

The xylanase activity was determined following previoulsy published method (de Queiroz Brito Cunha et al., 2018) with some modifications. Briefly, 160 µL of 1% BW xylan (w/v) was prepared in citrate phosphate buffer, pH 6.5 (0.1 M citric acid/0.2 M disodium hydrogen phosphate), and pre-incubated at 60 °C, 900 rpm in a Thermomixer Comfort (Eppendorf AG, Germany) for 30 min. Subsequently, 40 µL of the enzyme at an appropriate dilution was added to the reaction. After 5 min, the reaction was stopped by adding 200 µL of DNS (dinitro-salicylic acid) and centrifuged at 12,000 × g for 3 min to remove insoluble xylan. The supernatant was heated at 100 °C for 20 min for color development, then put on ice for 5 min. The reducing sugars released from the reaction were measured using a microplate reader (Tecan, Austria) at 540 nm. One unit (U) of xylanase activity was defined as the amount of the enzyme that releases 1 µmol of reducing sugars per minute, using D-xylose as a standard.

Protein concentration was determined by Brad-Ford (Bradford, 1976) using the Micro BCA Protein Assay Kit (#23235, Thermo Scientific, USA) and Bovine Serum Albumin (BSA) as a standard.

### 3.5 Gel electrophoresis and zymogram analysis

The Laemmli method was employed for gel electrophoresis (SDS-PAGE) using 12% (w/v) polyacrylamide gel. Protein samples were heated for 10 min in the loading

buffer at 100 °C, using a heat block (Eppendorf), then cooled on ice before loading into the gel. Visualization of protein bands was achieved through staining with Coomassie Brilliant Blue R-250 (Laemmli, 1970). All Blue Standards (Bio-rad) were used as a molecular weight marker.

For Zymogram analysis, the pure enzyme was electrophoresed on a 12% (w/v) SDS-PAGE gel containing 0.5% BW xylan. After electrophoresis, the gel was incubated in citrate-phosphate buffer (pH 6.5) at 50 °C for 1 h, followed by soaking in 2% Triton X-100 at 4 °C, 50 rpm for 1.5 h. Subsequently, the gel was stained with a 0.1% Congo red solution for 30 min, and destained twice with 1 M NaCl for 30 min each time.

## 3.6 Effect of temperature and pH on enzyme activity

The optimal temperature of xylanases was determined by incubating 0.6 μg of purified enzyme with 1% xylan solution at pH 6.5, over a temperature range from 0–80 °C in a Thermomixer for 5 min. The thermal stability of the enzymes in a buffer was investigated by incubating 1.2 μg of purified enzyme in citrate-phosphate buffer pH 6.5 at different temperatures, ranging from 4–80 °C, with shaking at 900 rpm for 30 min. The remaining enzyme activity was then measured based on the standard assay condition. The thermal inactivation kinetics of enzymes were assessed by incubating 7.0 μg of purified enzymes in 200 μL of 1% xylan in citrate-phosphate buffer pH 6.5 or buffer alone, at 40 and 50 °C, 900 rpm for various time duration (0, 1, 2, 3, 6, 12, 18, 24, 48, 72 h). Following incubation, the mixtures were diluted 2 times in a total volume of 400 μL. Then 40 μL was taken to measure the remaining activity under standard assay conditions, along with the corresponding blanks.

The pH profiles of recombinant xylanase activity were determined by incubating 40 μL (0.3 μg) of the enzyme with 160 μL of 1% xylan solution prepared in citrate-phosphate buffer (pH 2.2–8) and Tris-HCl (pH 8–10), under standard assay condition. For the pH stability analysis, 16 μg of enzymes were incubated at various pH values using citrate-phosphate buffer (pH 2.2–8) or Tris-HCl (pH 8–10) at 30 °C for 24 h. Subsequently, the reaction was diluted to 250 μL, and 40 μL (1.08 μg) was used to measure the remaining activity under standard assay conditions.

## 3.7 Enzyme kinetic

The kinetic parameters were analyzed using various BW xylan concentrations ranging from 0.5–30 mg/mL. The reaction was performed at 60 °C for 30 min. The

kinetic parameters ($V_{max}$, $K_m$, and $k_{cat}$) were calculated through nonlinear regression. The data were fitted to the Michaelis-Menten equation using GraphPad Prism 10 software (GraphPad Software Inc., USA).

## 3.8 Xylan solution preparation

BW xylan solution:

BW xylan with different concentrations was prepared by devolving the xylan powder in buffers under room temperature in a magnetic bar at 500 rpm for 30 min before use.

Sugarcane bagasse xylan (BG-xylan) solution:

The liquid part is obtained from the lignin extraction process from SCB by alkaline treatment. Alcohol 96% (1:1, v/v) was added into the liquid phase to precipitate xylan. Crude xylan was then separated by centrifuge at 4000 x g for 10 min. To remove the NaCl, the crude xylan was washed 3 times (50 mL each) with 96% ethanol and 3 times (50 mL each) of DI by vortexing, followed by centrifuging at 4000 x g for 10 min. BG-xylan was then dried at 45 °C overnight to get the solid form and stored at 4 °C for further assay.

**Figure 10.** BG-xylan preparation process


## 3.9 Xylooligosaccharide product identification by HPLC

Small-scale bioconversion of XOS was conducted in a 1.5 mL Eppendorf tube. The reaction contained various concentrations of BW xylan (1%, 2%, 4% w/v) and

enzyme concentrations (500 U, 1000 U, and 1500 U/mg) in a total reaction volume of 1 mL at 40 °C, 900 rpm. The reaction was stopped at various time points (0.5, 1, 2, 3, 6, 12, 24, and 48 h) by heat-inactivation at 100 °C for 10 min before centrifugation. The XOS profiles were determined using an HPLC system with an Aminex HPX42A column (300 x 7.8 mm with Micro-guard cartridges, Bio-rad) and a refractive index detector (Hitachi, Japan). Ten µL of filtered sample was injected into the HPLC. The column temperature was set at 80 °C with ultra-pure water as the mobile phase at a 0.6 mL/min flow rate. A mixture of xylose (X1), xylobiose (X2), xylotriose (X3), xylotetraose (X4), xylopentaose (X5), xylohexaose (X6) at concentrations ranging from from 0—5 g/L were used as the standards. The XOS bioconversion yield (%) was determined by calculating the ratio of the total amount of X2-X6 to the initial amount xylan.

### 3.10 Xylooligosaccharides product identification by TLC

TLC silica gel 60 F254 aluminum plates (Merck, Germany) were employed to analyze the XOS profiles derived from BW xylan. A 1 µL volume of hydrolyzed products was applied twice to the TLC plates, dried, and then placed into the developing tank. Separation was performed using a mobile phase comprising butanol, acetic acid, and water (2:1:1) for 2 h at room temperature (Amorim et al., 2019b). Visualization of XOS products on the TLC plates was achieved by dipping the plate into a solution containing 5% $H_2SO_4$ in ethanol and 0.05% thymol, followed by heating at 110 °C for 10 min. A mixture of X1 and XOS (X2–X6) at a concentration of 0.5 g/L was utilized as a reference.

### 3.11 Lab-scale of XOS bioconversion by MBP-*Bs*XynA11

Lab-scale production of MBPBW-XOS was conducted in a 250 mL Erlenmeyer flask containing 100 mL of 2% BW-xylan at pH 6.5. BW xylan was pre-incubated at 40 °C, with shaking at 250 rpm for 30 min before 0.42 mg purified xylanase was added. The bioconversion was continued for another 48 h under the same conditions. The reaction was stopped by heating at 100 °C for 10 min. The XOS product was recovered by centrifugation at 2,000 × g for 5 min, followed by lyophilization. The samples were kept at 4 °C for further biological activities analysis. Scanning Electron Microscopy (SEM) was used to analyze the xylan and XOS morphology.

## 3.12 Effect of XOS on probiotic growth in synthetic media

The prebiotic activity of XOS *in vitro* was studied by measuring the growth rate of bacteria in MRS media containing 2% (w/v) MBPBW-XOS. Probiotic strains were inoculated overnight in 5 mL MRS media at 37 °C under static anaerobic conditions. The cells were collected by centrifuge 4,000 × g at 4 °C for 10 min and resuspended in 0.85% normal saline to reach an $OD_{600}$ of 0.05. Subsequently, 20 µL of resuspended cells were added to 180 µL MRS media in a 96-well plate. The plates were then incubated under static anaerobic conditions at 37 °C in anaerobic jars. The growth of bacteria was monitored by measuring the absorbance of the culture broth at 600 nm using a microplate reader (Tecan, Austria) every 3 h for 24 h of incubation. The comparison was conducted by replacing 2% (w/v) glucose or inulin (Giffarine, Thailand) under the same incubation conditions. The respective media without a carbon source were used as the control. The cell density value ($OD_{600}$), prebiotic index (Kathiresan et al., 2024), and prebiotic score (Reque et al., 2019) at 24 h were used to analyze the impact of XOS with each probiotic following the formulas:

$$Prebiotic\ Index = \frac{OD600nm\ of\ probiotic\ growth\ in\ XOS\ supplemented\ media}{OD600nm\ of\ probiotic\ growth\ in\ control\ media}$$

$$Prebiotic\ Score = OD600nm\ at\ 24\ h - OD600nm\ at\ 0\ h$$

## 3.13 Effect of XOS on probiotic growth in yogurt

The yogurt production process involved heating a mixture containing 0 and 10% (w/v) sucrose in fresh cow milk from the Suranaree University of Technology Farm to 85 °C for 15 min and then cooling to 40 °C. Five percent (w/v) of yogurt (Meiji-Thailand, containing *L. delbrueckii* subsp. *bulgaricus* and *S. thermophilus*) was then thoroughly mixed. The mixture was divided into three aliquots. The first portion served as a negative control (no additional prebiotics), while 0.05% (w/v) of inulin (positive control) was added to the second, and 0.05% (w/v) of MBPBW-XOS was added to the third portion. All formulations were incubated at 42 °C for 7 h to produce yogurts. Subsequently, the yogurts were stored at 4 °C to analyze bacterial viability (CFU/g) every 7 days for 3 weeks.

### 3.14 XOS anti-inflammatory activity assay

The impact of XOS on the production of the pro-inflammatory cytokine IL-1β in human macrophages was investigated following a previously established protocol (Yamabhai et al., 2024). The THP-1 cell line was cultured in a 24-well plate with RPMI media containing 0.2 μM Vitamin D3 (Merck, Germany) for 48 h. Subsequently, cells were pre-treated with varying concentrations of MBPBW-XOS, HISBW-XOS, MBPBG-XOS, HISBG-XOS (1, 10, 50, 200, 500, and 1000 μg/mL) for 24 h or with 0.2 μg/mL dexamethasone (Sigma-Aldrich, USA) as a positive control. In the next step, 0.1 μg/mL LPS (Invivogen, USA) was added to each well and incubated for 6 h to stimulate inflammatory reactions. The supernatant was collected by centrifugation to measure the IL-1β concentration using an ELISA-based method (Human IL-1 β/IL-1F2 DuoSet ELISA, Cat #DY-201), following the manufacturer's instructions. The absorbance (OD) of the ELISA assay was determined with a microplate reader (Tecan, Austria) at a measurement wavelength of 450 nm.

### 3.15 Statistic analysis

The data were analyzed using a one-way analysis of variance (ANOVA), and the results are presented as mean ± standard deviation and Dunnett's multiple comparisons test. Statistical analysis was performed using GraphPad Prism 10 software (GraphPad Software Inc., USA). Statistical analysis was performed using GraphPad Prism 10 software (GraphPad Software Inc., USA)

# CHAPTER 4
# RESULTS AND DISCUSSION

## 4.1 Cloning, expression, and purification of xylanase

A 555 bp DNA fragment of *Bs*XynA11 encoding xylanase without its original signal peptide was isolated from the *B. subtilis* 168 genome and subcloned into different vectors pMAL-p5x and pMY202 to generate MBP-*Bs*XynA11 and *Bs*XynA11-His, respectively (Figure 11a, 11b). The *Bs*XynA11 gene was fused with corresponding signal peptides of the expression vector (*malE* in pMAL-p5x and *OmpA* in pMY202) to promote the enzyme secretion out of the cell under the control of *tac* promoter.

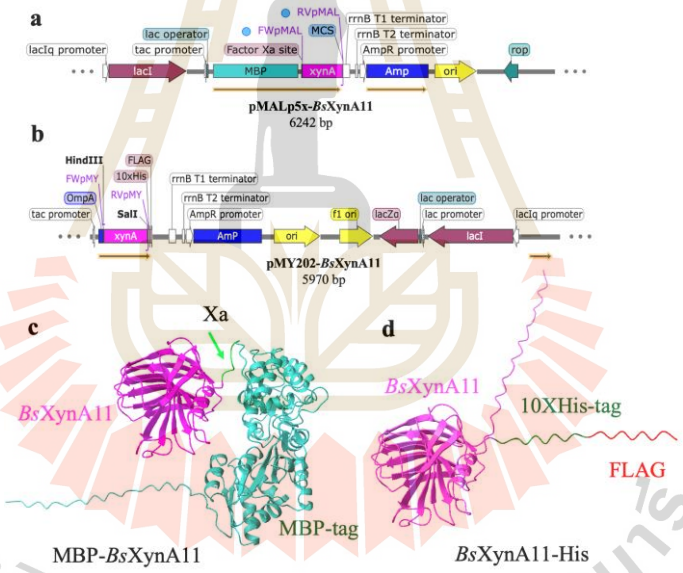


**Figure 11**. Expression and purification of recombinant MBP-*Bs*XynA11 and *Bs*XynA11-His from *B. subtilis* 168. The vector construction of MBP-*Bs*XynA11 (a) and *Bs*XynA11-His (b) was designed using SnapGene software (www.snapgene.com). The 3D prediction structure of MBP-*Bs*XynA11 (c) and *Bs*XynA11-His (d) was modeled using Alphafold3. The structure of the free xylanase completely matched that of MBP and HIS xylanase.

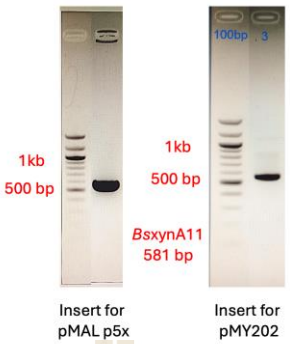


**Figure 12.** Agarose gel analysis of colony PCR reaction by KOD Hot start polymerase for preparing the insert for pMAL-p5x and pMY202

The agarose gel (Fig.12) show the expected size of the PCR product of *Bs*XynA11 without signal peptide. After that, the inserts and vectors were digested by the corresponding restriction enzyme and ligated by T4 ligase under manufactural instruction. Table 8 shows the concentration and purification degree of constructed plasmids.

**Table 8**. The mini prep result of ligation plasmid of MBP-*Bs*XynA11 and *Bs*XynA11-His

| MBP-*Bs*XynA11 | | | *Bs*XynA11-His | | |
|---|---|---|---|---|---|
| Colony | Conc. (ng/uL) | 260/280 | Colony | Conc. (ng/uL) | 260/280 |
| M1 | 96.7 | 1.86 | H1 | 65.4 | 1.81 |
| M2 | 130.6 | 1.98 | H2 | 54.7 | 1.83 |
| M3 | 174.3 | 2.04 | H3 | 76.4 | 1.85 |
| M4 | 157.8 | 2.09 | H4 | 42.1 | 1.89 |
| M5 | 87.6 | 2.01 | H5 | 82.4 | 1.87 |
| M6 | 167.9 | 2.13 | | | |
| M7 | 106.2 | 1.85 | | | |
| M8 | 91.9 | 1.87 | | | |

Before sending the plasmid to sequence, the clones were screened for positive recombinants using the restriction fragment analysis technique. MBP-*Bs*XynA11 was digested using *NheI-HF* (located on *Bs*XynA11) and *HindIII-HF* (the cloning site). *Bs*XynA11-His was cut by *HindIII-HF* and *SalI-HF* (both cloning sites). After digestion under optimal enzyme activity conditions, the products were loaded into agarose gel to check the size of the DNA. The restriction fragment analysis is shown in Figure 13.

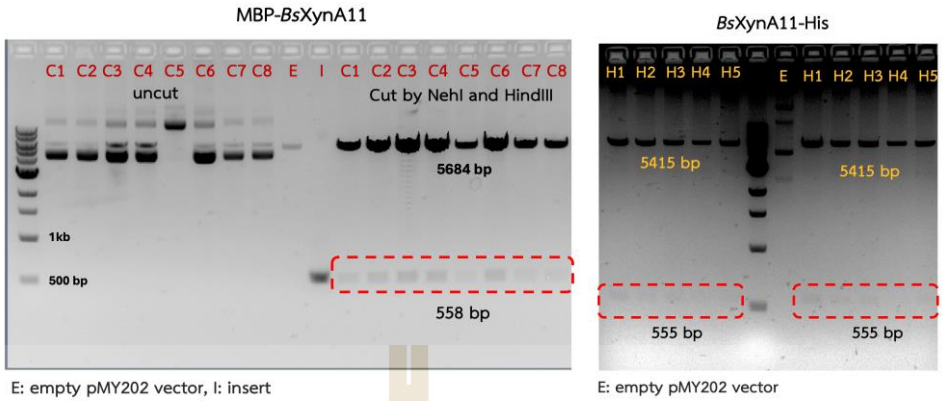


**Figure 13.** The agarose gel of restriction fragment analysis

The results of restriction fragment analysis were positive with both constructs. For MBP-*Bs*XynA11, 2 expected bands with the size of 5,600 bp and 560 bp were shown white the uncut plasmids showed the supercoiling of DNA. For *Bs*XynA11-His, 2 bands with the corresponding size were also observed at 5,400 bp and 550 bp. To confirm the results, plasmid C4 and C6 of MBP-*Bs*XynA11, and plasmid H1 and H5 of *Bs*XynA11-His were sent to sequence by Sanger DNA sequencing method.

The sequencing analysis (Figure 14, 15) shows the similar DNA sequence of both constructions compared with the original sequences designed by Snapgene.

**Figure 14.** The DNA sequencing chromatogram analysis of MBP-*Bs*XynA11

**Figure 15.** The DNA sequencing chromatogram analysis of *Bs*XynA11-His

To select the media for enzyme expression, 3 types of media (LB, TB, and Rich, see the component in Appendix 1) were used to cultivate the freshly transformed *E. coli* TOP10 colony. The result (Figure 16) shows that TB medium is the best medium for the growth of *E. coli* containing the constructs. Based on these initial results, TB media were selected for enzyme expression.

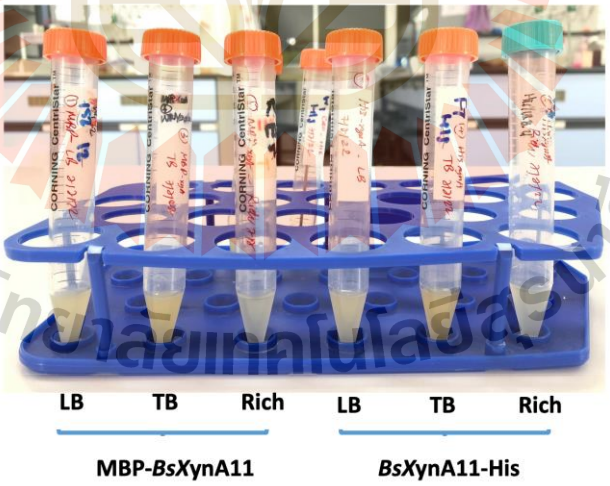


**Figure 16.** The growth of *E. coli* TOP10 carried MBP-*Bs*XynA11 and *Bs*XynA11-His xylanase in LB, TB, and Rich medium

To optimize IPGT concentration, IPTG of 0.1-1 mM was used to induce enzyme expression in 10 mL TB media at $OD_{600}$ 0.5 and continued incubation at 27 °C for 20h. The results in Figure 17 show the optimal IPTG concentration for MBP-*Bs*XynA11 expression is 0.2 mM. For *Bs*XynA11-His, 0.1 mM was chosen for safety cost, although 90% of the enzyme activity was achieved at 0.1 mM IPTG compared to 100% at 0.5 mM.

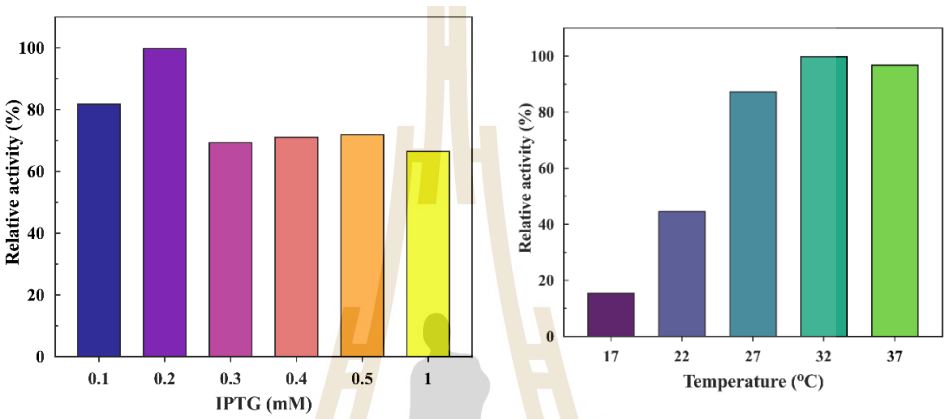


**Figure 17.** Effect of IPTG concentration on enzyme activity expression. A, MBP-*Bs*XynA11 and B, *Bs*XynA11-His

To invest the optimized temperature expression for MBP-*Bs*XynA11, after inducer, the culture was incubated at different temperature ranges from 17-37 °C for 20 h, 250 rpm. The results show that the optimal temperature for MBP xylanase expression is 32 °C with 100% relative activity compared to 95% at 37 °C and 88% at 27 °C (Figure 18).

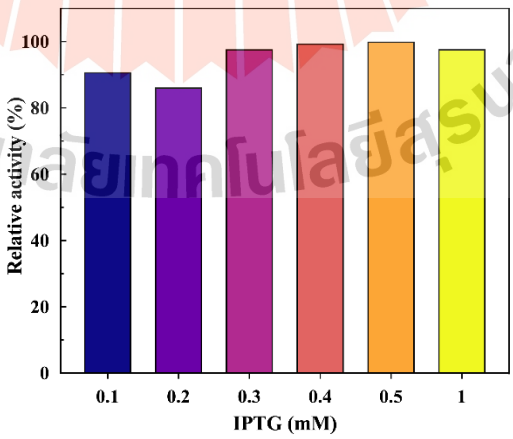


**Figure 18.** Optimize temperature for MBP-*Bs*XynA11 expression

For *Bs*XynA11-His, 2 different temperatures (27 °C and 32 °C) and OD inducer points (0.5 and 0.7) were used to compare the enzyme expression. The results show that a higher OD inducer point (0.7) and lower temperature (27 °C) are good conditions for *Bs*XynA11-His expression. The relative activity is 3 times higher than enzyme expression at OD 0.5 and 32 °C.

The MBP-*Bs*XynA11/ *Bs*XynA11-His could be overexpressed after induction with 0.2/0.1 mM IPTG after 20 h at 32/27 °C. Under these optimal conditions, $14 \times 10^6$ U (MBP-*Bs*XynA11) and $8.6 \times 10^6$ U (*Bs*XynA11-His) of total activity was obtained from 1 liter of culture. After the purification, 44.6 mg of purified MBP-*Bs*XynA11 was obtained from 1-liter media, eight times higher than 5.5 mg per 1-liter of *Bs*XynA11-His. At the same amount of purified enzyme, *Bs*XynA11-His shows the specific activity at 4,800 U/nmol protein, MBP-*Bs*XynA11 shows 7,900 U/nmol protein compared with 3,800 U/nmol of commercial xylanase from *Trichoderma reesei* (Figure 19). It is the highest enzyme activity from *B. subtilis* sp. have been reported to date. Differences in expression efficiency and enzyme activity may be due to variations in the media and conditions for enzyme expression, the host, or the methods used to analyze enzyme activity, such as different substrates, buffers, temperatures, times, or standards. Different xylanase activities have been reported include 436.5 U/mL from *B. subtilis* Lucky9 expressed by *E. coli* BL21 (Chang et al., 2017a) and 490.58 U/mL from *B. subtilis* ARSE2 (El-Gendi et al., 2023); 8,873.07 IU/mL from *B. australimaris* KS2 (Kumari et al., 2023); 3067.68 U/mg from *B. velezensis* expressed by *E. coli* DE3 (Zhang et al., 2023); 6,576.96 U/mg from B. *altitudinis* XYL17 (Phukon et al., 2024). In this study, *E. coli* was chosen for recombinant xylanase production due to its ease of genetic manipulation, rapid growth in inexpensive media, ability to secrete proteins with high yield, and the simple purification process that can be applied on a large scale (Ahmadi et al., 2023). MBP and HIS xylanase are secreted by the Sec pathway, which includes the *malE* and *OmpA* signal peptides. *OmpA* has been shown to have higher protein secretion efficiency than native signal peptide (Pechsrichuang et al., 2016). Meanwhile, *malE* has the advantage of not only providing a targeting signal but also stabilizing proteins (Singh et al., 2013).

Figure 19a shows the specific protein bands on SDS-PAGE gel after purification observed by Coomassie blue staining corresponding with approx. size of MBP-*Bs*XynA11 66 kDa and *Bs*XynA11-His 23 kDa. On the Zymogram gel (Figure 19b), the band of

*Bs*XynA11-His could not move to the correct MW position. However, it could be seen that xylan was hydrolyzed in the upper part of the gel, showing the enzyme activity. It could be due to the influence of high temperature (50 °C) for a long time (1 h) during the incubation step that reduced the activity of *Bs*XynA11-His. MW of MBP-*Bs*XynA11 fused with MBP 42.5 kDa (Schubeis et al., 2021) is higher three times than *Bs*XynA11-His. To confirm the fusion, Factor Xa protease (NEB #P8010) was used to cleave MBP-*Bs*XynA11 (Figure 20). The result shows that MBP-*Bs*XynA11 was cleaved into 2 parst: MBP (43 kDa) and *Bs*XynA11 (~20 kDa).

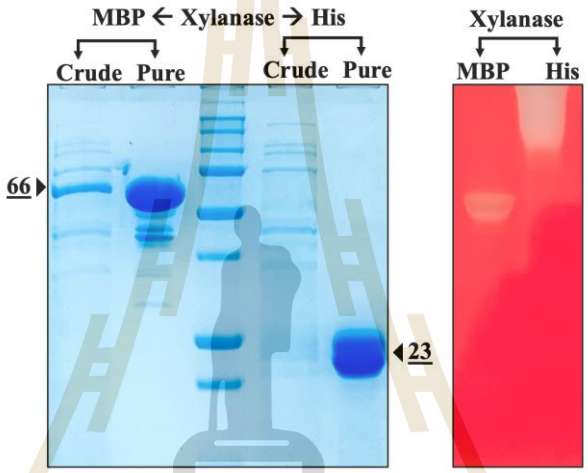


**Figure 19.** SDS-PAGE and Zymogram analysis of crude and pure MBP-*Bs*XynA11 and *Bs*XynA11-His with corresponding approx. size 66 and 23 kDa. On SDS-PAGE gel, 20µL of the crude enzyme was loaded, whereas 5µL and 15µL of pure MBP-*Bs*XynA11 and *Bs*XynA11-His were loaded.

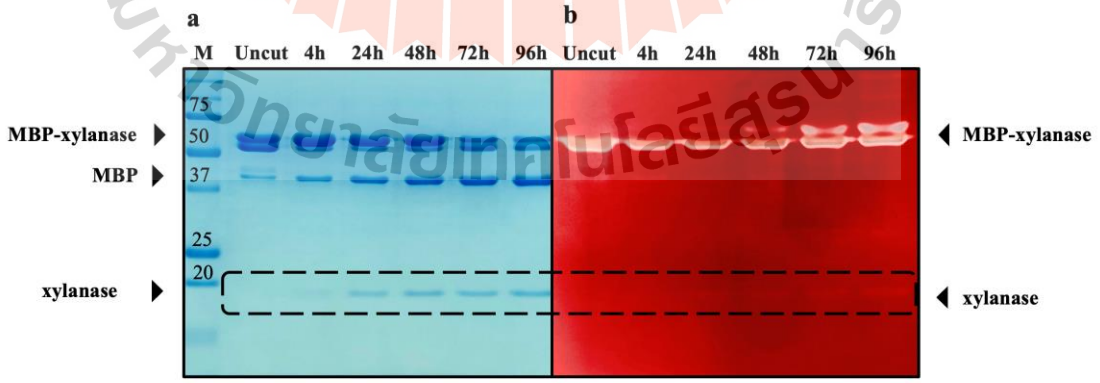


**Figure 20.** SDS-PAGE (a) and zymogram (b) assay of MBP-*Bs*XynA11 cleaved by Xa factor. The MBP-*Bs*XynA11 (66 kDa) was cleaved into MBP (43 kDa) and free xylanase (~20 kDa). The reaction was conducted using 1% (w/w) Xa in 100

μL of MBP-*Bs*XynA11 (1.45 mg/mL) at 37 °C for 96 h. For SDS-PAGE and the zymogram, a 5 μL mixture of enzyme and dye was loaded.

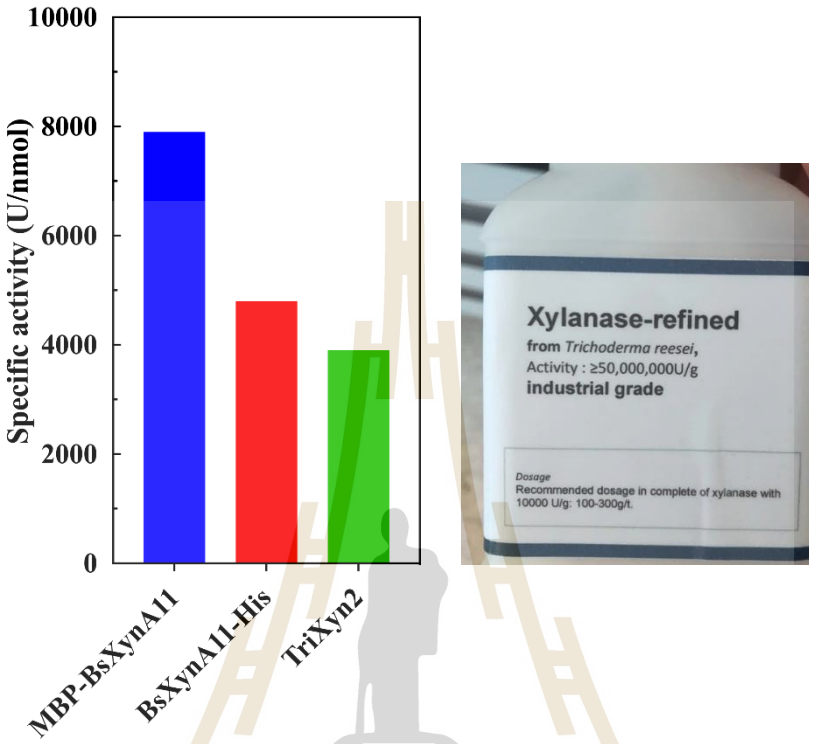


**Figure 21.** The specific activity comparison of MBP-*Bs*XynA11, *Bs*XynA11-His and TriXyn2 from *Tri. reesei* by standard condition assay

To enhance the efficiency and purity of hydrolyzed products, xylanase has been purified using the corresponding affinity chromatography method. Immobilized Metal Affinity Chromatography (IMAC) is a widely used method for purifying proteins with His-tags. IMAC columns contain agarose resins bonded to nickel via a nitrilotriacetic acid (NTA) linkage. The $Ni^{2+}$ ion, an intermediate metal, binds to the histidine residues in the polyhistidine tag of proteins. This method offers advantages such as ease of use, safety, and suitability for industrial applications. However, it also has drawbacks, including high cost and a lack of specificity for histidine-containing proteins (Hajihassan et al., 2024). While His is an affinity tag, MBP (Maltose-Binding Protein) is an affinity and solubility domain tag. MBP has a two-domain globular structure separated by a groove that contains a tightly bound ligand-binding site for maltose/maltodextrin. The rapid folding into the secondary structure, regulated by the signal peptide, contributes to the enhanced thermal stability of the mature protein (Beena et al., 2004). MBP can increase expression levels, simplify purification, enhance solubility, and stability, and

does not promote aggregation of the fusion protein (Lénon et al., 2021; Mahmoudi Gomari et al., 2020; Reuten et al., 2016). Therefore, MBP is also widely used in the expression and purification of proteins from *E. coli*.

## 4.2 Effect of temperatures and pH on enzyme catalytic activity and stability

Under standard conditions, both MBP-*Bs*XynA11 and *Bs*XynA11-His from *B. subtillis* 168 show the optimal temperature for catalytic activity at 60 °C (Figure 22a, d, red solid line). In citrate phosphate buffer pH 6.5, MBP-*Bs*XynA11 is more stable with 92% remaining activity compared to *Bs*XynA11-His with 72% after incubation at 50 °C for 30 min. The stability of xylanase with the substrate under the same conditions as above was also evaluated after incubation with 10 g/L xylooligosaccharides (X1-X6) or 1% xylan (Figure 23). The results showed that a higher degree of polymerization (DP) substrates can better protect the enzyme from thermal inactivation.

Thermal inactivation experiments provided more details about the stability of xylanases with or without substrate, as shown in Figure 22c and 22f. At 40 °C, pH 6.5 for 72 h, with substrate, MBP-*Bs*XynA11 (green solid line) was more stable than *Bs*XynA11-His (purple dashed line), with 76.5% compared to 65.5% remaining activity. The same trend was observed without the substrate, where MBP-xylanase (green dashed line) was 35 times more stable than *Bs*XynA11-His (purple dashed line), with 81% compared to 2.3% remaining activity. At 50 °C, MBP-*Bs*XynA11 showed greater thermal stability than *Bs*XynA11-His. With substrate, MBP-*Bs*XynA11 (orange solid line) retained 58.5% activity, 5.5 times higher than MBP-*Bs*XynA11 (ruby solid line), which retained only 10.7%. Without the substrate, MBP-*Bs*XynA11 (orange dashed line) retained 22.5% activity, compared to just 1.6% for *Bs*XynA11-His (ruby dashed line), showing a 14-fold difference. From these results, we can confirm that MBP-*Bs*XynA11 is more stable than *Bs*XynA11-His under the same conditions. The notable exception is at 40 °C, where MBP-*Bs*XynA11 shows no difference in stability with or without the presence of substrate. Under other conditions, both enzymes exhibit higher stability in substrate.

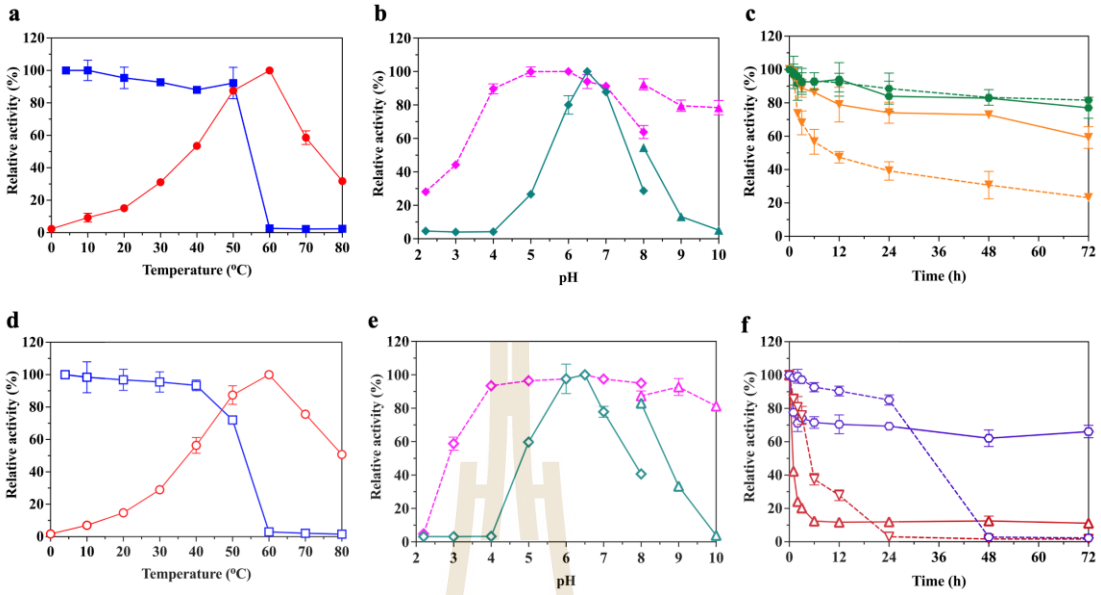


**Figure 22.** The effect of temperature and pH on MBP-*Bs*XynA11 and *Bs*XynA11-His activity and stability with/without substrate. The effect of temperature and pH on activity (red and sapphire lines) and stability (blue and pink lines) of MBP-*Bs*XynA11 (a, b) and *Bs*XynA11-His (d, e) was examined. The optimal temperature was determined using 1% BW xylan in citrate-phosphate buffer at pH 6.5. Thermal stability was assessed by measuring the remaining activity after incubation in citrate buffer at pH 6.5 for 30 min, using the standard assay. The optimal pH was determined at 60 °C using 1% BW. pH stability was evaluated by measuring the remaining activity after incubation at various pH values at 30 °C for 24 h. The buffers used were citrate-phosphate buffer (diamond) from pH 2.2—8.0, and Tris-HCl buffer (triangle) from pH 8.0—10. Thermal inactivation of MBP-*Bs*XynA11 (c) and *Bs*XynA11-His (f) with substrate (solid line) and without substrate (dashed line) was assessed by measuring the remaining activity after incubation at 40 °C (circle) or 50 °C (triangle) in citrate buffer for 0–72 h.

The optimal pH for both *B. subtilis* 168 recombinant xylanases was 6.5 in citrate phosphate buffer. At pH 8, both enzymes exhibited higher activity in Tris-HCl buffer than in citrate phosphate buffer (Figure 22b, e, sapphire solid line). The reason for this could be the effect of a high concentration of $Na^+$ ions in citrate phosphate buffer at pH 8. Notably, the activity of the xylanases remained stable between pH 4 and 10 after

incubation at 30 °C for 24 h in both Citrate phosphate and Tris-HCl buffers, with more than 80% of activity retained (Figure 22b, e, pink dashed line).

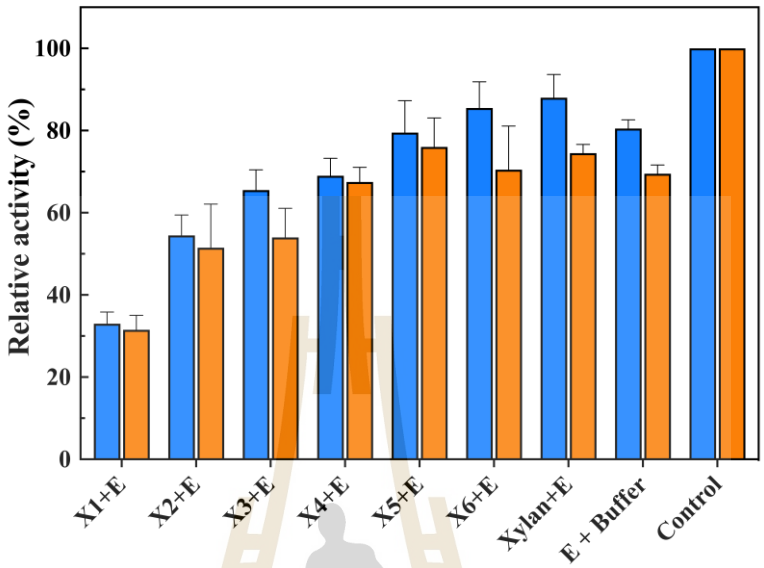


**Figure 23.** Thermal stability of MBP-*Bs*XynA11 and *Bs*XynA11-His in the presence of substrate. The remaining enzyme activity was measured after incubating the enzyme with 10 g/L XOS (X1–X6) or 1% BW at 50°C, pH 6.5 for 30 min, compared with the control, where the enzyme was kept at 4°C.

Table 9 summarizes the characteristics of MBP-*Bs*XynA11 and *Bs*XynA11-His in terms of expression, purification, optimal activity conditions, and stability. The optimal activity conditions and stability of MBP and HIS xylanase are quite similar to the xylanase from *B. subtilis* reported in previous studies. NS-*xyn*LC9 from *B. subtilis* Lucky9 showed optimal activity at pH 6.5 and 60 °C. It exhibited 80% residual activity in the pH range of 6.0–9.0 for 24 h and retained 60% of its activity at 60 °C after 2 h (Chang et al., 2017a). *Ba*xyl11 from *B. agaradhaerens* showed maximal activity at 60 °C and pH 8.0–8.5, retaining more than 60% of its activity at 70 °C after 4 h of incubation (Liu et al., 2022). *Bs*xyn10 from *B. safensis* had optimal activity at 60 °C and pH 7.0, with a half-life ($\tau_{1/2}$) of 315 minutes at 50 °C and 25 minutes at 60 °C. It retained more than 60% of its residual activity at pH 5.0–8.0 at 4 °C for 24 h (Glekas et al., 2022). Similarly, rXynT6 from *B. sonorensis* T6 had an optimal pH of 7.0 but a lower optimal temperature of 55 °C. It showed high pH stability with 100% activity after 10 h in the pH range of 3–11 and 68% after 1 h at pH 2.0 (Kiribayeva et al., 2022). Meanwhile, rational mutagenesis strategies can improve the thermostability and alkaline tolerance

of xylanase. The mutant Xyn30Y5 from *Bacillus* sp. 30Y5 had optimal activity at 70 °C and pH 8.0, and it maintained stability at pH 6.0–10 after incubation at 37 °C for 12 h with over 80% residual activity (Lai et al., 2021). The mutant *Bh*S7Xy from *B. halodurans* S7 exhibited optimal activity at 70 °C and pH 9.0, with a $\tau_{1/2}$ of 383 min (Zhou et al., 2024). Based on these results and discussions, it can be indicated that xylanase from various *Bacillus* sp. strains have quite similar optimal temperature and pH for enzyme activity. They are thermostable and can function across a wide pH range, offering advantages for the application of xylanase in various hydrolytic environments in industry.

**Table 9.** Summary of the characteristics of MBP-*Bs*XynA11 and *Bs*XynA11-His

| Characterictics \ Enzyme | MBP-*Bs*XynA11 | ***Bs*XynA11 -His** |
|---|---|---|
| **Optimal expression conditions** | | |
| Temperature (°C) | 32 | 27 |
| IPTG concentration (mM) | 0.2 | 0.1 |
| Time (h) | 20 | 20 |
| Expression yield (mg xylanase.L$^{-1}$ culture)[a] | 44.6 (0.68 mmol.L$^{-1}$) | 5.5 (0.24 mmol.L$^{-1}$) |
| Molecular weight (kDa) | 66 | 23 |
| **Optimal activity conditions** | | |
| Temperature (°C) | 60 | 60 |
| pH | 6.5 | 6.5 |
| **Enzyme activity** | | |
| Volumetric activity of crude xylanase (U.mL$^{-1}$)[b] | $14 \times 10^6$ | $8.6 \times 10^6$ |
| Specific activity of pure xylanase (U.nmol$^{-1}$)[b] | 7,900 ± 430<br>120,000 ± 6,500 (U/mg) | 4,800 ± 28<br>210,000 ± 1,200 (U/mg) |
| **Stability (remaining activity %)** | | |
| At 40 °C for 72h | | |
| With substrate | 76.5 | 65.5 |
| Without substrate | 81 | 2.3 |
| At 50 °C for 72h | | |
| With substrate | 58.5 | 10.7 |
| Without substrate | 22.5 | 1.6 |

[a]The Lowry method measured the protein concentration using BSA as the standard.

[b] Activity was measured in citrate phosphate buffer pH 6.5 at 60 °C for 5 min using 1% (w/v) BW xylan by DNS method.

## 4.3 Enzyme kinetic

The kinetic parameters, *Km, Vmax*, and *kcat*, for MBP and HIS xylanases were assessed using BW xylan as the substrate. The *Vmax* and *kcat* values for MBP-*Bs*XynA11 were higher than those for *Bs*XynA11-His, indicating a faster reaction rate for the former. However, the *Km* value for MBP-*Bs*XynA11 was also higher, suggesting a lower affinity and efficiency of MBP-*Bs*XynA11 with substrate compared to *Bs*XynA11-His. A comparison of the kinetic parameters of MBP and HIS xylanases with those from other sources is presented in Table 10

**Table 10.** Optimal activity conditions and kinetic parameters of MBP-*Bs*XynA11 and *Bs*XynA11-His compared with other sources

| Xylanase | Sources of enzyme | Optimal activity | | Enzyme kinetic | | | References |
|---|---|---|---|---|---|---|---|
| | | Temperature (°C) | pH | $V_{max}$ | $K_m$ ($mg.mL^{-1}$) | $k_{cat}$ ($s^{-1}$) | |
| *endo*-β-1,4-MBP-*Bs*XynA11 | B. subtilis 168 (expressed in *E. coli* TOP10) | 60 | 6.5 | 4,530 ($\mu mol.min^{-1}.nmol^{-1}$) | 19.3 | 5,976 | This study |
| *endo*-β-1,4-*Bs*XynA11-His | B. subtilis 168 (expressed in *E. coli* TOP10) | 60 | 6.5 | 3,470 ($\mu mol.min^{-1}.nmol^{-1}$) | 12.9 | 4,788 | This study |
| Xylanase (Intrustrial grade) | T. reesei | ND | ND | 2,150 ($\mu mol.min^{-1}.nmol^{-1}$) | 10.15 | 2,524 | Comparison, *this study* |
| *endo*-β-1,4-xylanase | Bacillus sp. 30Y5 (expressed in *E. coli* BL21) | 70 | 8.0 | ND | 1.4 ($g.L^{-1}$) | 783.2 ($s^{-1}$) | (Lai et al., 2021) |
| *endo*-β-1,4-xylanase | B. agaradhaerens (expressed in *E. coli* BL21) | 60 | 8.0-8.5 | 44.2 ($\mu M.s^{-1}$) | 10.9 ($g.L^{-1}$) | 599 ($s^{-1}$) | (Liu et al., 2022) |
| *endo*-β-1,4-xylanase | B. safensis (expressed in *E. coli* BL21) | 60 | 7.0 | 58.6 ($\mu mole.min^{-1}$) | 1.96 ($g.L^{-1}$) | 49 ($s^{-1}$) | (Glekas et al., 2022) |
| *endo*-β-1,4-xylanase | B. sonorensis T6 (expressed in *P. pastoris* X-33) | 55 | 7.0 | 667.9 ($U.mg^{-1}$) | 3.0 | 100 ($s^{-1}$) | (Kiribayeva et al., 2022) |
| *endo*-β-1,4-xylanase | B. subtilis ARSE2 | 50-60 | 8.0-9.0 | 1,481.5 ($U.mL^{-1}$) | 0.187 (mM) | ND | (El-Gendi et al., 2023) |
| *endo*-β-1,4-xylanase | B. subtilis subsp. *subtilis* JJBS250 | 60 | 7.0 | 23.92 ($U.mL^{-1}$) | 1.62 | ND | (Alokika et al., 2023) |
| *endo*xylanase | B. velezensis (expressed in *E. coli* DE3) | 50 | 6.0 | 3,067.68 ($U.mg^{-1}$) | 1.45 ($g.L^{-1}$) | ND | (Zhang et al., 2023) |
| *endo*-β-1,4-xylanase | B. halodurans S7 (expressed in *E. coli* BL21) | 70 | 9.0 | 41.9 ($\mu mol.min^{-1}.mg^{-1}$) | 32.1 (mM) | 185.9 ($s^{-1}$) | (Zhou et al., 2024) |

## 4.4 XOS bioconversion and product identification

Based on the characteristics of xylanases that have been explored, XOS bioconversion using xylanases was performed at 40 °C in citrate phosphate buffer pH 6.5. The reaction was monitored for 48 h with varying BW xylan concentrations (1–4%), enzyme doses (500–1500 U), and a reaction volume of 1 mL. The XOS composition and conversion yield were qualitative and quantitative using TLC and HPLC (Figure 24). In Figure 22a-b, all reactions demonstrated the effectiveness of both xylanases in converting XOS from BW xylan compared to the control (B-blank). TLC showed an increase in XOS content and a decrease in the DP of xylan from 1–48 h. This indicates that xylanase cleaved the β-1,4-xylosidic bonds of the xylan backbone, resulting in low molecular weight products. Qualitative analysis by TLC also revealed a trace amount of X1 produced as the hydrolysis time was extended. X1 is an undesirable product in this case since the goal is to produce oligomers with biological activities. Therefore, the hydrolysis time plays an important role in the yield and composition of products. Notably, increasing the substrate and enzyme concentrations led to an increase in the amount of product obtained. However, this does not necessarily mean that the hydrolysis yield will increase.

The hydrolysis yield under different substrate and enzyme conditions is shown in Figure 24c-d. At 1% xylan, increasing the enzyme dose from 500 to 1500 U/mL increased the XOS yield from 58.24% to 87.91% for MBP-*Bs*XynA11 and from 59.58% to 71.49% for *Bs*XynA11-His. Interestingly, at xylan concentrations of 2–4%, increasing the enzyme dosage did not improve the XOS yield. Similarly, with the same enzyme dosage, increasing the substrate concentration did not necessarily lead to increased product yield.

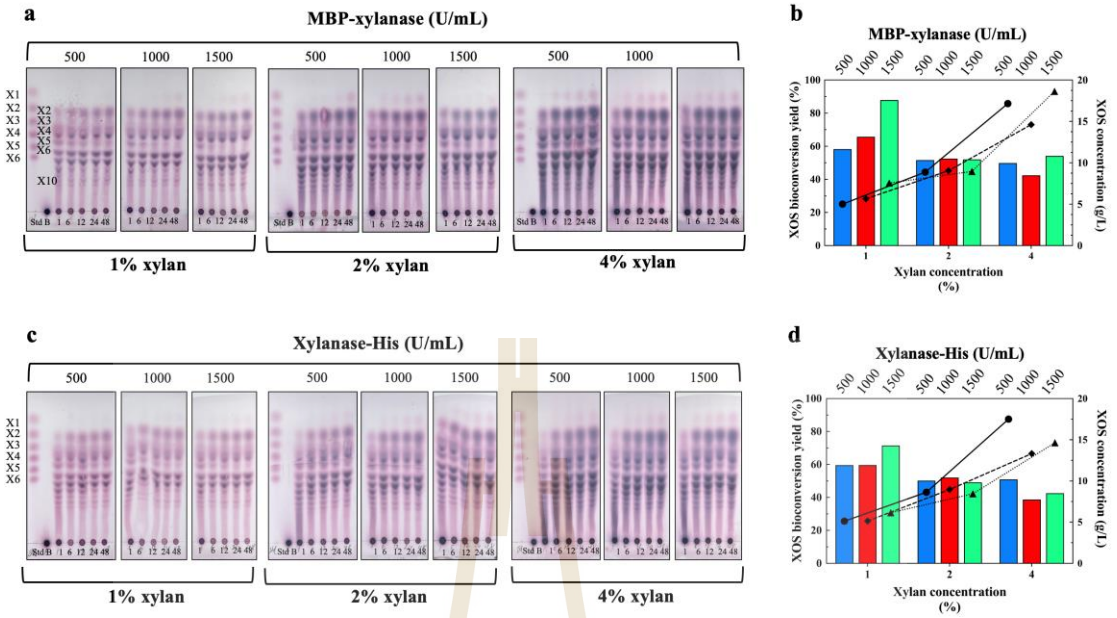


**Figure 24.** Identification of XOS release from BW xylan using MBP-*Bs*XynA11 and *Bs*XynA11-His. Thin layer chromatography (TLC) analysis was performed at varying xylan concentrations (1-4% w/v) and enzyme doses (500-1500 U/mL reaction) for MBP-*Bs*XynA11 (a) and *Bs*XynA11-His (c). The yield (%) and concentration (g/L) of XOS were quantified by high-performance liquid chromatography (HPLC) using mixture of xylose (X1), xylobiose (X2), xylotriose (X3), xylotetraose (X4), xylopentaose (X5), and xylohexaose (X6) as standards (0-5 g/L). Reactions were conducted at 40 °C, 900 rpm in citrate phosphate buffer (pH 6.5) for 48 h.

The composition of oligomers in XOS was also reported, with the main products being X2, X3, and X4, which accounted for over 90% (Figure 25). The biological activity of XOS depends on its DP, where DP 2–6 has potential health benefits (Saini et al., 2022). Reports indicate that X2 and X3 are oligomers that cannot be hydrolyzed by saliva, pancreatin, gastric juice, or intestinal mucosa homogenate, allowing intestinal bacteria to utilize them (Vazquez et al., 2000). X2 and X3 have been reported as the main products of xylan degradation by xylanase, with X2 exhibiting the highest prebiotic activity in promoting the proliferation of *Bifidobacterium* (Sukri & Mimi Sakinah, 2018). Based on these results, we propose that the hydrolysis process be carried out with a xylan concentration of 2% and an enzyme dosage of 500 U/mL to optimize yield and product quantity with a low enzyme dosage. The hydrolysis reaction was conducted at 40 °C, pH 6.5 in citrate phosphate buffer for 48 h. Under

these conditions, the XOS yield by MBP-*Bs*XynA11 and *Bs*XynA11-His reached 51.59% and 50.18% reducing sugar, respectively.

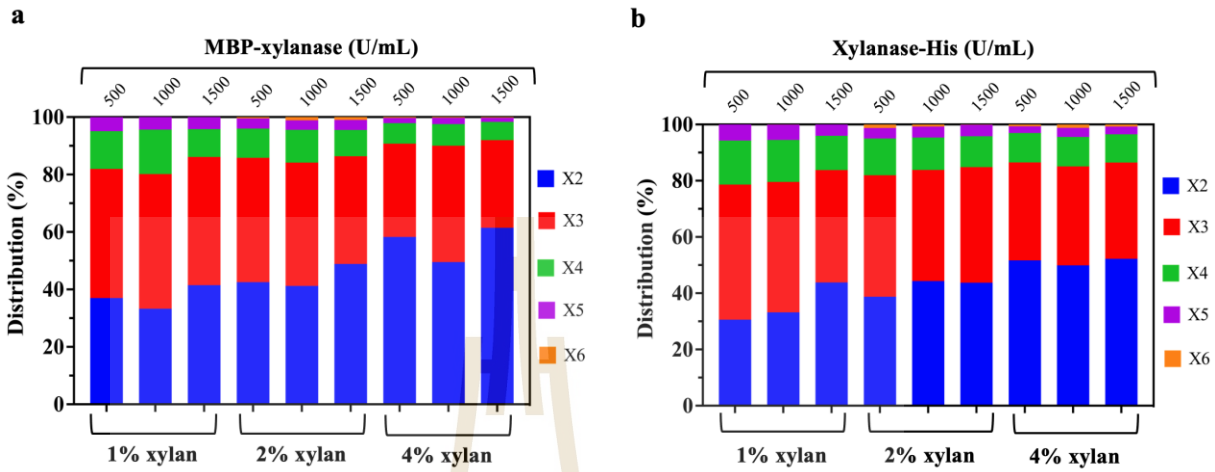


**Figure 25.** Composition of XOS released from BW xylan using MBP-*Bs*XynA11 and *Bs*XynA11-His under different conditions. Reactions were conducted with varying xylan concentrations (1–4% w/v) and enzyme doses (500–1500 U/mL) for MBP-*Bs*XynA11 (a) and *Bs*XynA11-His (b) at 40 °C and 900 rpm in citrate phosphate buffer (pH 6.5). XOS distribution after 48 h was quantified by high-performance liquid chromatography (HPLC) using mixture of xylose (X1), xylobiose (X2), xylotriose (X3), xylotetraose (X4), xylopentaose (X5), and xylohexaose (X6) as standards (0–5 g/L).

## 4.5 Lab-scale of XOS bioconversion

To prepare XOS for assessing biological activity, MBP-*Bs*XynA11 was used to perform the BW xylan hydrolysis reaction. Lab-scale production of XOS was carried out in 100 mL with 2% xylan and 0.42 mg MBP-*Bs*XynA11 at 40 °C, 250 rpm, pH 6.5 for 48 h. After hydrolysis, XOS was recovered by centrifugation at 2,000 × g for 10 min to remove the insoluble part and then lyophilized. XOS was stored at 4 °C for further analysis of biological activity. Figure 26a-b illustrates the molecular structure of xylan in polymer form with β-1,4-xylosidic bonds and XOS in oligomer form with xylose units ranging from 2–6 after enzymatic hydrolysis. The changes in surface morphology of xylan and XOS before and after hydrolysis were also analyzed using SEM (Figure 27). The SEM images of xylan before hydrolysis show a flat, smooth surface (Figure 27a, b). In contrast, the surface of XOS is rough and heterogeneous (Figure 27c), indicating the action of xylanase in xylan degradation. Similar results were observed for the hydrolysis

of wheat bran-extracted xylan by xylanase from *B. australimaris* KS2. The untreated samples exhibited a rough, flaky morphology, while after treatment with xylanase, the cell wall structure was disrupted. The breakdown of cross-links between cellulose and hemicellulose led to the solubilization of hemicellulose, resulting in a change in morphology compared to the original structure (Kumari et al., 2023). Figure 26c shows the qualitative analysis of XOS using TLC, illustrating the change in XOS composition over time. The product composition was analyzed by HPLC (Figure 26d). The HPLC chromatographic peaks represent individual components of xylobiose (X2, 13.6 min), xylotriose (X3, 12.0 min), xylotetraose (X4, 10.8 min), xylopentaose (X5, 9.8 min), xylohexaose (X6, 9.0 min), and a trace amount of xylose (X1, 15.6 min). Notably, a part of XOS with DP > 6 that has not been quantified will not be counted towards the hydrolysis yield but will still be considered part of the product composition. After centrifugation to remove insoluble residue and subsequent freeze-drying, the product recovery yield based on weight reached 890 mg/g.

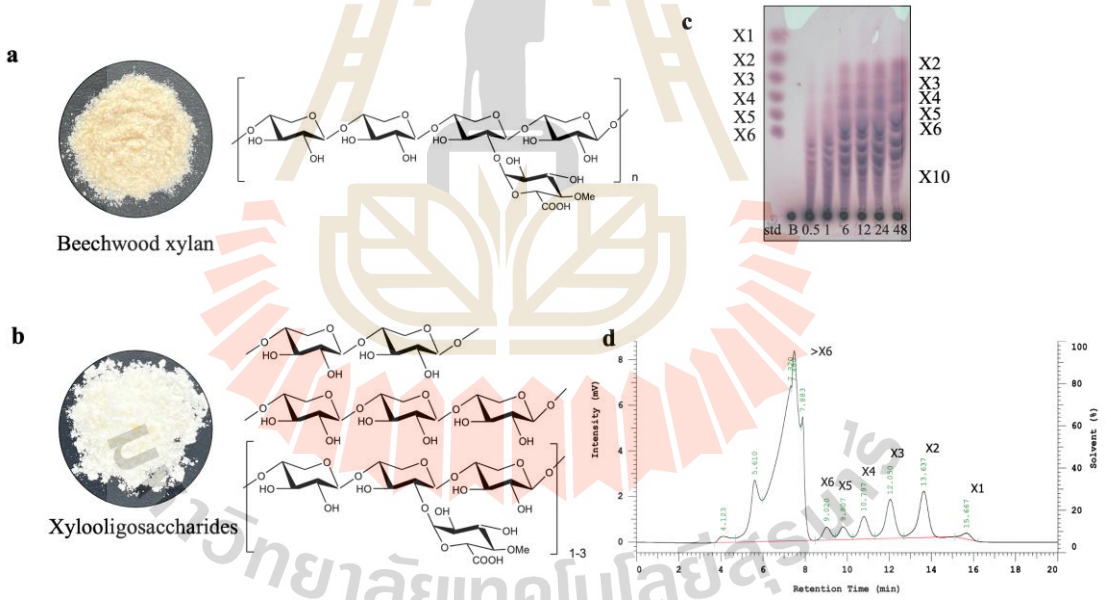


**Figure 26.** Lab-scale bioconversion of XOS from BW xylan by MBP-*Bs*XynA11. The powder and chemical structure of BW xylan (a) and the XOS product after hydrolysis and lyophilization (b); TLC plate (c) and HPLC chromatogram (d) analysis of the XOS product. The lab-scale bioconversion of XOS was conducted using 2% xylan, 500 U/mL, at 250 rpm and 40℃ for 48 h. Xylose, xylobiose, xylotriose, xylotetraose, xylopentaose, and xylohexaose were used for TLC and HPLC standards.

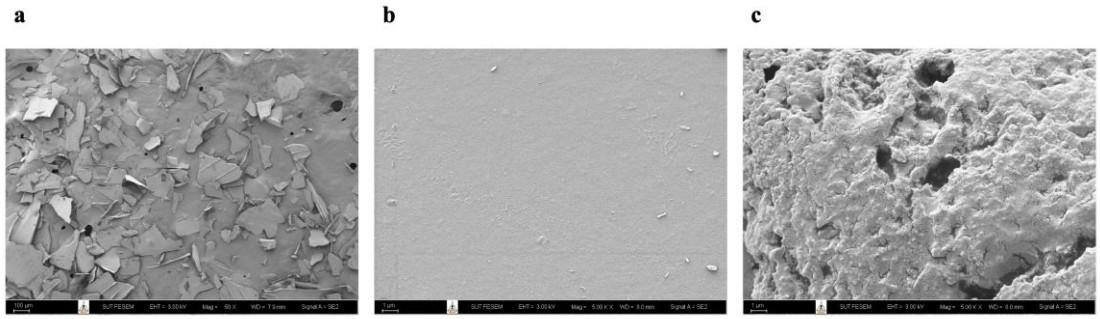


**Figure 27.** SEM analysis of BW xylan at 50× magnification (a) and 5000× magnification (b), and XOS at 5000× (c) magnification after hydrolysis and lyophilization.

The composition and yield of XOS are influenced by various factors, including hydrolysis conditions (temperature, pH, duration), xylanase dosage, and the xylan source. The yield and composition of XOS are specifically impacted by the xylan source, making it necessary to optimize XOS composition for each substrate independently (Gufe et al., 2022). For instance, hydrolysis conducted at 60 °C and pH 7.0 for 24 h using 2% BG-xylan resulted in a total XOS yield of 449 mg/g, with 90% of the products being X2 and X3 (Tseng et al., 2022). Hydrothermal pre-treatment followed by *endo*xylanase hydrolysis of poplar xylan produced 446 mg/g of XOS (DP 2–6), with 78.7% comprising X2 and X3 (Su et al., 2021). In another study, rice straw xylan pre-treat with sodium carbonate followed by enzymatic hydrolysis using 20 U/g of xylanase at 60 °C and pH 7.0 for 48 h yielded 151.65 mg/g XOS with DP 2–6 (Alokika et al., 2023). Rice husks hydrolyzed by 3,000 U/g of xylanase at 50 °C for 3 h yielded 150.9 mg/g XOS (Tian et al., 2024). Despite xylose being an unwanted byproduct, is still generated during enzymatic hydrolysis. A yield of 5.3 mg/mL XOS, consisting of 23.1% X1, 37.3% X2, and 39.6% X3, was obtained from 10% (w/v) wheat bran xylan (Liu et al., 2022). Under hydrolysis conditions of 55 °C, pH 6, and 375 U of xylanase after 16 h, wheat bran xylan yielded 588 mg/g XOS, with X2, X3, and X5 as the predominant products (Kumari et al., 2023). The composition of XOS derived from various agro-waste xylan sources using xylanase has been previously studied, revealing that X5 is the major component from rice straw xylan, X4 dominates in BG-xylan, and X3 is prominent in BW xylan but absent in rice straw, corncob, and BG-xylan (Phukon et al., 2024).

Variations in xylan sources result in different yields and compositions of XOS, which in turn affect their biological activities. In this study, the main components of

XOS are X2–4 (>90%), considered oligomers with high biological activity. The next section will evaluate the biological activity of XOS from BW or BG xylan hydrolyzed by MBP-*Bs*XynA11 and *Bs*XynA11-His through prebiotic activity (MBPBW-XOS) and anti-inflammatory assessments (MBPBW-XOS, HISBW-XOS, MBPBG-XOS, HISBG-XOS).

## 4.6 The effect of XOS on probiotics growth in MRS medium

In the subsequent experiment, we demonstrated that XOS-BW-MBP (XOS delivery from beechwood xylan by MBP-*Bs*XynA11) promoted the growth of specific probiotic strains in synthetic media (Figure 28a-g). In MRS media, the effects of different carbon sources (2%, w/v), including glucose, inulin, and XOS-BW-MBP on the growth of *Bifidobacterium longum*, *Lactobacillus acidophilus* DSM20079, *L. amylovorus* DSM20552, *L. delbrueckii* subsp. *bulgaricus* DSM20081, *L. gasseri*, *Streptococcus salivarius* DSM2059, and *S. thermophilus* APC151 were compared. The lowest growth for all strains was observed in the control (without a carbon source), followed by XOS, inulin, and glucose, which promoted the highest growth. The prebiotic activity of XOS is detailed in Table 11. Among the strains evaluated, *B. longum* showed the highest XOS prebiotic index (6.67), followed by *S. thermophilus* (6.23), while *L. gasseri* had the lowest index (4.94). The highest prebiotic score for XOS was observed in *S. thermophilus*, with a value of 0.60. A previous study reported prebiotic scores of 1.73 and 1.61 for *L. acidophilus* LA-5 after 24 and 72 h, respectively, using a mixture of XOS produced by *B. subtilis* from wheat middlings (Reque et al., 2019). Additionally, XOS derived from SCB through enzymatic hydrolysis combined with alkali extraction exhibited prebiotic index and score values of 1.92 and 1.61, 1.9 and 1.7 for *L. plantarum* and *L. fermentum*, respectively (Kathiresan et al., 2024).

**Table 11.** Evaluation of prebiotic index and prebiotic score of MBPBW-XOS by comparing the growth of different probiotics after 24 h

| Probiotic strains | Prebiotic Index[a] | Prebiotic score[b] |
|---|---|---|
| *Bifidobacterium longum* | 6.67 | 0.35 |
| *Lactobacillus acidophilus* DSM20079 | 5.16 | 0.24 |
| *Lactobacillus amylovorus* DSM20552 | 5.09 | 0.23 |
| *Lactobacillus delbrueckii* sub. Bulgaricus DSM20081 | 5.10 | 0.22 |
| *Lactobacillus gasseri* | 4.92 | 0.22 |
| *Streptococcus salivarius* DSM2059 | 5.23 | 0.24 |
| *Streptococcus thermophilus* APC151 | 6.23 | 0.60 |

[a]The prebiotic index was calculated based on the $OD_{600}$ of probiotics in XOS-supplemented media compared to control media after 24 h.

[b]The prebiotic score was calculated based on the $OD_{600}$ of probiotics in XOS-supplemented media at 24 h compared to the $OD_{600}$ at 0 h.

Xylooligosaccharides are well-known for their prebiotic properties, selectively promoting the growth of beneficial gut bacteria, which contributes to overall gut health. Specifically, XOS stimulate the proliferation of *Bifidobacterium* sp. and *Lactobacillus* sp., helping to maintain a balanced gut microbiota (Amorim et al., 2020; Tian et al., 2024). In addition to promoting beneficial bacteria, XOS also inhibit the growth of harmful bacteria such as *E. coli*, enhancing gastrointestinal health (Hafidah et al., 2018). The fermentation of XOS by gut bacteria generates short-chain fatty acids (SCFAs) like acetic and butyric acids, which have been shown to promote colon health. These SCFAs not only provide energy for colon cells but also help maintain the structural integrity of the intestinal mucus lining and modulate immune responses (Chinbat et al., 2024). Moreover, XOS can be easily incorporated into various food products to improve their nutritional value, offering benefits at low doses with low caloric impact (Aita & Moon, 2020; Chen et al., 2021b).

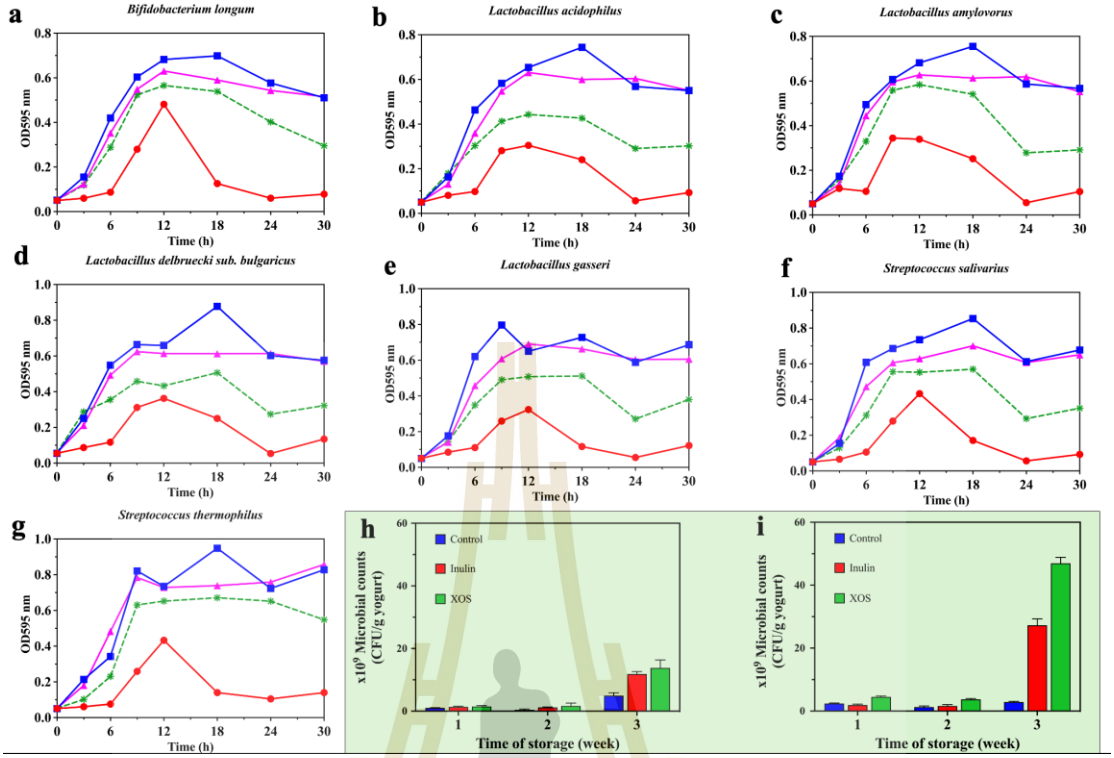


**Figure 28.** The effect of MBPBW-XOS and other carbon sources on the growth of probiotics. Growth of probiotic bacteria (OD600): *Bifidobacterium longum* (a), *Lactobacillus acidophilus* (b), *L. amylovorus* (c), *L. delbrueckii* (d), *L. gasseri* (e), *Streptococcus salivarius* (f), and *S. thermophilus* (g) in MRS media with different 2% carbon sources: glucose (blue), inulin (pink), XOS (green), and control (red). The CFU values of *L. bulgaricus* and *S. thermophilus* in yogurt without sucrose (h) and with 10% sucrose (i) in the presence of 0.05% inulin (red), XOS (green), and control (blue, no supplementation). Data are presented as mean ± SD (n = 2).

## 4.7 The effect of XOS on probiotics growth in yogurt

To further evaluate the prebiotic activity of XOS, yogurt formulations were supplemented with 0.05% (w/v) MBPBW-XOS and inulin, both with and without sucrose (10% w/v), and their effects on probiotic growth were monitored. The colony-forming unit (CFU/g) values were evaluated every 7 days for 3 weeks of storage at 4 °C. During the first two weeks, there were no significant differences in CFU between the XOS, inulin, and control groups under both sucrose conditions (Figure 28h-i). However, by the third week, in yogurt without sucrose (Figure 28h), the CFU values in the inulin-

supplemented yogurt reached 11.85 × $10^9$, which was 2.4 times higher than the control group. In the XOS-supplemented yogurt, the CFU level reached 13.8 × $10^9$, which was 2.8 times higher than the control. A similar trend was observed in yogurt containing 10% sucrose (Figure 28i), where CFU reached 27.25 × $10^9$ in inulin-supplemented yogurt and 46.95 × $10^9$ in XOS-supplemented yogurt, representing increases of 9.6 and 16.5 times compared to the control, respectively. In this case, the CFU in XOS-supplemented yogurt was 1.7 times higher than in inulin-supplemented yogurt. Interestingly, these results demonstrate that XOS not only supported the growth of probiotics during storage but also more effectively than inulin. In the presence of sucrose, XOS and inulin significantly enhanced probiotic viability, suggesting that XOS can serve as an effective prebiotic in dairy products, promoting the proliferation of beneficial bacteria over long storage periods. The comparisons of the protective effects of sucrose and various prebiotics on *L. plantarum* during freeze-drying and storage have been previously reported (Oluwatosin et al., 2022). Accordingly, 10% (w/v) of skimmed milk, inulin, maltodextrin, and sucrose all can protect cells during the freeze-drying process. Among them, skimmed milk has the highest cell survival rate, at 91%. During storage, maltodextrin and sucrose were effective in maintaining cell viability at 4 °C after 12 weeks, while inulin offered the lowest protection, with a survival rate of less than 1%. In *in vivo* conditions, the growth ability of *L. plantarum* in maltodextrin and inulin was lower than in sucrose (67% and 33%, respectively). This suggests that sucrose plays an important role in food, serving not only as a sweetening ingredient but also as a preservative and promoting probiotics. In another report, adding 2% XOS and *L. plantarum* S61 to orange juice significantly increased phenolic content, antioxidant activity, and preserved VitC in a synbiotic beverage product (Abouloifa et al., 2024). In our study, the combination of sucrose and prebiotics (XOS) in yogurt containing probiotics (*L. delbrueckii* subsp. *bulgaricus* and *S. thermophilus*) can be considered a synbiotic yogurt, which is a promising product with potential health benefits for humans.

## 4.8 XOS anti-inflammatory activity assay

The anti-inflammatory activity of XOS was investigated using differentiated THP-1 human monocytes. The cells were first differentiated with 0.2 μM Vitamin D3 for 48 h to simulate primary human monocytes. Following differentiation, the THP-1 cells were pre-treated with different XOS (MBPBW-XOS, HISBW-XOS, MBPBG-XOS,

HISBG-XOS) at various concentration range 0–1,000 μg/mL for 24 h. Afterward, the cells were exposed to bacterial lipopolysaccharides (LPS) at 100 ng/mL for 7 h. As a control, cells were treated with 0.2 μg/mL of the steroid dexamethasone (Dexa). The level of the pro-inflammatory cytokine IL-1β (pg/mL) secreted into the culture medium was quantified using ELISA, as shown in Figure 29.

LPS stimulation significantly increased IL-1β release 202.22 pg/mL in differentiated THP-1 cells compared to the untreated control 29.77 pg/mL. However, treatment with MBPBW-XOS, HISBW-XOS (Figure 29a) at concentrations between 1–200 μg/mL and MBPBG-XOS, HISBG-HIS (Figure 29b) at concentrations between 1–50 μg/mL markedly reduced IL-1β levels, demonstrating a dose-dependent anti-inflammatory effect. The lowest concentration of XOS (1 μg/mL) exhibited an anti-inflammatory response, with the effect increasing with higher concentrations and peaking at 50 μg/mL, resulting in the release of 76 pg/mL (MBPBW-XOS), 64.5 pg/mL (HISBW-XOS), 70.6 pg/mL (MBPBG-XOS) and 47.4 pg/m (HISBG-XOS) of IL-1β. At this concentration, the anti-inflammatory effect of XOS was comparable to that of Dexa (0.2 μg/mL). However, at 200 μg/mL, XOS began to induce higher IL-1β, and at concentrations between 500–1,000 μg/mL, IL-1β levels increased further. Notably, at 1,000 μg/mL, MBPBW-XOS, MBPBG-XOS, and HISBG-XOS induced IL-1β secretion (317, 854, and 840 pg/mL) in the absence of LPS (Figure 29c). XOS derived from BG-xylan shows higher toxicity than XOS derived from BW-xylan. This may be due to the low purity of BG-xylan compared to BW-xylan (Megazyme). Therefore, xylan's source and purification process are crucial in XOS activity.

These findings suggest that while XOS exhibits anti-inflammatory properties at low concentrations, high concentrations may provoke an inflammatory response, indicating the need for further investigation to optimize its therapeutic use. In response to inflammatory stimuli, macrophages rapidly secrete “early response cytokines”, such as TNF-α and IL-1β, which promote the expression of adhesion molecules on endothelial cells, facilitating macrophage migration to inflamed tissues. Thus, changes in cytokine levels serve as key indicators of immune system activation and are used to evaluate the efficacy of anti-inflammatory treatments. However, excessive cytokine production by macrophages can result in tissue damage. XOS's anti-inflammatory effects were initially observed in the murine macrophage cell line RAW 264.7, where pre- and post-treatment with XOS (0.1–100 μg/mL, containing 83% of X2 and X3,

autohydrolysis method) significantly reduced LPS-induced inflammation by inhibiting the production of TNF-α, IL-1β, IL-6, and nitric oxide (NO), without causing cytotoxicity (Chen et al., 2012).

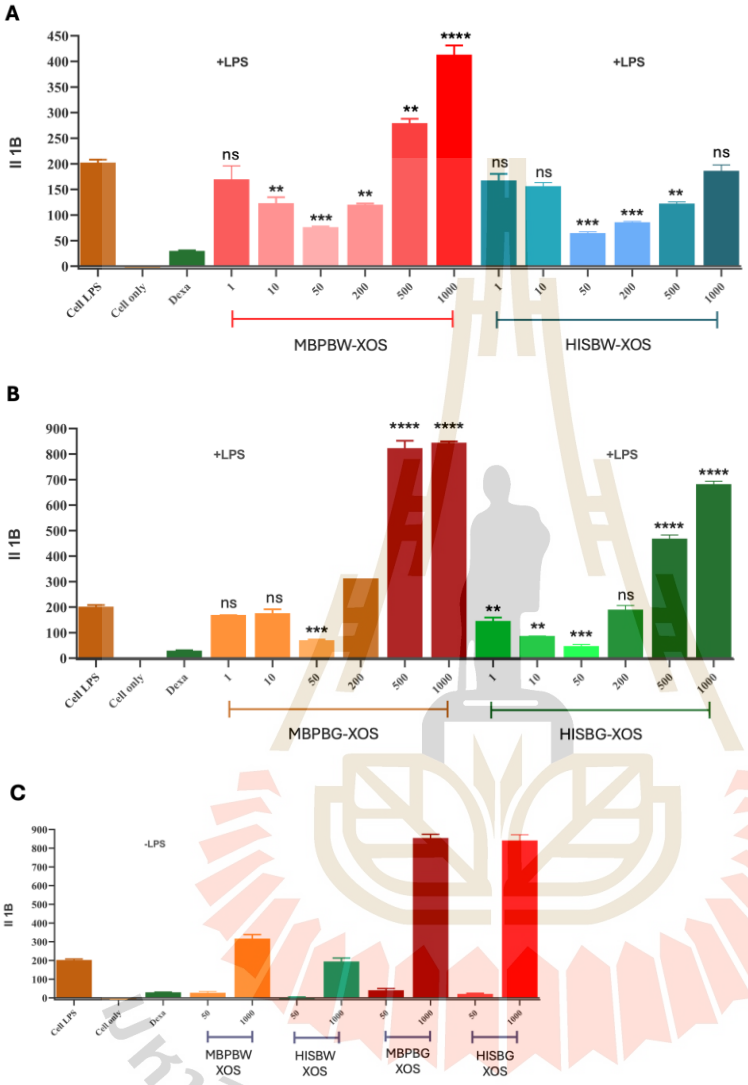


**Figure 29.** Anti-inflammatory properties of XOS. THP-1 cells were differentiated using VitD3 and then pretreated with XOS at concentrations of 1–1000 µg/mL, while dexamethasone (0.2 µg/mL) served as the control. Relative IL-1β levels, stimulated by LPS (a) and without LPS (b), represent the average of duplicates, with error bars indicating the standard deviation of the mean. One-way ANOVA and Dunnett's multiple comparisons test were performed: ns (non-significant), **P = 0.0025, ***P = 0.0001, ****P < 0.0001. MBPBW-XOS: XOS delivery from beechwood xylan by MBP-*Bs*XynA11, HISBW-XOS: XOS delivery from beechwood xylan by *Bs*XynA11-His, MBPBG-XOS: XOS delivery

from sugarcane bagasse xylan by MBP-*Bs*XynA11, **HISBG-XOS**: XOS delivery from sugarcane bagasse xylan by *Bs*XynA11-HIS.

Other oligosaccharides, including chitooligosaccharides (COS), manno-oligosaccharides (β-MOS), and synbiotics, have also been shown to exert anti-inflammatory effects on cells. For instance, COS at concentrations of 10 to 100 μg/mL demonstrated potent anti-inflammatory activity in human THP-1 macrophages (Yamabhai et al., 2024). Similarly, MOS derived from copra meal exhibited the most significant anti-inflammatory response at 200 μg/mL (Cuong et al., 2024). However, as with xylooligosaccharides (XOS) in this study, increasing concentrations of COS and MOS led to heightened inflammation in macrophages. Synbiotics, which consist of three probiotic strains *Leuconostoc lactis* CCK940, *L. lactis* SBC001, and *Weissella cibaria* YRK005 along with the oligosaccharides (CCK, SBC, YRK) produced by these strains, also displayed both immunostimulatory and anti-inflammatory effects in RAW264.7 mice macrophages by modulating the expression of TNF-α and IL-1β (Jeong et al., 2023). Importantly, this study is the first to report the anti-inflammatory properties of XOS in human cell lines. Our findings indicate that XOS, at concentrations ranging from 1–200 μg/mL, activates THP-1 cells and reduces the production of IL-1β, a key pro-inflammatory cytokine in the innate immune response.

# CHAPTER 5
# CONCLUSION AND RECOMMENDATION

In summary (Figure 30), two different xylanases cloned from *Bacillus subtilis* and expressed in *E. coli* were evaluated for their activity characteristics. Both enzymes demonstrated functionality across a broad pH range, while MBP-*Bs*XynA11 exhibited higher expression levels and thermal stability than *Bs*XynA11-His. In Lab scale, both MBP-*Bs*XynA11 and *Bs*XynA11-His effectively hydrolyzed xylan into functional xylooligosaccharides (XOS) with a degree of polymerization (DP) of 2–6, with 90% of the products being xylobiose, xylotriose, and xylotetraose. The prebiotic activity of XOS derived from BW xylan using MBP-*Bs*XynA11 for probiotics was fully evaluated in synthetic media and synbiotic yogurt. Additionally, XOS from various xylan sources hydrolyzed by MBP and His xylanase showed additional attractive properties, as their potent dose-dependent anti-inflammatory activity in LPS-induced THP-1 monocytes. However, further studies on the toxicity of XOS at high doses are needed to ensure efficacy and safety. Moreover, extraction and purification processes for xylan from sugarcane bagasse and other lignocellulosic biomass should be optimized to create substrate sources for XOS production via the enzymatic method. The findings from this study open up potential applications of xylanase for producing functional XOS from agricultural byproducts, which can be applied in health-beneficial products for humans and animals.

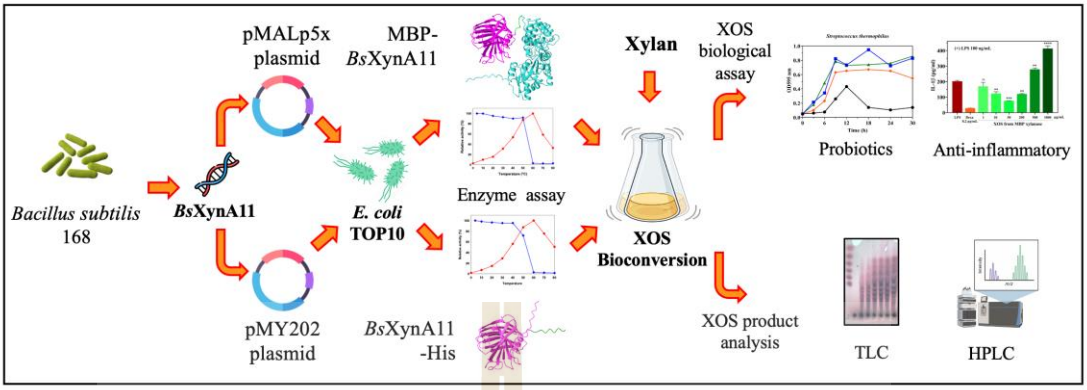


**Figure 30.** Summary of the research diagram. The study includes three main steps: the first step is the production and characterization of xylanase; the second step involves optimizing the xylan hydrolysis process and analyzing the composition of XOS products; the third step involves experiments to evaluate the biological activities of XOS, such as prebiotic and anti-inflammatory activity.

# REFERENCES


A. Parnell, J., A. Reimer, R.J.G.m. 2012. Prebiotic fiber modulation of the gut microbiota improves risk factors for obesity and the metabolic syndrome. 3(1), 29-34.

Aachary, A.A., Gobinath, D., Srinivasan, K., Prapulla, S.G. 2015. Protective effect of xylooligosaccharides from corncob on 1,2-dimethylhydrazine induced colon cancer in rats. *Bioactive Carbohydrates and Dietary Fibre*, **5**(2), 146-152.

Abouloifa, H., Gaamouche, S., Ghabbour, N., Hasnaoui, I., Moumnassi, S., Bentouhami, N., Yahyaoui, M.I., Bellaouchi, R., Rokni, Y., Karboune, S., Saalaoui, E., Asehraou, A. 2024. The impact of probiotic Lactiplantibacillus plantarum S61 and prebiotic Xylooligosaccharide on the functional properties of fermented orange juice. *Journal of Food Measurement and Characterization*, **18**(8), 7044-7051.

Abramson, J., Adler, J., Dunger, J., Evans, R., Green, T., Pritzel, A., Ronneberger, O., Willmore, L., Ballard, A.J., Bambrick, J., Bodenstein, S.W., Evans, D.A., Hung, C.-C., O'Neill, M., Reiman, D., Tunyasuvunakool, K., Wu, Z., Žemgulytė, A., Arvaniti, E., Beattie, C., Bertolli, O., Bridgland, A., Cherepanov, A., Congreve, M., Cowen-Rivers, A.I., Cowie, A., Figurnov, M., Fuchs, F.B., Gladman, H., Jain, R., Khan, Y.A., Low, C.M.R., Perlin, K., Potapenko, A., Savy, P., Singh, S., Stecula, A., Thillaisundaram, A., Tong, C., Yakneen, S., Zhong, E.D., Zielinski, M., Žídek, A., Bapst, V., Kohli, P., Jaderberg, M., Hassabis, D., Jumper, J.M. 2024. Accurate structure prediction of biomolecular interactions with AlphaFold 3. *Nature*, **630**(8016), 493-500.

Adiguzel, G., Faiz, O., Sisecioglu, M., Sari, B., Baltaci, O., Akbulut, S., Genc, B., Adiguzel, A. 2019. A novel endo-beta-1,4-xylanase from Pediococcus acidilactici GC25; purification, characterization and application in clarification of fruit juices. *Int J Biol Macromol*, **129**, 571-578.

Ahmadi, Z., Farajnia, S., Farajzadeh, D., Pouladi, N., Pourvatan, N., Karbalaeimahdi, M., Shayegh, F., Arya, M. 2023. Optimized Signal Peptide for Secretory Expression of Human Recombinant Somatropin in E. coli. *Adv Pharm Bull*, **13**(2), 339-349.

Aita, G., Moon, Y. 2020. Prebiotics from energy cane bagasse. *Sugar Industry*, 488-494.

Akpinar, O., Erdogan, K., Bostanci, S. 2009. Enzymatic production of Xylooligosaccharide from selected agricultural wastes. *Food and Bioproducts Processing*, **87**(2), 145-151.

Alokika, Kumar, V., Singh, B. 2023. Biochemical characteristics of a novel ethanol-tolerant xylanase from Bacillus subtilis subsp. subtilis JJBS250 and its applicability in saccharification of rice straw. *Biomass Conversion and Biorefinery*, **13**(3), 1937-1949.

Amorim, C., Silverio, S.C., Cardoso, B.B., Alves, J.I., Pereira, M.A., Rodrigues, L.R. 2020. In vitro assessment of prebiotic properties of xylooligosaccharides produced by Bacillus subtilis 3610. *Carbohydr Polym*, **229**, 115460.

Amorim, C., Silverio, S.C., Goncalves, R.F.S., Pinheiro, A.C., Silva, S., Coelho, E., Coimbra, M.A., Prather, K.L.J., Rodrigues, L.R. 2019a. Downscale fermentation for xylooligosaccharides production by recombinant Bacillus subtilis 3610. *Carbohydr Polym*, **205**, 176-183.

Amorim, C., Silvério, S.C., Rodrigues, L.R. 2019b. One-step process for producing prebiotic arabino-xylooligosaccharides from brewer's spent grain employing Trichoderma species. *Food Chem*, **270**, 86-94.

Ando, H., Ohba, H., Sakaki, T., Takamine, K., Kamino, Y., Moriwaki, S., Bakalova, R., Uemura, Y., Hatate, Y. 2004. Hot-compressed-water decomposed products from bamboo manifest a selective cytotoxicity against acute lymphoblastic leukemia cells. *Toxicol In Vitro*, **18**(6), 765-71.

Ávila, P.F., Martins, M., de Almeida Costa, F.A., Goldbeck, R. 2020. Xylooligosaccharides production by commercial enzyme mixture from agricultural wastes and their prebiotic and antioxidant potential. *Bioactive Carbohydrates and Dietary Fibre*, **24**.

Basit, A., Liu, J., Miao, T., Zheng, F., Rahim, K., Lou, H., Jiang, W. 2018. Characterization of Two Endo-beta-1, 4-Xylanases from Myceliophthora thermophila and Their Saccharification Efficiencies, Synergistic with Commercial Cellulase. *Front Microbiol*, **9**, 233.

Bedford, M.R.J.B.P.S. 2018. The evolution and application of enzymes in the animal feed industry: the role of data interpretation. **59**(5), 486-493.

Beena, K., Udgaonkar, J.B., Varadarajan, R. 2004. Effect of signal peptide on the stability and folding kinetics of maltose binding protein. *Biochemistry*, **43**(12), 3608-19.

Bhardwaj, N., Kumar, B., Agarwal, K., Chaturvedi, V., Verma, P. 2019a. Purification and characterization of a thermo-acid/alkali stable xylanases from Aspergillus oryzae LC1 and its application in Xylo-oligosaccharides production from lignocellulosic agricultural wastes. *International Journal of Biological Macromolecules*, **122**, 1191-1202.

Bhardwaj, N., Kumar, B., Verma, P. 2019b. A detailed overview of xylanases: an emerging biomolecule for current and future prospective. *Bioresources and Bioprocessing*, **6**(1).

Bouiche, C., Boucherba, N., Benallaoua, S., Martinez, J., Diaz, P., Pastor, F.I.J., Valenzuela, S.V. 2020. Differential antioxidant activity of glucuronoxylooligosaccharides (UXOS) and arabinoxylooligosaccharides (AXOS) produced by two novel xylanases. *Int J Biol Macromol*, **155**, 1075-1083.

Bradford, M.M. 1976. A rapid and sensitive method for the quantitation of microgram quantities of protein utilizing the principle of protein-dye binding. *Analytical biochemistry*, **72**(1-2), 248-254.

Brienzo, M., Carvalho, A. F. A., Figueiredo, F. C., & Neto, P. O. 2016. Sugarcane bagasse hemicellulose properties, extraction technologies and xylooligosaccharides production. Food waste: Practices, management and challenges, pp. 155-188.

Buruiana, C.-T., Gómez, B., Vizireanu, C., Garrote, G.J.L. 2017. Manufacture and evaluation of xylooligosaccharides from corn stover as emerging prebiotic candidates for human health. **77**, 449-459.

Butt, M.S., Tahir-Nadeem, M., Ahmad, Z., Sultan, M.T.J.F.T., Biotechnology. 2008. Xylanases and their applications in baking industry. **46**(1), 22-31.

Canilha, L., Kumar Chandel, A., dos Santos Milessi, T.S., Fernandes Antunes, F.A., da Costa Freitas, W.L., das Gracas Almeida Felipe, M., da Silva, S.S. 2012. Bioconversion of sugarcane biomass into ethanol: an overview about composition, pretreatment methods, detoxification of hydrolysates, enzymatic saccharification, and ethanol fermentation. *J Biomed Biotechnol*, **2012**, 989572.

Carrillo, I., Mendonça, R.T., Ago, M., Rojas, O.J. 2018. Comparative study of cellulosic components isolated from different Eucalyptus species. *Cellulose*, **25**(2), 1011-1029.

Chang, S., Guo, Y., Wu, B., He, B. 2017a. Extracellular expression of alkali tolerant xylanase from Bacillus subtilis Lucky9 in E. coli and application for

xylooligosaccharides production from agro-industrial waste. *International Journal of Biological Macromolecules*, **96**, 249-256.

Chang, S., Guo, Y., Wu, B., He, B. 2017b. Extracellular expression of alkali tolerant xylanase from Bacillus subtilis Lucky9 in E. coli and application for xylooligosaccharides production from agro-industrial waste. *Int J Biol Macromol*, **96**, 249-256.

Chapla, D., Pandit, P., Shah, A.J.B.T. 2012. Production of xylooligosaccharides from corncob xylan by fungal xylanase and their utilization by probiotics. **115**, 215-221.

Chaudhary, R., Kuthiala, T., Singh, G., Rarotra, S., Kaur, A., Arya, S.K., Kumar, P. 2021. Current status of xylanase for biofuel production: a review on classification and characterization. *Biomass Conversion and Biorefinery*.

Chen, H.H., Chen, Y.K., Chang, H.C., Lin, S.Y. 2012. Immunomodulatory Effects of Xylooligosaccharides. *Food Science and Technology Research*, **18**(2), 195-199.

Chen, M.-H., Bowman, M.J., Cotta, M.A., Dien, B.S., Iten, L.B., Whitehead, T.R., Rausch, K.D., Tumbleson, M., Singh, V.J.C.p. 2016. Miscanthus× giganteus xylooligosaccharides: Purification and fermentation. **140**, 96-103.

Chen, M.H., Bowman, M.J., Dien, B.S., Rausch, K.D., Tumbleson, M.E., Singh, V. 2014. Autohydrolysis of Miscanthus x giganteus for the production of xylooligosaccharides (XOS): kinetics, characterization and recovery. *Bioresour Technol*, **155**, 359-65.

Chen, Y., Xie, Y., Ajuwon, K.M., Zhong, R., Li, T., Chen, L., Zhang, H., Beckers, Y., Everaert, N. 2021a. Xylo-Oligosaccharides, Preparation and Application to Human and Animal Health: A Review. *Frontiers in Nutrition*, **8**.

Chen, Y., Xie, Y., Ajuwon, K.M., Zhong, R., Li, T., Chen, L., Zhang, H., Beckers, Y., Everaert, N. 2021b. Xylo-Oligosaccharides, Preparation and Application to Human and Animal Health: A Review. *Front Nutr*, **8**, 731930.

Chinbat, O., Erdenetsog, P., Tuvshintur, B., Gantumur, A., Burenjargal, M., Chimeddorj, B., Janlav, M. 2024. In vitro and in vivo investigation of the biological action of xylooligosaccharides derived from industrial waste. *Food Science & Nutrition*.

Costa, S., Almeida, A., Castro, A., Domingues, L. 2014. Fusion tags for protein solubility, purification and immunogenicity in Escherichia coli: the novel Fh8 system. *Front Microbiol*, **5**, 63.

Cuong, N.C., Haltrich, D., Min, T.T., Nguyen, T.-H., Yamabhai, M. 2024. Value creation of copra meal mannan into functional manno-oligosaccharides (β-MOS) using the mannanase Bacillus man B (BlMan26B). *Scientific Reports*, **14**(1), 22363.

de Freitas, C., Carmona, E., Brienzo, M. 2019. Xylooligosaccharides production process from lignocellulosic biomass and bioactive effects. *Bioactive Carbohydrates and Dietary Fibre*, **18**.

de Queiroz Brito Cunha, C.C., Gama, A.R., Cintra, L.C., Bataus, L.A.M., Ulhoa, C.J. 2018. Improvement of bread making quality by supplementation with a recombinant xylanase produced by Pichia pastoris. *PLoS One*, **13**(2), e0192996.

Demirbaş, A. 2006. Estimating of Structural Composition of Wood and Non-Wood Biomass Samples. *Energy Sources*, **27**(8), 761-767.

Dewulf, E.M., Cani, P.D., Neyrinck, A.M., Possemiers, S., Van Holle, A., Muccioli, G.G., Deldicque, L., Bindels, L.B., Pachikian, B.D., Sohet, F.M.J.T.J.o.n.b. 2011. Inulin-type fructans with prebiotic properties counteract GPR43 overexpression and PPARγ-related adipogenesis in the white adipose tissue of high-fat diet-fed mice. **22**(8), 712-722.

Diaz-Arenas, G.L., Lebanov, L., Sanz Rodriguez, E., Sadiq, M.M., Paull, B., Garnier, G., Tanner, J. 2022. Chemometric optimisation of enzymatic hydrolysis of beechwood xylan to target desired xylooligosaccharides. *Bioresour Technol*, **352**, 127041.

Ebersbach, T., Andersen, J.B., Bergstrom, A., Hutkins, R.W., Licht, T.R. 2012. Xylo-oligosaccharides inhibit pathogen adhesion to enterocytes in vitro. *Res Microbiol*, **163**(1), 22-7.

El-Gendi, H., Badawy, A.S., Bakhiet, E.K., Rawway, M., Ali, S.G. 2023. Valorization of lignocellulosic wastes for sustainable xylanase production from locally isolated Bacillus subtilis exploited for xylooligosaccharides' production with potential antimicrobial activity. *Archives of Microbiology*, **205**(9), 315.

Geetha, K., Gunasekaran, P. 2017a. Purification of Endoxylanase from Bacillus pumilus B20 for Production of Prebiotic Xylooligosaccharide Syrup; An In vitro Study. *Iran J Biotechnol*, **15**(4), 232-240.

Geetha, K., Gunasekaran, P.J.I.j.o.b. 2017b. Purification of endoxylanase from Bacillus pumilus B20 for production of prebiotic xylooligosaccharide syrup; an in vitro study. **15**(4), 232.

Glekas, P.D., Kalantzi, S., Dalios, A., Hatzinikolaou, D.G., Mamma, D. 2022. Biochemical and Thermodynamic Studies on a Novel Thermotolerant GH10 Xylanase from Bacillus safensis. *Biomolecules*, **12**(6), 790.

Gufe, C., Ngenyoung, A., Rattanarojpong, T., Khunrae, P.J.B.T. 2022. Investigation into the effects of CbXyn10C and Xyn11A on xylooligosaccharide profiles produced from sugarcane bagasse and rice straw and their impact on probiotic growth. **344**, 126319.

Gupta, M., Bangotra, R., Sharma, S., Vaid, S., Kapoor, N., Dutt, H.C., Bajaj, B.K. 2022. Bioprocess development for production of xylooligosaccharides prebiotics from sugarcane bagasse with high bioactivity potential. *Industrial Crops and Products*, **178**.

Gupta, P.K., Agrawal, P., Hedge, P., Akhtar, M.S. 2018. Xylooligosaccharides and Their Anticancer Potential: An Update. in: *Anticancer Plants: Natural Products and Biotechnological Implements*, pp. 255-271.

Gusakov, A.V., Kondratyeva, E.G., Sinitsyn, A.P.J.I.j.o.a.c. 2011. Comparison of two methods for assaying reducing sugars in the determination of carbohydrase activities. **2011**.

Hafidah, A.H., Sulistyaningsih, E., Handayani, W., Ratnadewi, A.A.I. 2018. Prebiotic Potential of Xylooligosaccharides Derived from Cassava Dregs in Balb/c Mice Colon. *Pertanika Journal of Tropical Agricultural Science*, **41**(3).

Hajihassan, Z., Ghaee, A., Bazargannia, P., Shahrivar, E.S. 2024. Affinity purification/immobilization of poly histidine-tagged proteins by nickel-functionalized porous chitosan membranes. *Journal of Chromatography A*, **1722**, 464902.

Hansen, C.H., Frokiaer, H., Christensen, A.G., Bergstrom, A., Licht, T.R., Hansen, A.K., Metzdorff, S.B. 2013. Dietary xylooligosaccharide downregulates IFN-gamma and the low-grade inflammatory cytokine IL-1beta systemically in mice. *J Nutr*, **143**(4), 533-40.

Heinen, P.R., Bauermeister, A., Ribeiro, L.F., Messias, J.M., Almeida, P.Z.d., Moraes, L.A.B.d., Vargas-Rechia, C.G., De Oliveira, A., Ward, R.J., Kadowaki, M.J.I.j.o.b.m. 2018. GH11 xylanase from Aspergillus tamarii Kita: Purification by one-step chromatography and xylooligosaccharides hydrolysis monitored in real-time by mass spectrometry. **108**, 291-299.

hen, H.H., Chen, Y. K., Chang, H. C., & Lin, S. Y. 2012. Immunomodulatory effects of xylooligosaccharides. *Food Science and Technology Research*, **18**, 195–199.

Hesam, F., Tarzi, B.G., Honarvar, M., Jahadi, M.J.B.C., Biorefinery. 2020. Valorization of sugarcane bagasse to high value-added xylooligosaccharides and evaluation of their prebiotic function in a synbiotic pomegranate juice. 1-13.

Hsu, C.-K., Liao, J.-W., Chung, Y.-C., Hsieh, C.-P., Chan, Y.-C. 2004. Xylooligosaccharides and Fructooligosaccharides Affect the Intestinal Microbiota and Precancerous Colonic Lesion Development in Rats. *The Journal of Nutrition*, **134**(6), 1523-1528.

Hu, H., Dai, S., Wen, A., Bai, X.J.A. 2019. Efficient expression of Xylanase by codon optimization and its effects on the growth performance and carcass characteristics of broiler. **9**(2), 65.

Huang, X., Ouyang, X., Hendriks, B.M.S., Gonzalez, O.M.M., Zhu, J., Koranyi, T.I., Boot, M.D., Hensen, E.J.M. 2017. Selective production of mono-aromatics from lignocellulose over Pd/C catalyst: the influence of acid co-catalysts. *Faraday Discuss*, **202**, 141-156.

Jagtap, S., Deshmukh, R.A., Menon, S., Das, S. 2017. Xylooligosaccharides production by crude microbial enzymes from agricultural waste without prior treatment and their potential application as nutraceuticals. *Bioresour Technol*, **245**(Pt A), 283-288.

Jeong, S., Kwon, A., Jeong, H., Park, Y.-S. 2023. Synergistic Immunostimulatory Activities of Probiotic Strains, Leuconostoc lactis and Weissella cibaria, and the Prebiotic Oligosaccharides They Produce. *Microorganisms*, **11**(5), 1354.

Jiang, Y., Wang, X., Wu, Z., Xu, J., Hu, L., Lin, L.J.R.i.C. 2021. Purification of xylooligosaccharides from bamboo with non-organic solvent to prepare food grade functional sugars. **3**, 100153.

Kathiresan, N., Karuppiah, V., Gopal, L., Abraham, D.R., Thangavel, K. 2024. Production and characterization of xylooligosaccharides from sugarcane bagasse using response surface methodology and its prebiotic properties. *Biomass Conversion and Biorefinery*.

Khaleghipour, L., Linares-Pasten, J.A., Rashedi, H., Ranaei Siadat, S.O., Jasilionis, A., Al-Hamimi, S., Sardari, R.R.R., Karlsson, E.N. 2021. Extraction of sugarcane bagasse

arabinoxylan, integrated with enzymatic production of xylo-oligosaccharides and separation of cellulose. *Biotechnol Biofuels*, **14**(1), 153.

Khangwal, I., Shukla, P.J.I.J.o.M. 2022. A Comparative Analysis for the Production of Xylooligosaccharides via Enzymatic Hydrolysis from Sugarcane Bagasse and Coconut Coir. **62**(2), 317-321.

Kiribayeva, A., Mukanov, B., Silayev, D., Akishev, Z., Ramankulov, Y., Khassenov, B. 2022. Cloning, expression, and characterization of a recombinant xylanase from Bacillus sonorensis T6. *PLoS One*, **17**(3), e0265647.

Koh, A., De Vadder, F., Kovatcheva-Datchary, P., & Bäckhed, F. 2016. From Dietary Fiber to Host Physiology: Short-Chain Fatty Acids as Key Bacterial Metabolites. *Cellulose*, **165**(6), 1332–1345.

Kumar, V., Bahuguna, A., Ramalingam, S., Kim, M. 2021. Developing a sustainable bioprocess for the cleaner production of xylooligosaccharides: An approach towards lignocellulosic waste management. *Journal of Cleaner Production*, **316**.

Kumar, V., Satyanarayana, T. 2015a. Generation of xylooligosaccharides from microwave irradiated agroresidues using recombinant thermo-alkali-stable endoxylanase of the polyextremophilic bacterium Bacillus halodurans expressed in Pichia pastoris. *Bioresour Technol*, **179**, 382-389.

Kumar, V., Satyanarayana, T.J.B.t. 2015b. Generation of xylooligosaccharides from microwave irradiated agroresidues using recombinant thermo-alkali-stable endoxylanase of the polyextremophilic bacterium Bacillus halodurans expressed in Pichia pastoris. **179**, 382-389.

Kumari, K., Nagar, S., Goyal, S., Maan, S. 2023. Hyper xylanase production and potential of xylooligosaccharides formation from a novel Bacillus australimaris KS2. *Biocatalysis and Agricultural Biotechnology*, **54**, 102899.

L, F., P. Andrade, C.C., A. Sant, M.H. 2013. A Review of Xylanase Production by the Fermentation of Xylan: Classification, Characterization and Applications. in: *Sustainable Degradation of Lignocellulosic Biomass - Techniques, Applications and Commercialization*.

Laemmli, U.K. 1970. Cleavage of structural proteins during the assembly of the head of bacteriophage T4. *nature*, **227**(5259), 680-685.

Lai, Z., Zhou, C., Ma, X., Xue, Y., Ma, Y. 2021. Enzymatic characterization of a novel thermostable and alkaline tolerant GH10 xylanase and activity improvement by multiple rational mutagenesis strategies. *International Journal of Biological Macromolecules*, **170**, 164-177.

Lecerf, J.M., Depeint, F., Clerc, E., Dugenet, Y., Niamba, C.N., Rhazi, L., Cayzeele, A., Abdelnour, G., Jaruga, A., Younes, H., Jacobs, H., Lambrey, G., Abdelnour, A.M., Pouillart, P.R. 2012. Xylo-oligosaccharide (XOS) in combination with inulin modulates both the intestinal environment and immune status in healthy subjects, while XOS alone only shows prebiotic properties. *Br J Nutr*, **108**(10), 1847-58.

Lénon, M., Ke, N., Ren, G., Meuser, M.E., Loll, P.J., Riggs, P., Berkmen, M. 2021. A useful epitope tag derived from maltose binding protein. *Protein Sci*, **30**(6), 1235-1246.

Li, T., Li, S., Du, L., Wang, N., Guo, M., Zhang, J., Yan, F., Zhang, H. 2010. Effects of haw pectic oligosaccharide on lipid metabolism and oxidative stress in experimental hyperlipidemia mice induced by high-fat diet. *Food Chemistry*, **121**(4), 1010-1013.

Liu, J., Liu, C., Qiao, S., Dong, Z., Sun, D., Zhu, J., Liu, W. 2022. One-step fermentation for producing xylo-oligosaccharides from wheat bran by recombinant Escherichia coli containing an alkaline xylanase. *BMC biotechnology*, **22**(1), 6.

Liu, M.Q., Huo, W.K., Xu, X., Weng, X.Y. 2017. Recombinant Bacillus amyloliquefaciens xylanase A expressed in Pichia pastoris and generation of xylooligosaccharides from xylans and wheat bran. *Int J Biol Macromol*, **105**(Pt 1), 656-663.

M.J. Va´zquez, J.L.A., H. Domı´nguez and J.C. Parajo´ 2000. Xylooligosaccharides manufacture and applications *Trends in Food Science & Technology*, **11**, 387–393.

Maccioni, R.B., Calfio, C., Gonzalez, A., Luttges, V. 2022. Novel Nutraceutical Compounds in Alzheimer Prevention. *Biomolecules*, **12**(2).

Maeda, R., Ida, T., Ihara, H., Sakamoto, T. 2012. Induction of apoptosis in MCF-7 cells by beta-1,3-xylooligosaccharides prepared from Caulerpa lentillifera. *Biosci Biotechnol Biochem*, **76**(5), 1032-4.

Mahmoudi Gomari, M., Saraygord-Afshari, N., Farsimadan, M., Rostami, N., Aghamiri, S., Farajollahi, M.M. 2020. Opportunities and challenges of the tag-assisted protein

purification techniques: Applications in the pharmaceutical industry. *Biotechnology Advances*, **45**, 107653.

Mai-Moulin, T., Visser, L., Fingerman, K.R., Elbersen, W., Elbersen, B., Nabuurs, G.-J., Fritsche, U.R., Del Campo Colmenar, I., Rutz, D., Diaz-Chavez, R.A., Roozen, A., Weck, M., Iriarte, L., Pelkmans, L., Sanchez Gonzalez, D., Janssen, R., Junginger, M. 2019. Sourcing overseas biomass for EU ambitions: assessing net sustainable export potential from various sourcing countries. *Biofuels, Bioproducts and Biorefining*, **13**(2), 293-324.

Martínez, P., Pereira, M., Mendonça, R.T.J.J.o.W.C., Technology. 2015. Retention and structure of xylans from Eucalyptus globulus genotypes with different pulpwood characteristics. **35**(2), 129-136.

McCleary, B.V., McGeough, P. 2015. A Comparison of Polysaccharide Substrates and Reducing Sugar Methods for the Measurement of endo-1,4-beta-Xylanase. *Appl Biochem Biotechnol*, **177**(5), 1152-63.

Mohanta, B., Sen, D.J., Mahanti, B., Nayak, A.K. 2022. Antioxidant potential of herbal polysaccharides: An overview on recent researches. *Sensors International*, **3**.

Nabarlatz, D., Montane, D., Kardosova, A., Bekesova, S., Hribalova, V., Ebringerova, A. 2007. Almond shell xylo-oligosaccharides exhibiting immunostimulatory activity. *Carbohydr Res*, **342**(8), 1122-8.

Oluwatosin, S.O., Tai, S.L., Fagan-Endres, M.A. 2022. Sucrose, maltodextrin and inulin efficacy as cryoprotectant, preservative and prebiotic - towards a freeze dried Lactobacillus plantarum topical probiotic. *Biotechnol Rep (Amst)*, **33**, e00696.

Otieno, D.O., Ahring, B.K. 2012a. The potential for oligosaccharide production from the hemicellulose fraction of biomasses through pretreatment processes: xylooligosaccharides (XOS), arabinooligosaccharides (AOS), and mannooligosaccharides (MOS). *Carbohydr Res*, **360**, 84-92.

Otieno, D.O., Ahring, B.K. 2012b. A thermochemical pretreatment process to produce xylooligosaccharides (XOS), arabinooligosaccharides (AOS) and mannooligosaccharides (MOS) from lignocellulosic biomasses. *Bioresour Technol*, **112**, 285-92.

Palaniappan, A., Antony, U., Emmambux, M.N. 2021. Current status of xylooligosaccharides: Production, characterization, health benefits and food application. *Trends in Food Science & Technology*, **111**, 506-519.

Pechsrichuang, P., Songsiriritthigul, C., Haltrich, D., Roytrakul, S., Namvijtr, P., Bonaparte, N., Yamabhai, M. 2016. OmpA signal peptide leads to heterogenous secretion of B. subtilis chitosanase enzyme from E. coli expression system. *Springerplus*, **5**, 1-10.

Pechsrichuang, P., Yoohat, K., Yamabhai, M. 2013. Production of recombinant Bacillus subtilis chitosanase, suitable for biosynthesis of chitosan-oligosaccharides. *Bioresource technology*, **127**, 407-414.

Phukon, L.C., Abedin, M.M., Chourasia, R., Singh, S.P., Tayung, K., Rai, A.K. 2024. Valorization of agro-wastes by Bacillus altitudinis XYL17 through simultaneous production of xylanase, xylooligosaccharides, and antioxidant compounds. *Industrial Crops and Products*, **213**, 118395.

Poletto, P., Pereira, G.N., Monteiro, C.R.M., Pereira, M.A.F., Bordignon, S.E., de Oliveira, D. 2020. Xylooligosaccharides: Transforming the lignocellulosic biomasses into valuable 5-carbon sugar prebiotics. *Process Biochemistry*, **91**, 352-363.

Pu, J., Zhao, X., Wang, Q., Wang, Y., Zhou, H.J.F.C. 2016. Development and validation of a HPLC method for determination of degree of polymerization of xylo-oligosaccharides. **213**, 654-659.

Rashad, M., El-Torky, A., Nooman, M., Keshta, A., Mahmoud, H., Mahmoud, A.J.A.J.M.B.E.S., a. 2015. Enhanced production of cellulase-free xylanase from Bacillus amyloliquifaciens NNRL B-14393 by solid state fermentation of water hyacinth and its application in degradation of agricultural residues. **17**, 865-877.

Rashad, M., Mahmoud, A., Nooman, M., Mahmoud, H., El-Torky, A., Keshta, A. 2016. Production of antioxidant xylooligosaccharides from lignocellulosic materials using Bacillus amyloliquifaciens NRRL B-14393 xylanase. *Journal of Applied Pharmaceutical Science*, 030-036.

Rashid, R., Sohail, M. 2021. Xylanolytic Bacillus species for xylooligosaccharides production: a critical review. *Bioresources and Bioprocessing*, **8**(1).

Reque, P.M., Pinilla, C.M.B., Gautério, G.V., Kalil, S.J., Brandelli, A. 2019. Xylooligosaccharides production from wheat middlings bioprocessed with Bacillus subtilis. *Food Research International*, **126**, 108673.

Reuten, R., Nikodemus, D., Oliveira, M.B., Patel, T.R., Brachvogel, B., Breloy, I., Stetefeld, J., Koch, M. 2016. Maltose-Binding Protein (MBP), a Secretion-Enhancing Tag for Mammalian Protein Expression Systems. *PLoS One*, **11**(3), e0152386.

Roslan, A.M., Mustafa Kamil, A., Chandran, C., Song, A.A., Yusoff, K., Abdul Rahim, R. 2020. Secretion of recombinant xylanase in Lactococcus lactis using signal peptides Usp45 and Spk1. *Biotechnol Lett*, **42**(9), 1727-1733.

Saini, R., Patel, A.K., Saini, J.K., Chen, C.-W., Varjani, S., Singhania, R.R., Di Dong, C. 2022. Recent advancements in prebiotic oligomers synthesis via enzymatic hydrolysis of lignocellulosic biomass. *Bioengineered*, **13**(2), 2139-2172.

Santibanez, L., Henriquez, C., Corro-Tejeda, R., Bernal, S., Armijo, B., Salazar, O. 2021. Xylooligosaccharides from lignocellulosic biomass: A comprehensive review. *Carbohydr Polym*, **251**, 117118.

Schubeis, T., Stanek, J., Pintacuda, G. 2021. Backbone assignment of crystalline E. coli maltose binding protein. *Biomolecular NMR Assignments*, **15**(2), 317-322.

Sharma, N., Sharma, N.J.G.J.B.A.H.S. 2017. Microbial xylanases and their industrial applications as well as future perspectives: a review. **6**, 5-12.

Shi, H., Zhang, Y., Zhong, H., Huang, Y., Li, X., Wang, F.J.B.l. 2014. Cloning, over-expression and characterization of a thermo-tolerant xylanase from Thermotoga thermarum. **36**(3), 587-593.

Silva, L.d.O., Terrasan, C.R.F., Carmona, E.C.J.E.J.o.B. 2015. Purification and characterization of xylanases from Trichoderma inhamatum. **18**(4), 307-313.

Singh, P., Sharma, L., Kulothungan, S.R., Adkar, B.V., Prajapati, R.S., Ali, P.S., Krishnan, B., Varadarajan, R. 2013. Effect of signal peptide on stability and folding of Escherichia coli thioredoxin. *PLoS One*, **8**(5), e63442.

Singh, R.D., Muir, J., Arora, A.J.B., Bioproducts, Biorefining. 2021. Concentration of xylooligosaccharides with a low degree of polymerization using membranes and their effect on bacterial fermentation. **15**(1), 61-73.

Singh, R.S., Singhania, R.R., Pandey, A., Larroche, C. 2019. *Biomass, Biofuels, Biochemicals: Advances in Enzyme Technology*. Elsevier.

Songsiriritthigul, C., Lapboonrueng, S., Pechsrichuang, P., Pesatcha, P., Yamabhai, M. 2010. Expression and characterization of Bacillus licheniformis chitinase (ChiA), suitable for bioconversion of chitin waste. *Bioresource Technology*, **101**(11), 4096-4103.

Su, Y., Fang, L., Wang, P., Lai, C., Huang, C., Ling, Z., Sun, S., Yong, Q. 2021. Efficient production of xylooligosaccharides rich in xylobiose and xylotriose from poplar

by hydrothermal pretreatment coupled with post-enzymatic hydrolysis. *Bioresource Technology*, **342**, 125955.

Sukri, S.S.M., Mimi Sakinah, A.M. 2018. Production of High Commercial Value Xylooligosaccharides from Meranti Wood Sawdust Using Immobilised Xylanase. *Appl Biochem Biotechnol*, **184**(1), 278-290.

Sun, J., Sun, X., Sun, R., Su, Y.J.C.p. 2004. Fractional extraction and structural characterization of sugarcane bagasse hemicelluloses. **56**(2), 195-204.

Terrone, C.C., de Freitas, C., Terrasan, C.R.F., de Almeida, A.F., Carmona, E.C.J.E.J.o.B. 2018. Agroindustrial biomass for xylanase production by Penicillium chrysogenum: Purification, biochemical properties and hydrolysis of hemicelluloses. **33**, 39-45.

Tian, S., Yang, Z., Yan, F., Xue, X.a., Lu, J. 2024. Preparation of xylooligosaccharides from rice husks and their structural characterization, antioxidant activity, and probiotic properties. *International Journal of Biological Macromolecules*, **271**, 132575.

Tseng, Y.-H., Lee, W.-C., Krisomdee, K., Natesuntorn, W., Chatsurachai, S., Sriroth, K. 2022. Xylooligosaccharide Production from Sugarcane Bagasse using Recombinant Endoxylanase of Bacillus Halodurans. *Sugar Tech*, **24**(4), 1029-1036.

Valladares-Diestra, K.K., de Souza Vandenberghe, L.P., Soccol, C.R.J.B.T. 2021a. A biorefinery approach for enzymatic complex production for the synthesis of xylooligosaccharides from sugarcane bagasse. **333**, 125174.

Valladares-Diestra, K.K., de Souza Vandenberghe, L.P., Torres, L.A.Z., Nishida, V.S., Zandoná Filho, A., Woiciechowski, A.L., Soccol, C.R.J.C.E.J. 2021b. Imidazole green solvent pre-treatment as a strategy for second-generation bioethanol production from sugarcane bagasse. **420**, 127708.

Valladares-Diestra, K.K., Porto de Souza Vandenberghe, L., Soccol, C.R. 2022. Integrated xylooligosaccharides production from imidazole-treated sugarcane bagasse with application of in house produced enzymes. *Bioresour Technol*, **362**, 127800.

Valls, C., Pastor, F.I.J., Vidal, T., Roncero, M.B., Diaz, P., Martinez, J., Valenzuela, S.V. 2018. Antioxidant activity of xylooligosaccharides produced from

glucuronoxylan by Xyn10A and Xyn30D xylanases and eucalyptus autohydrolysates. *Carbohydr Polym*, **194**, 43-50.

Vazquez, M.J., Alonso, J.L., Domınguez, H., Parajo, J.C. 2000. Xylooligosaccharides: manufacture and applications. *Trends in Food Science & Technology*, **11**(11), 387-393.

Walia, A., Guleria, S., Mehta, P., Chauhan, A., Parkash, J.J.B. 2017. Microbial xylanases and their industrial application in pulp and paper biobleaching: a review. **7**(1), 1-12.

Wang, L., Li, Z., Liu, Y.J.J.o.F.P.E. 2022. Ultrasonic-assisted extraction and purification of xylo-oligosaccharides from wheat bran. **45**(11), e14152.

Wijaya, H., Sasaki, K., Kahar, P., Rahmani, N., Hermiati, E., Yopi, Y., Ogino, C., Prasetya, B., Kondo, A.J.P. 2020. High enzymatic recovery and purification of xylooligosaccharides from empty fruit bunch via nanofiltration. **8**(5), 619.

Yadav, P., Maharjan, J., Korpole, S., Prasad, G.S., Sahni, G., Bhattarai, T., Sreerama, L. 2018. Production, Purification, and Characterization of Thermostable Alkaline Xylanase From Anoxybacillus kamchatkensis NASTPD13. *Front Bioeng Biotechnol*, **6**, 65.

Yamabhai, M., Buranabanyat, B., Jaruseranee, N., Songsiriritthigul, C. 2011. Efficient E. coli expression systems for the production of recombinant beta-mannanases and other bacterial extracellular enzymes. *Bioeng Bugs*, **2**(1), 45-9.

Yamabhai, M., Khamphio, M., Min, T.T., Soem, C.N., Cuong, N.C., Aprilia, W.R., Luesukprasert, K., Teeranitayatarn, K., Maneedaeng, A., Tuveng, T.R., Lorentzen, S.B., Antonsen, S., Jitprasertwong, P., Eijsink, V.G.H. 2024. Valorization of shrimp processing waste-derived chitosan into anti-inflammatory chitosan-oligosaccharides (CHOS). *Carbohydrate Polymers*, **324**, 121546.

Yang, J., Summanen, P.H., Henning, S.M., Hsu, M., Lam, H., Huang, J., Tseng, C.H., Dowd, S.E., Finegold, S.M., Heber, D., Li, Z. 2015. Xylooligosaccharide supplementation alters gut bacteria in both healthy and prediabetic adults: a pilot study. *Front Physiol*, **6**, 216.

Yu, X., Yin, J., Li, L., Luan, C., Zhang, J., Zhao, C., Li, S. 2015. Prebiotic Potential of Xylooligosaccharides Derived from Corn Cobs and Their In Vitro Antioxidant Activity When Combined with Lactobacillus. *J Microbiol Biotechnol*, **25**(7), 1084-92.

Zhang, J., Qin, Y., Wang, Q., Liu, S., Zhou, J., He, B., Liang, X., Xian, L., Wu, J. 2023. Gene cloning, expression, and characterization of two endo-xylanases from Bacillus velezensis and Streptomyces rochei, and their application in xylooligosaccharide production. *Front Microbiol*, **14**, 1292726.

ZHANG, Y., HUANG, L.J., WANG, Z.F.J.C.J.o.C. 2007. A sensitive derivatization method for the determination of the sugar composition after pre-column reductive amination with 3-amino-9-ethylcarbazole (AEC) by high-performance liquid chromatography. **25**(10), 1522-1528.

Zhao, S., Zhang, G.-L., Chen, C., Yang, Q., Luo, X.-M., Wang, Z.-B., Wu, A.-M., Feng, J.-X. 2021. A combination of mild chemical pre-treatment and enzymatic hydrolysis efficiently produces xylooligosaccharides from sugarcane bagasse. *Journal of Cleaner Production*, **291**.

Zhou, H., Cai, Y., Long, M., Zheng, N., Zhang, Z., You, C., Hussain, A., Xia, X. 2024. Computer-Aided Reconstruction and Application of Bacillus halodurans S7 Xylanase with Heat and Alkali Resistance. *Journal of Agricultural and Food Chemistry*, **72**(2), 1213-1227.

# APPENDIX

**Appendix 1.** The components of LB, TB and Rich media in 1 L

| Component | LB (Luria-Bertani) | TB (Terrific Broth) | Rich Media |
|---|---|---|---|
| Peptone (g) | 10 | | |
| Tryptone | | 12 | 10 |
| Yeat extract (g) | 5 | 24 | 5 |
| NaCl (g) | 5 | | 5 |
| Glycerol (mL) | | 4 | |
| $KH_2PO_4$ (g) | | 2.31 | |
| $K_2HPO_4$ (g) | | 12.54 | |
| Glucose (g) | | | 2 |

# BIOGRAPHY

Mr. Nguyen Cao Cuong was born in 1985 in Nghe An, Vietnam. In 2008, he graduated with a bachelor's degree in Post-harvest and Food Processing in Agriculture, with a thesis titled "*Optimization of Protein Hydrolysis and Deacetylation Process to Produce Chitosan from Shrimp Shells"* under the supervision of Prof. Do Thi Bich Thuy. He became a lecturer at the University of Agriculture and Forestry, Hue University, in the same year. From 2009 to 2018, he participated in teaching and scientific research activities as a lecturer. On 07/2019, he received a scholarship for a master's program at Suranaree University of Technology, Thailand. On 02/2021, he completed his master's degree with a thesis titled *"Production of Xylitol from Sugarcane Bagasse Xylan by Candida guilliermondii TISTR 5068"* supervised by Assoc. Prof. Dr. Apichat Boontawan. He then continued with a Ph.D program on the topic *"Bioconversion of xylan into functional xylooligosaccharides (XOS) by recombinant endo-β-1,4-xylanase"* under the supervision of Prof. Dr. Montarop Yamabhai (SUT, Thailand), Assoc. Prof. Dr. Apichat Boontawan (SUT, Thailand) and Prof. Dr. Dietmar Haltrich (BOKU, Austria).

During his career, he has published 23 scientific papers (in both Vietnamese and English), participated in 07 scientific projects, 01 Provincial Science and Technology Award (2018), and 01 Gold Award for the International Innovation Project Competition in Malaysia, with *chitosan-oligosaccharides project* (2024). He joined the exchange research program for 3 months at BOKU University (Austria) under the supervision of Assoc. Prof. Dr. Clemens Karl Peterbauer, Dr. Thu-Ha Nguyen and Prof. Dr. Dietmar Haltrich. His main research topic is "Applying biotechnology to enhance the value of agricultural by-products."

Contact information: Email: nguyencaocuong@hueuni.edu.vn

**Reference:**

Prof. Dr. Montarop Yamabhai, Email: montarop@g.sut.ac.th

Assoc. Prof. Dr. Apichat Boontawan, Email: apichat@sut.ac.th